

Document made available under the Patent Cooperation Treaty (PCT)

International application number: PCT/CA05/000438

International filing date: 23 March 2005 (23.03.2005)

Document type: Certified copy of priority document

Document details: Country/Office: US
Number: 60/555,316
Filing date: 23 March 2004 (23.03.2004)

Date of receipt at the International Bureau: 15 June 2005 (15.06.2005)

Remark: Priority document submitted or transmitted to the International Bureau in compliance with Rule 17.1(a) or (b)



World Intellectual Property Organization (WIPO) - Geneva, Switzerland
Organisation Mondiale de la Propriété Intellectuelle (OMPI) - Genève, Suisse

PA 1323581

THE UNITED STATES OF AMERICA

~~TO ALL TO WHOM THESE PRESENTS SHALL COME:~~

UNITED STATES DEPARTMENT OF COMMERCE

United States Patent and Trademark Office

May 24, 2005

THIS IS TO CERTIFY THAT ANNEXED HERETO IS A TRUE COPY FROM THE RECORDS OF THE UNITED STATES PATENT AND TRADEMARK OFFICE OF THOSE PAPERS OF THE BELOW IDENTIFIED PATENT APPLICATION THAT MET THE REQUIREMENTS TO BE GRANTED A FILING DATE UNDER 35 USC 111.

APPLICATION NUMBER: 60/555,316

FILING DATE: March 23, 2004

PCT/CA05/00438

By Authority of the
COMMISSIONER OF PATENTS AND TRADEMARKS



L. Edelen

L. EDELEN
Certifying Officer

16698 U.S. PTO

PTO/SB/16 (08-03)

Approved for use through 07/31/2006. OMB 0651-0032
U.S. Patent and Trademark Office; U.S. DEPARTMENT OF COMMERCE

Under the Paperwork Reduction Act of 1995, no persons are required to respond to a collection of information unless it displays a valid OMB control number.

PROVISIONAL APPLICATION FOR PATENT COVER SHEET

This is a request for filing a PROVISIONAL APPLICATION FOR PATENT under 37 CFR 1.53(c).

Express Mail Label No.

2264 U.S. PTO
60/555316

032304

INVENTOR(S)					
Given Name (first and middle [if any])		Family Name or Surname		Residence (City and either State or Foreign Country)	
Jose Krishan		MARTI SRIVASTAVA		Vancouver, CANADA Vancouver, CANADA	
Additional inventors are being named on the <u>1</u> separately numbered sheets attached hereto					
TITLE OF THE INVENTION (500 characters max)					
Electric Winding Displacement Detection Method and Apparatus					
Direct all correspondence to: CORRESPONDENCE ADDRESS					
<input type="checkbox"/> Customer Number: <div style="border: 1px solid black; width: 250px; height: 20px;"></div>					
OR					
<input checked="" type="checkbox"/> Firm or Individual Name		The University of British Columbia - Industry Liaison Office			
Address		#103 -6190 Agronomy Road			
Address					
City		Vancouver	State	BC	Zip V6T 1Z3
Country		CANADA	Telephone	6048228594	Fax 6048225998
ENCLOSED APPLICATION PARTS (check all that apply)					
<input checked="" type="checkbox"/> Specification Number of Pages <u>45</u>		<input type="checkbox"/> CD(s), Number _____			
<input checked="" type="checkbox"/> Drawing(s) Number of Sheets <u>19</u>		<input type="checkbox"/> Other (specify) _____			
<input type="checkbox"/> Application Date Sheet. See 37 CFR 1.76					
METHOD OF PAYMENT OF FILING FEES FOR THIS PROVISIONAL APPLICATION FOR PATENT					
<input checked="" type="checkbox"/> Applicant claims small entity status. See 37 CFR 1.27.				FILING FEE Amount (\$)	
<input type="checkbox"/> A check or money order is enclosed to cover the filing fees.				<div style="border: 1px solid black; width: 100px; height: 50px; text-align: center; vertical-align: middle;">80.00</div>	
<input type="checkbox"/> The Director is hereby authorized to charge filing fees or credit any overpayment to Deposit Account Number: _____					
<input checked="" type="checkbox"/> Payment by credit card. Form PTO-2038 is attached.					
The invention was made by an agency of the United States Government or under a contract with an agency of the United States Government.					
<input checked="" type="checkbox"/> No.					
<input type="checkbox"/> Yes, the name of the U.S. Government agency and the Government contract number are: _____					

Respectfully submitted,

[Page 1 of 2]

Date 22 March 2004

SIGNATURE



REGISTRATION NO. _____

TYPED or PRINTED NAME ANNARI FAURIE

(if appropriate)

Docket Number: UBC 04-032

TELEPHONE 604-822-8594

USE ONLY FOR FILING A PROVISIONAL APPLICATION FOR PATENT

This collection of information is required by 37 CFR 1.51. The information is required to obtain or retain a benefit by the public which is to file (and by the USPTO to process) an application. Confidentiality is governed by 35 U.S.C. 122 and 37 CFR 1.14. This collection is estimated to take 8 hours to complete, including gathering, preparing, and submitting the completed application form to the USPTO. Time will vary depending upon the individual case. Any comments on the amount of time you require to complete this form and/or suggestions for reducing this burden, should be sent to the Chief Information Officer, U.S. Patent and Trademark Office, U.S. Department of Commerce, P.O. Box 1450, Alexandria, VA 22313-1450. DO NOT SEND FEES OR COMPLETED FORMS TO THIS ADDRESS. SEND TO: Mail Stop Provisional Application, Commissioner for Patents, P.O. Box 1450, Alexandria, VA 22313-1450.

If you need assistance in completing the form, call 1-800-PTO-9199 and select option 2.

PROVISIONAL APPLICATION COVER SHEET
Additional Page

PTO/SB/18 (08-03)

Approved for use through 07/31/2006. OMB 0651-0032

U.S. Patent and Trademark Office; U.S. DEPARTMENT OF COMMERCE

Under the Paperwork Reduction Act of 1995, no persons are required to respond to a collection of information unless it displays a valid OMB control number.

Docket Number UBC 04-032

INVENTOR(S)/APPLICANT(S)		
Given Name (first and middle [if any])	Family or Surname	Residence (City and either State or Foreign Country)
Qiaoshu	JIANG	Vancouver, CANADA

[Page 2 of 2]

Number 1 of 1

WARNING: Information on this form may become public. Credit card information should not be included on this form. Provide credit card information and authorization on PTO-2038.

TO:

Commissioner for Patents
P.O. Box 1450
Alexandria, VA 22313-1450

Enclosures:

1. Provisional application for patent cover sheet
2. Specifications, 45 pages
3. Drawings, 19 pages
4. Credit card payment form PTO-2038 for \$80.00 filing fee

THE UNIVERSITY OF BRITISH COLUMBIA

March 22, 2004

Hon. Commissioner for Patents
P.O. Box 1450
Alexandria, VA 22313-1450

Dear Sir:

Re: Provisional Patent Application for "Electric Winding Displacement Detection
Method and Apparatus"
UBC file no: 04-032

Enclosed please find the necessary documents for filing a Provisional Patent
Application for the above-identified technology on behalf of The University of British
Columbia. Also enclosed is Credit Card payment form PTO-2038 to cover the cost
of the \$80.00 application fee.

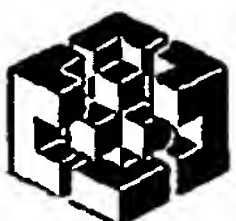
Thank you,

Sincerely,



Annari Faurie
Patent Manager

Encl.



U·I·L·O

UNIVERSITY-INDUSTRY
LIAISON OFFICE

#103 - 6190 Agronomy Road
Vancouver, BC
V6T 1Z3

Tel: (604) 822-8580
Fax: (604) 822-8589
Web: www.uilo.ubc.ca

Transmission Line Diagnostic

ELECTRIC WINDING DISPLACEMENT DETECTION METHOD AND APPARATUS

Technical Field

[0001] This application relates to a highly sensitive method and apparatus for detecting small deformation or movement of the windings in transformers, electric motors and generators.

Background

[0002] It is known that the displacement of windings in transformers, electric motors and generators can lead to insulation deterioration. When the insulation deteriorates, windings can electrically contact each other, resulting in high current flow, partial discharges, and very severe and expensive faults. It is useful to be able to assess the health of a winding to enable prediction of remaining life, capacity limits, and preventive maintenance.

[0003] There are several known methods to assess the health of a winding, including detection of insulation degradation. By way of example, insulation degradation in transformers can be monitored by methods that detect partial discharges. Partial discharge detection methods include Dissolved Gas Analysis and Tan-Delta techniques. It is notable that Dissolved Gas Analysis methods detect the chemical reaction products of insulation degradation, and therefore partial discharge must have occurred before these techniques are useful. The Tan-Delta similarly detects damage that has already occurred.

[0004] Another known method of detecting winding damage is the winding ratio test, which measures the numbers of turns of both primary and secondary windings and calculates the ratio between them. By comparing the measured winding ratio with the ratio of rated primary and secondary voltages as shown on the nameplate of the transformer, shorted turns or open winding faults may be detected. However, an outage and isolation of the transformer is required for the purpose of measurements.

[0005] Another known method of detecting winding damage is the winding resistance test, which is similar to the winding ratio test except that it measures the winding resistance rather than the number of winding turns. Additionally, a very precise ohmmeter is needed, which will assure the accuracy of a fraction of an ohm. The measured resistance will be compared with the previous measurement referred to the same temperature. Measurements are conducted for different phases and different tap-changer positions. This method detects the condition of the winding conductor directly. However, it requires a transformer outage and is usually performed in the factory or a laboratory.

[0006] Another known method of detecting winding damage is the 60 Hz transformer impedance test. This method measures the input voltage, input current and input power while shorting the low voltage winding of the transformer. The before and after results are then compared with the before and after short circuit. This test is insensitive to small winding movements.

Transmission Line Diagnostic

[0007] Another known method of detecting winding damage is the Leakage reactance measurement (LRM), which can be achieved with the same test set-up as the short circuit impedance measurement. LRM is based on the increased leakage reactance, resulting from the radial outward force on the outer winding and the radial inward force on the inner winding induced by short circuits.

[0008] Another way to assess the health of a winding is to detect winding displacement. Detection of winding displacement is advantageous because such methods permit detection of deterioration prior to actual winding damage. Known winding displacement detection methods include detection of increases of the audible noise, visual inspection, short-circuit impedance measurement, vibration analysis, low voltage impulse, and Frequency Response Analysis ('FRA') techniques.

[0009] The subject invention (Transmission Line Diagnostic or 'TLD') also belongs to a class of techniques for detecting winding structural aging by measuring winding displacement, but is a superior way of obtaining winding displacement information than FRA or other techniques.

Transmission Line Diagnostic

Brief Description of Drawings

[0010] In drawings which illustrate non-limiting example embodiments of the invention:

- Figure 1.2 is a Core Type Transformer
- Figure 1.3 is a Shell Type Transformer
- Figure 1.4 is a Distortion of a Transformer Winding
- Figure 2.2 is a Transformer Circuit by Physical Parameters
- Figure 2.3 is a Frequency Response for the Physical Transformer Model with 8 Sections
- Figure 2.4 is a Decoupled Circuit I by High Frequency Transformer Model
- Figure 2.5 is a Decoupled Circuit II by High Frequency Transformer Model
- Figure 2.6 is a Symmetrical Circuit by High Frequency Transformer Model
- Figure 2.7 is a Simulation Result for the High Frequency Transformer Model
- Figure 2.8 is a Equivalent p Model by Nodal Analysis
- Figure 2.9 is a Simulation Results for Equivalent p Model Using Nodal Analysis
- Figure 3.1 is a Transmission Line
- Figure 3.2 is a Equivalent Frequency-dependent Line Model
- Figure 3.3 is a Connection of the Winding under Investigation
- Figure 3.4 is a Winding Model
- Figure 3.5 is a Faulted Winding Model
- Figure 3.6 is a Experiment Set-up
- Figure 3.7 is a 10kVA Transformer in the University Lab
- Figure 3.8 is a Z_c with Different External Insulating Distances
- Figure 3.9 is a Z_c Obtained from Different Experiment Locations
- Figure 3.10 is an Original Time Domain Measurements in a Utility Research Lab
- Figure 3.11 is a Modified Time Domain Measurements in a Utility Research Lab
- Figure 3.12 is a Simulation Results of Z_c in a Utility Research Lab
- Figure 3.13 is a Simulation Results of Travelling Time and Equivalent Length in a Utility Research Lab
- Figure 3.14 is an Overall View of the Transformer
- Figure 3.15 is a Cross-section View of the Transformer
- Figure 3.16 is a Cross-section View of the Transformer
- Figure 3.17 is an Illustration of the Skin Depth of a Conducting Material
- Figure 3.18 is a Z_c for Different Inner Separation by TLD Method with Model II
- Figure 3.19 is a Z_c for Different Inner Separation by TLD Method with Model I
- Figure 3.20 is a Shortest Distance among Z_{c5} , Z_{c7} and Z_{c8}
- Figure 3.21 is a Shortest Distance Percentage Comparison When b is Small
- Figure 3.22 is a Z_c for Bigger Inner Separation by TLD Method
- Figure 3.23 is a Shortest Distance among Z_{c1} , Z_{c2} and Z_{c4}
- Figure 3.24 is a Shortest Distance Percentage Comparison When b is Large
- Figure 3.25 is a Z_c for Different Outer Separation by TLD Method
- Figure 3.26 is a Shortest Distance among Z_{c8} , Z_{c9} and Z_{c10}
- Figure 3.27 is a Shortest Distance Percentage Comparison among Z_{c9} , Z_{c8} and Z_{c10}
- Figure 3.28 is a Z_c Comparison 1
- Figure 3.29 is a Z_c Comparison 2

Transmission Line Diagnostic

Figure 3.30 is a Shortest Distance & Distance Percentage Comparison 1

Figure 3.31 is a Shortest Distance & Distance Percentage Comparison 2

Figure 3.32 is a Z_c Comparison for Fault Situations

Description

[0011] Throughout the following description, specific details are set forth in order to provide a more thorough understanding of the TLD invention. However, the invention may be practiced without these particulars. In other instances, well known elements have not been shown or described in detail to avoid unnecessarily obscuring the invention. Accordingly, the specification and drawings are to be regarded in an illustrative, rather than a restrictive, sense.

[0012] This invention provides a system and method for obtaining the surge impedance Z_c of the winding by measuring the input and output voltages and the currents within a winding. The system has particular application in detection of winding condition and prediction of winding failure in transformers, electric generators, and electric motors.

[0013] Z_c is the signature of the winding and it is independent of external circuits. Any changes of Z_c will reflect movements of the winding. Z_c obtained by TLD is a simple exponential-like curve, whose vertical shift gives obvious indication to the overall axial or radial winding movements. This simple means for obtaining Z_c is different from the complex transfer function of numerous resonant frequencies in FRA.

[0014] The following discussion describes the background, features, embodiment, and use of the invention in the context of detecting winding displacement in, by way of example, transformers.

[0015] Description of the TLD method to detect winding displacement in transformers

Power transformers play a vital role in the operation of a power grid. A power transformer converts electricity from one potential level to another, and it is one of the most important and expensive pieces in a power grid. However, transformer failures happen, which lead to power outages, high cost of repair or replacement, personal injuries and environmental damages. Winding movement and/or distortion account for a large percentage of transformer failures.

The current diagnostic techniques used for detecting winding movements are discussed and compared. The Frequency Response Analysis (FRA) technique is today's most commonly used and effective technique; however, it highly depends on the test frequency range, test set-up, external circuits and different physical structures of different transformers. The FRA's dependence on so many parameters can result in inaccurate data.

Based on the wave propagation property and the frequency dependent transmission line model, a new approach for winding movement detection is proposed,

Transmission Line Diagnostic

the Transmission Line Diagnostics (TLD). In this method, by measuring the input and output voltages and the currents, the surge impedance Z_c of the winding can be uniquely obtained. Z_c is the signature of the winding and it is independent of the external circuits. Any changes of Z_c will reflect movements of the winding. Different from the complex transfer function of numerous resonant frequencies in FRA, Z_c obtained by TLD is a simple exponential-like curve, whose vertical shift gives obvious indication to the overall axial or radial winding movements. Furthermore, TLD is very efficient in low frequency range. With all these advantages, TLD can be effectively applied to on-line transformer winding condition monitoring.

LIST OF ABBREVIATIONS

BILs - basic insulation levels
DGA - dissolved gas analysis
LRM - leakage reactance measurement
LVI - low voltage impulse
FRA - frequency response analysis
FRA(S) - swept frequency response analysis
FRA(I) - impulse frequency response analysis
HIFRA - high-frequency internal frequency response analysis
TLD - transmission line diagnostics
EMI - electromagnetic interference
OWA - objective winding asymmetry
SDE - spectral density estimate

Transmission Line Diagnostic

Overview

Introduction to Power Transformers

In an AC power system, power transformers are used to convert electric power from one potential level to another. A power transformer comprises of two or more windings that are coupled through a common magnetic core. A time-varying flux created by one winding induces voltages in all of the other windings.

The main components of a transformer include: a laminated iron core, two or more windings, an insulation medium, a tank, bushings and accessories. Transformers can be categorized into different types according to different criteria. Depending on the insulation medium, transformers can be categorized as: dry type transformers and fluid-filled transformers. If the core and coils are in a gaseous or dry compound insulation, the transformer is called dry-type transformer; while fluid-filled transformers have the core and coils impregnated with an insulating fluid and immersed in the same insulating medium. Depending on the construction of the core, transformers can be categorized as core-type or shell-type transformers. In core-type transformers, shown in Figure 1.2, the windings are wrapped around two sides of a simple rectangular window iron core; while in shell-type transformers, shown in Figure 1.3, the windings are only wrapped around the center leg of a three-legged iron core.

An iron core is used because of its high relative permeability. As a result of its higher relative permeability, a smaller magnetizing current is required as compared to a non-ferromagnetic core. Furthermore, the iron core is usually laminated in order to minimize eddy current losses, which are generated in the core by the time varying magnetic flux.

The insulation must be capable of withstanding voltages greatly exceeding the rated winding voltages. Voltages much larger than the rated values can appear across the windings of the transformer during network transients, such as switching operations, lightning strikes, short circuit faults, and fluctuations in the load. Table 1.1 shows the insulation levels for different voltage ratings, which are defined as the values of the required test voltages. BIL, that is basic insulation levels, are given in the column 3 and column 7 for Europe and North America respectively.

Table 1.1
Standardized Test Voltages for Rated Voltages

IEC Publication 71, 1972				Coordination of Insulation		
European practice and other countries				U.S.A. and Canada		
Rated voltage Vm	Test voltage 50 Hz, 1min	Lightning Impulse voltage 1.2/50 μ sec	Switching surge voltage 250/2500 μ sec	Rated voltage	Test voltage 60Hz, 1min	Lightning Impulse voltage 1.2/50 μ sec
KV in RMS	KV in RMS	KV in peak	KV in peak	KV in RMS	KV in RMS	KV in peak
3.6	10	40		4.76	19	60
7.2	20	60		8.25	26	75
12	28	75		15	36	95
17.5	38	95		15.5	50	110
24	50	125		25.8	60	125
36	70	170		38	80	150
100	185	450		100	185	450
145	275	650		145	275	650
175	325	750		175	325	750
245	460	1050		245	460	1050
300	380	1050	850			
362	450	1175	950			
420	520	1425	1050			
525	620	1550	1175			
765	830	2100	1425			

Note: 1. Vm is the maximum service voltage of the network between phases.

2. Test voltage is the voltage to earth.

The windings are usually made of copper or aluminum. The winding conductors may be either wires or sheets. Successive layers are insulated by sheets of insulation. Ceramic bushings are used to isolate the windings from grounded structures of the transformer such as the oil tank. Transformers with increasingly larger voltages require increasingly longer bushings to prevent an external flashover. Mineral oil is typically used as insulation medium. It is also used to cool the transformer.

Transformers are one of the most essential elements of an electric power system. They are widely used in electric networks because the generation, transmission, and distribution of power require different voltage levels. For example, in a large power utility, the number of transformers can exceed 1000. They link electric loads to power

Transmission Line Diagnostic

supplies through an interconnected power network and satisfy the requirements of both parts. The use of transformers helps to reduce losses in an AC power system.

Transformers are one of the most expensive pieces of equipment in a power grid. A large power transformer in a 500kV system may cost up to a million dollars. In 1996, the total sale of power transformers in the United States was over US\$ 11 million. In terms of numbers, more than 8000 transformers, of at least 2MVA and up to more than 100 MVA, were sold in the same year all over the world.

Since transformers play a vital role in the operation of AC or HVDC electric networks, it is important to ensure that they are operating efficiently and reliably.

1.2 Transformer Failures

Inevitably in service transformer failures occur. Generally, the failures can be divided into two categories: internal failures and external failures. Internal faults are faults that happen inside the tank, such as short circuit between windings, short circuit between turns, insulation deterioration, loss of winding clamping, partial discharges and winding resonance. External faults are related to bushing, leads and accessories that are outside the tank, and may be caused by system switching operations, lightning strikes and short circuits. The internal faults can be further divided into two main categories: thermal faults and electric faults. Thermal faults cause the transformers to overheat. According to the severity of the faults, thermal faults are often categorized as slight overheating (lower than 150°C), low temperature overheating (150-300°C), medium temperature overheating (300~700°C), and high temperature overheating (higher than 700°C). Electric faults lead to the degradation of the insulation under high electric field. According to the degree of discharge intensity, electric faults are further divided into partial discharge, spark discharge and arc discharge.

There are many different ways to categorize transformer failures. The above categorization is one way. Failures can also be split according to "circuitry", structure of main body, and fault location. By circuitry, failures can be divided into electric faults, magnetic faults, and oil path faults; by structure of the main body of the transformers, failures can be divided into winding faults, core faults, oil faults, and accessory faults; by fault location, failures can be divided into insulation faults, core faults and tap-changer faults, etc. All of the above failures can either reflect thermal failures, electric failures or both. Thus, transformer failures may be caused by a multitude of reasons.

A survey over the last several decades on thousands of transformer failures conducted by Hartford Steam Boiler listed several reasons of transformer failures as shown in Table 1.2.

Table 1.2
Causes for Transformer Failures

	1975	1983	1998	Related to winding movement
Lightning Surges	32.3%	30.2%	12.4%	*
Line Surges/External Short Circuit	13.6%	18.6%	21.5%	*
Poor Workmanship-Manufacturer	10.6%	7.2%	2.9%	*
Deterioration of Insulation	10.4%	8.7%	13%	
Overloading	7.7%	3.2%	2.4%	
Moisture	7.2%	6.9%	6.3%	
Inadequate Maintenance	6.6%	13.1%	11.3%	*
Sabotage, Malicious Mischief	2.6%	1.7%	0	
Loose Connections	2.1%	2.0%	6%	*
All others	6.9%	8.4%	24.2%	

As can be seen in Table 1.2, lightning surges, switching surges, deterioration of insulation and inadequate maintenance are the main reasons of transformer failures.

An international survey conducted by the CIGRE Working Group on failures in large power transformer in service shows the percentage of failures related to the structural components of the transformers, as given in Table 1.3.

Table 1.3
Failures for Large Power Transformers with On-load Tap Changers

Location	Percentage
On-load tap changers	41%
Windings	19%
Tank/Fluid	14%
Accessories	12%
Terminal	10%
Core	4%
Total	100%

Table 1.3 shows that on-load tap changers, windings, and tank/fluid are the main parts that cause failures in large power transformers.

Transmission Line Diagnostic

The following tabulates transformer failures by their components as given in Table 1.4.

Table 1.4
Transformer Component Failures

Transformer Component Failures	
High Voltage Windings*	48%
Low Voltage Windings*	23%
Bushings*	2%
Leads	6%
Tap Changers	0%
Gaskets	2%
Other	19%
Total	100%
* Components of Insulation System	

Table 1.4 clearly shows that components of insulation system contribute the most significant portion of transformer failures. In particular, the failure of the insulation protecting the windings contributes more than 71% of total failures.

A survey of records of modern power transformer breakdown that occurred over a period of years concludes that between 70 and 80% of the failures are finally traced back to short-circuits between winding turns.

Chemical reactions such as pyrolysis, oxidation and hydrolysis age the insulation material. The moisture content, presence of oxygen and temperature levels affects the speed of these chemical reactions.

The surveys presented here are typical of results obtained from other published surveys. From these results, one can see that failures of transformers are in a large part due to problems with its windings. Furthermore, winding faults occur when the insulation around the winding is compromised. In general, the insulation of the winding is compromised either by ageing or by mechanical forces acting upon it or both.

The failure of a transformer can be potentially devastating to the personnel safety and to the environment. Transformers may fail explosively causing great personal injuries to people around them and damage to the surrounding equipment. The environment can be adversely affected by the leakage of oil. A failure also has a large economic impact due to its high cost of replacement and repair and lost revenue while it is out of service. During its outage, the customers of a utility can be greatly inconvenienced, which could result in a loss of goodwill towards the utility, especially in a deregulated power market. Table 1.5 illustrates the economic impact of transformer failures. This table originally appeared in a working group report to the 29th Conference of the International Machinery Insurer's Association. The report is based on 75 cases of

Transmission Line Diagnostic

failures of large oil-cooled transformers rated at 100MVA and above from 1989 to 1996. As can be seen in the table, the average loss per case is in excess of US\$ 1.5 million.

Table 1.5

Numbers and Amounts of Losses due to Transformer Failure

Year	Number		Total MVA	Amount (US \$) millions	Average per case \$ millions	Average per case MVA
	(a)	(b)				
1989	5	3	1626	12.360	2.472	542
1990	8	6	2205	12.797	1.600	368
1991	14	10	2828	26.359	1.883	283
1994	13	11	4482	37.706	2.900	407
TOTAL S	75	59	22048	152.650	2.035	374

NOTE: (a) total number of cases for which loss amounts are known.

(b) total number of cases for which MVA capacity is known, in addition to loss amount

1.3 Causes of Winding Movement

A short circuit fault, for example, created by lightning strike or ground fault, is the most likely factor to cause the winding movement. Assuming a copper winding is wound on a ferromagnetic core and the transformer is in service, the currents carried by the windings will produce the predominant flux in the axial direction. The interaction of the current in the coils in the circumferential direction and the axial flux field will therefore produce a radial outward electro-magnetic force. There is, however, a leakage flux around individual turns and near the ends of the windings which has a component in the radial direction. This radial flux induces an axial inward electro-magnetic force. Under normal operation of power transformer, the windings are designed to withstand the mechanical pressure described above. However, when short circuits happen, the electro-magnetic forces induced in the windings are increased dramatically and threaten the insulation layers severely. For example, if a transformer's leakage impedance is 10%, its short circuit current will be 10 times the rated current and the mechanical stress will be roughly 100 times of the normal stress under the rated load current.

Short circuit force studies have special meanings for autotransformers. Autotransformers are normally used for coupling transmission systems where both input and output sides are at high voltage, such as 230/500KV or 500/765KV. They usually have very low impedance, about 5% to 8%. For a leakage impedance of 5% the

Transmission Line Diagnostic

mechanical stresses during a short circuit will be in the order of 400 times the normal. To withstand the high pressure from both high voltage level and large short circuit force, these autotransformers have to be designed and manufactured to be much stronger than in a normal two winding transformers.

For insulation and other manufacturing reasons, a transformer's high voltage winding is usually on the outside of the low voltage winding. Assume the two windings have the opposite ampere-turns. As above, the predominant flux is in axial direction and will induce radial force to both windings. This radial force will pull the outer winding (i.e. HV winding in this case) outward and inner winding inward the core. Meanwhile, the flux near the ends of the windings will induce suppressive force in axial direction as well. Furthermore, the axial suppressive force will cause a hoop stress on the outer winding and a compressive stress on the inner winding, which strengthens the outward force on the outer winding and inward force on the inner winding both caused by the axial flux.

In summary, when a short circuit happens, the winding will stretch out in the radial direction and compress in the axial direction. The radial forces in a 10MVA transformer can exceed 100,000lbs. Such huge electro-magnetic forces will inevitably loosen the winding clamp structure, which is the main mechanical support of the winding and cause the distortion or movement of the winding. A twisted transformer winding is shown in Figure 1.4.

Inrush currents, due to the powering up of the transformer circuit and vibration force increase the electro-magnetic forces in the same way as short circuits. The frequent fluctuation in generation or load will also put burdens to the electrical and mechanical strength of the windings, accelerate the loosening of the winding clamps, and eventually cause the winding to move or even break down.

The main reason of winding movement is the loosening of the clamps holding the windings. The clamps can be loosened by the vibration forces, external forces, like short-circuits forces discussed above, or by the compression and deterioration of the solid insulation.

In service, the inter-turn insulation, usually an oil impregnated insulating tape, undergoes changes. Over a period in service the taped insulation loses its elasticity. Moreover, under short-circuit forces the taped insulation may be permanently compressed or damaged. These mechanical changes in the taped winding insulation may significantly contribute to winding looseness. Overvoltages caused by system transients, mechanical deterioration due to the short circuits fault, vibration or inrush current, the rise of temperature inside the winding and oil, and the penetration of the moisture in the paper insulation will lead to the reduction of the dielectric strength of the cellulose paper. Winding movement may rupture the insulation paper and the rupture of the insulation can further deform the winding.

Transmission Line Diagnostic

Overheating caused by sustained heavy overloads or faulty cooling system, is another contributing factor to the winding movement. The temperature for the normal ageing of a power transformer is 98°C. Every rise or drop of 6°C either doubles or halves the electrical ageing. Exceeding the winding hot-spot temperature limit will accelerate the ageing process of the winding and therefore shorten the transformer's service life dramatically. In addition, temperatures higher than the design affect the clamping forces. One transformer fault detection study shows that clamping forces vary up to 10% with the temperature variations.

Structural defects due to poor quality control during manufacture may trigger winding failure in many ways. A winding bulge or sharp edge of the coil may cut through the insulation and cause short circuit between turns; deformed or disconnected leads, and bad connection may decrease the tightness of the winding and badly made joints may come apart and produce an open-circuit winding.

The huge impact of transformer failures on security of power systems motivates the development of monitoring systems and testing strategies. Since a large number of failures are due to the windings, an efficient on-line diagnostic technique for detecting winding movement is a necessity. The TLD method addresses this need.

1.4 Currently Available Winding Diagnostic Tools

An efficient on-line technique for monitoring transformer winding movement is of considerable interest due to the large number of aging transformers and the economic considerations under the deregulated electric power markets. Currently developed diagnostic techniques are discussed below.

Transformer winding movement detection can be done by an internal visual inspection. It requires draining the oil in the transformer, to perform a direct inspection of windings and clamps, and to observe any signs of looseness. Conventionally, such inspections are conducted on a time-based regular maintenance schedule; therefore, it may result in long-time transformer outage and consequent high costs. Sometimes, an increase of the audible noise can also indicate winding looseness. Recently, condition-based maintenance is becoming the new trend and will eventually replace the time-based maintenance.

Short-circuit impedance measurement is another technique to detect winding movement. One simply shorts the low voltage winding terminals and measures the input voltage, current and power. The result is then compared with the impedance before the transformer experienced a system short circuit. According to the IEC 60076-5, 2% deviation of the test results is the maximum value which can be accepted. The drawback of this technique is that it is an off-line diagnosis and usually done in a laboratory. In addition, it is only effective for a significant movement or distortion or looseness of the transformer windings.

Dissolved Gas Analysis (DGA) distinguishes the different types of insulation faults depending on the composition of gases liberated by solid insulation or oil

Transmission Line Diagnostic

breakdown. It can indirectly detect the winding displacement when this movement results in partial discharges. For example, when a partial discharge occurs, the most abundant gas among all the other dissolved gases is hydrogen. However, the method cannot locate where the displacement happened and how severe the displacement is. Also, in most cases the initial winding displacement does not result in partial discharges and may go undetected by DGA.

A winding ratio test measures the numbers of turns of both primary and secondary windings and calculates the ratio between them. By comparing the measured winding ratio with the ratio of rated primary and secondary voltages as shown on the nameplate of the transformer, shorted turns or open winding faults may be detected. However, an outage and isolation of the transformer is required for the purpose of measurements.

A winding resistance test is similar to the winding ratio test except that it measures the winding resistance rather than the number of winding turns. Additionally, a very precise ohmmeter is needed, which will assure the accuracy of a fraction of an ohm. The measured resistance will be compared with the previous measurement referred to the same temperature. Measurements are conducted for different phases and different tap-changer positions. This method detects the condition of the winding conductor directly. However, it requires a transformer outage and is usually performed in the factory or a laboratory.

A 60 Hz transformer impedance test is another off-site winding detection method. It measures the input voltage, input current and input power while shorting the low voltage winding of the transformer. The before and after results are then compared with the before and after short circuit. This test is insensitive to small winding movements.

Leakage reactance measurement (LRM) can be achieved with the same test set-up as the short circuit impedance measurement. LRM is based on the increased leakage reactance, resulting from the radial outward force on the outer winding and the radial inward force on the inner winding induced by short circuits. The main advantage of LRM method is that it is sensitive to winding distortion and insensitive to temperature or presence of contamination. However, it is not only an off-line and in-laboratory method, but also insufficient for frequencies more than 200 KHz, when compared with the FRA method, which will be discussed in the later part of this section. Furthermore, the deviation of measurement obtained from LRM is hardly found for some type of physical winding displacement for example, when the outward winding is simply bent inward to the core without any axial displacement, even when the distortion of the winding is severe.

Winding distortion can eventually develop into transformer failures, which can be catastrophic. Aging of the insulation has cumulative effects on transformer winding distortion. An effective on-line condition monitoring for transformer windings is required to provide instant detection of the winding integrity. Currently several on-line monitoring and diagnostic techniques are used for monitoring the windings

Transmission Line Diagnostic

Vibration test is an on-line monitoring technique. It monitors the vibration signals recorded on the tank wall by acoustic sensors and indicates the deviation or change of the internal winding position. Since the acoustic sensors are usually mounted on the tank wall, vibration testing doesn't require transformer outage. However, it is only effective for detecting large winding movement and can only be used as reference information. For an externally installed vibration sensor, it is even harder to distinguish whether the disturbance is caused by the winding distortion or by the surrounding environment.

Low voltage impulse (LVI) method is a well known technique for winding movement detection, which was proposed by W. Lech and L. Tyminsky in Poland in 1960 and first published in 1966. LVI technique was originally used off-line and later developed into on-line monitoring. It applies a few microsecond duration low voltage impulse to one winding and records the voltage or current response in the other winding or windings. Recorded response currents or voltages are compared during some time interval. However, the response waveform is heavily relying on the input waveform. It adds more difficulty to determine whether the changed response is due to the deviation of the input waveform or the displacement of the transformer winding.

With the acquisition of modern digital signal processing techniques, LVI method has been developed into a commonly used technique, called Frequency Response Analysis (FRA) technique. There are two types of FRA methods: FRA (I) and FRA (S). In FRA (I), LVI measurements are firstly taken and then converted into frequency domain by using Fourier transform, fast Fourier transform, short-time Fourier transform or wavelet transform. By dividing the response current by the input voltage, one can obtain the transfer function of the transformer, which is actually the transformer's transadmittance in frequency domain. Some researchers prefer transimpedance, i.e. the quotient between the input voltage and output current, and others prefer transadmittance. In both cases, the transfer function is freed from the input waveform, and it is a unique "signature" of the parameters of the internal windings. Winding movements result in the change of the RLC parameters of the winding, such as inter-turn capacitance, ground capacitance and series inductance. Hence, by comparing the changed "signature" with the "signature" obtained from the new transformer or from the previous measurements, one can detect the deformation of the winding. The drawback of this technique is that the maximum frequency that can be used is no more than 4 MHz and the results can be very sensitive to the test set-up and the arrangement of the physical test cables and leads. In addition, the experimental set up will have a big impact on the test results, for example, the cables layout, the leads connection and the choice of external circuit. The impedance of the external measuring circuit will vary with the frequency, so strictly speaking there is no way to avoid the deviation of the external impedance for FRA methods.

FRA technique can be applied to both off-line and on-line monitoring of transformer winding movement, for example, on-site measurements on a 200MVA 3-phase power transformer in service in Germany. Both monitoring systems consist of voltage sensors and current sensors which are mounted at the transformer, and a transient digital recorder with a resolution of 10 bits and a sampling frequency of 10MHz. Off-line

Transmission Line Diagnostic

transient monitoring is realized by switching operation of a SF₆ circuit breaker on the high-voltage side of the transformer while the low-voltage side is usually disconnected from the power network. On the other hand, on-line condition monitoring is realized by the dominant excitation transients that occur at only one phase. The transfer function (transadmittance) used here is the quotient between the spectra of the neutral current and the spectra of the terminal voltage. Both off-line and on-line monitoring measurements were taken during an 11-month period, and thus prove its feasibility.

Theoretically, the frequency response obtained from the above off-line and on-line measurements should not be identical to each other, but the resonance frequencies for both cases are the same up to 780 KHz. Therefore, a new resonance frequency can indicate the movement of the winding. However, this method requires a large amount of information about the dominant excitation modes accumulated over a long period of time and is only valid for up to 1MHz.

FRA (S) is also called SFRA, namely Swept Frequency Response Analysis. FRA (S) technique was first proposed by Dick and Erven in 1978. In this method, a signal from a network analyzer is applied and the swept frequency signal is generated by injecting a sinusoidal signal at a frequency, one at a time. SFRA technique maintains the constant energy level for each frequency. The analyzer used in SFRA provides better resolution due to the ability of autoscale. Compared with FRA (I) method, SFRA has better signal to noise ratio and wider frequency range. However it needs longer measurement time and is usually very expensive.

FRA techniques are still the most effective method used for winding movement detection. From the above discussion, we can see that currently used monitoring techniques are inadequate, especially for high frequencies. Therefore, a new high frequency transformer model and data conditioning technique are needed for the use of SFRA in on-line condition monitoring of transformer winding movement.

CHAPTER 2 Transformer Models

2.1 Modeling Background

Since the invention of power transformer in 1885, people have developed different transformer models for different purposes. Transformer models specifically used for the winding movement detection are discussed here.

A model based on multi-conductor transmission line theory uses a single turn as a circuit element, with the capacitance, inductance, and losses calculated as distributed parameters, are built up to simulate transformer windings. In the above model, transfer functions (i.e. frequency response) that describe how the location of a fault, such as a PD source, affects the current signals measured at the terminals of the winding, were calculated. The model shows how the position of the zeros in the frequency response of the measured current signals can be used to locate the winding distortion. However, it needs $(n+1)*(n+1)$ Y matrix for n conductors or layers or pancakes, which is a huge amount of calculation for a normal power transformer.

Transmission Line Diagnostic

Another model based on FRA is developed into condition monitoring technique for transformers in service. In this model, the applied voltage is measured on the high voltage winding using the HV bushing as a voltage divider. A custom designed "secondary" is installed on the capacitance tap to obtain a suitable signal, while the current is recorded on the other winding. By Fourier transformer, the transadmittance obtained gives the characteristic of the on-line transformer windings, but the usable frequency is about 0.8 MHz in the field and up to 3 MHz in a laboratory.

By evaluating the leakage factors in a transformer winding, a model for internal winding faults study is presented. The leakage factor between coil 1 and coil 2 is defined as $s_{12} = 1 - M_{12}^2 / (L_1 L_2)$ in the above papers, where L_1 and L_2 are the self inductance, and M_{12} is the mutual inductance. BCTRAN is used in the method. It is an auxiliary routine of EMTP and is used to produce an input file readable by EMTP. A matrix of inductance and a matrix of resistance of the transformer winding must be computed by BCTRAN first, which indicates that a full knowledge of the transformer winding has to be available. BCTRAN is an auxiliary routine of EMTP and is used to produce an input file readable by EMTP. Based on the above R and L matrices, a new set of R and L matrices must be developed to allow the simulation of any kind of internal winding fault, for example faults between any winding turns or faults between any winding turn and the earth.

This model is completely compatible with EMTP, but it adds lots of complication due to the computation of the new R, L matrices and the evaluation of leakage factor. The determination of the leakage factor largely depends on the methods chosen and the assumptions made. Based on the geometry information of the transformer and experimental results, a correcting factor is usually added to increase the calculation accuracy of the leakage factor. Different researchers may choose different correcting factors. Furthermore, the detailed transformer winding data is not usually obtained from the manufacturer, which is the fundamental data base needed in this model.

A newly developed model HIFRA, high-frequency internal frequency response analysis, uses an injected wide-band frequency signal through the transformer bushing, in combination with an internal FRA measurement. This model measures the signals inside the transformer tank by using appropriate non-contact sensors inside the transformer on the transformer winding leads, and therefore, the transfer function would then be calculated from the signals measured inside. This method increases the useful frequency range up to 10MHz.

Wavelet analysis and neural network are applied to the winding detection by the researchers in Texas A & M University. Based on the normal and faulty primary signals obtained from EMTP, this method uses wavelet transform as a processor to the four neural networks (two BP neural networks and two Elman networks) to identify the internal turn-to-turn faults in transformer winding. This method is not suitable for high-frequencies because the transformer model used in EMTP has lumped parameters. It also needs a big data base as the baseline.

Transmission Line Diagnostic

An analysis of internal winding stresses in EHV generator step-up transformer was performed at Ontario Hydro. In this analysis, a high accuracy frequency dependent transformer model is used to monitor the terminal condition of a transformer under transient conditions. An internal voltage distribution map is created by the measured transfer functions among terminals and various points of the winding, and is used to evaluate the insulation stress and therefore detect the winding displacement. This high frequency transformer model takes full account of frequency dependent parameter effects, thus it is only suitable for the transformer under study and the standard name plate data from other transformers give no information to the model.

Transformer winding turn-to-turn or turn-to-earth fault is modeled by coupled electromagnetic and structural finite elements. This model is based on the physical information of the specific transformer and the simulation is implemented by commercial software. A large amount of previous experiment data are available to compare with the present measurements and simulation results. However, in reality it is very hard to get the physical layout of a transformer; therefore detailed parameters are not available. Similar to the model in the previous paragraph, it doesn't have practical applications to a large number of transformers in service with different physical structure and electrical capacities.

Due to the disadvantage of the above transformer models, a new transformer model for winding movement diagnosis has to be established. FRA technique is the most used and effective detection method in winding displacement so far. With the increase of the frequency, the capacitance in the transformer becomes more important than the inductance. In FRA, it represents the higher resonances. As the fingerprint or signature of the transformer winding, admittance or transadmittance has more sensitivity for high frequency than impedance or transimpedance. In my trial and error of developing an effective transformer model, the value of transadmittance in frequency domain is considered as the fingerprint of the transformer under study, which is the quotient between the output current spectrum and input voltage spectrum of the transformer in this chapter.

2.2 Physical Transformer Model Simulated as a Transmission Line

A 167KVA single phase distribution transformer as shown in figure 2.1 is used in the model simulation for this chapter. The transformer's voltage rating is 14400V/347V, and the impedance is 2%. The high voltage and low voltage winding BILs are 125 kV and 30kV respectively. The weight of the transformer is 648 kg. The transformer looks like a cylinder, in which the two windings are wrapped on an iron core. The low voltage winding is split into the inner section and outer section with the high voltage winding in between. The closest winding to the core is the inner low voltage winding, then high voltage winding. The outer LV winding is closest to the tank.

The high voltage winding is made of copper coil with a 4 mm diameter cross section. The radius between the high voltage coil and the central point of the iron core is about 13.24 cm. Unlike the high voltage winding, the low voltage winding is made of aluminum sheet

Transmission Line Diagnostic

with thickness of 1.5 mm. For each section of the low voltage sheet, it has 16 turns. The distance between sheets is 0.5 mm. The radius of the most inner layer is 10.16 cm; the distance from the most outer layer of low voltage sheet to tank is 8.89 cm; the diameter of the tank is 50.8 cm. The height of the windings is 40.64 cm.

From the above detailed physical layout of the transformer, the electrical parameters RLC can be calculated and therefore a physical transformer model circuit is set up as shown in Figure 2.2. All resistance values are in ohm; the inductance values are in mili-henry; the capacitance values are in pico-farad.

From the perspective of electromagnetics, the transformer winding conductors are like transmission line conductors except that they are thinner and shorter. However, the same length of the transmission line or transformer winding "looks" longer for high frequency signal than low frequency signal. In this respect, the transformer winding can behave in a similar way when a megahertz range signal is applied as an overhead transmission line applied with kilohertz range frequencies.

A real transmission line has distributed parameters. In every single tiny section or fraction of the line, it includes a series resistance, a series inductance and two shunt capacitances. These R, L and C are uniformly distributed along the line. However, the physical transformer model of Figure 2.2 is lumped parameter characteristics. In order to simulate the distribution characteristics of the transmission line, the lumped parameter transformer model has to be evenly split into sections. The more the number of the sections, the more distributed the transformer winding model is. Theoretically, an increase in the number of sections creates more LC loops, which can lead to more resonance frequencies.

Whenever the winding has some movement, its physical layout will be distorted and lead to the variation of the RLC parameters in the model. Correspondingly, the resonances will change either in magnitude or shift in frequency. Consequently, the waveform of the frequency response may distort as well. By comparing the resonances and the general shape of the waveform from time to time, one should be able to detect whether there is noticeable change in the winding geometry in some time period.

Based on the physical transformer model in Figure 2.2, the simulations have been done in Microtran with the evenly divided sections of the circuit. An impulse voltage source V1 with 2.5 ns rising time is injected into the high voltage terminal 11'; while a 13.37 ohms load resistor is connected to the low voltage terminal 22'. The total simulation time is 80 μ s. Output current I2 and input signal V1 are transferred into Matlab script to obtain the frequency response of the transformer, i.e. transadmittance spectrum. The Matlab script is as follows.

```
%matlab script for physical transformer model in chapter 2
```

```
load orig1.txt; % load simulation results from Microtran
```

Transmission Line Diagnostic

```
%plot input voltage and output current in time domain
close all;
figure
subplot(3,1,1),plot(orig1(:,2)/1e-6,orig1(:,3));
ylabel('Input voltage in V');grid;
axis([19.8 20.2 50 350]);xlabel('time in us')

subplot(3,1,2),plot(orig1(:,2)/1e-6,orig1(:,5));grid;
ylabel('Output current in A');axis([19 21 -0.002 0.01]);
xlabel('time in us');

%plot I(f)/V(f) in frequency domain by FFT
dt=2.5e-9;%time step
t=orig1(:,2);%32001 time step
v=fft(orig1(:,3));
i=fft(orig1(:,5));
N=length(t);%801 odd number
%n=N%when N is even number
n=length(i)-1;%change odd number to even number
nyquist=1/2/dt;
freq=(1:n/2)/(n/2)*nyquist;
freq=freq-freq(1);%frequency from zero to near nyquist frequency
imag=abs(i(1:n/2));
vmag=abs(v(1:n/2));
b=imag./vmag;%transadmittance
subplot(3,1,3),plot(freq/1e6,b),grid;
xlabel('Frequency in MHz');ylabel('I(f)/V(f)');
axis([0 20 -0.5e-4 3e-4]);
```

More resonances are expected with the increase in the number of the sections. Simulations have been performed from one section to eight sections in Microtran and Matlab. However, the results are almost the same and only have two dominant resonance frequencies as shown in Figure 2.3.

The reason of only one resonance frequency is explained as follows. When the transmission line is so long that an equivalent π circuit is required instead of the nominal π circuit, the hyperbolic correcting functions must be applied to the line's parameters. The boundary length L_b for overhead line and cable are calculated as the function of frequency applied as shown in formula (1) and (2). In other word, L_b is the maximum length of each section in our model.

$$L_b = \frac{10,000}{f} \quad \text{for overhead line} \quad (1)$$

$$L_b = \frac{3,000}{f} \quad \text{for cable} \quad (2)$$

Transmission Line Diagnostic

For a transmission line with power frequency, L_b is 170 km; while for a cable with power frequency, L_b is about 50 km. The transformer winding is something in between the overhead line and cable, so if we combine formula (1) and (2) into formula (3) and the maximum frequency we are interested is around 20MHz, then L_b will be 0.25 meters. By the size of the transformer winding, we can calculate the total length of the winding, which is around 200 meters. By dividing the total length with L_b , we can get the minimum number of sections needed for this model, which is 800 sections in our case. Such a huge number of sections makes the transformer parameters as distributed as a real transmission line, but more critically, it limits the effectiveness of this physical model. For high capacity power transformers with much longer windings, the calculations in this model are too huge to be realistic.

$$L_b = \frac{5,000}{f} \quad \text{for transformer winding} \quad (3)$$

Another big disadvantage of this physical transformer model is that usually the detailed design parameters of transformers are not available.

2.3 Decoupled High Frequency Transformer Model

A simplified high frequency transformer model is used in Microtran to simulate the winding performance. By using the RLC conversion formulae in the paper, the coupled-coils constant parameter transformer model in Figure 2.2 can be decoupled firstly as shown in Figure 2.4.

Due to the two sections of the low voltage winding, the above figure is still coupled. By simply dropping the parallel branch with 8.48 pF capacitance and the shunt branch with -8952 pF capacitance, we can apply the conversion formulae again and get the totally decoupled high frequency transformer as shown in Figure 2.5.

To further improve the obtained circuit, an imaginary neutral plate is added to it and all the RLC parameters are equally split into two parts. The modification makes the circuit symmetrical, which is usually the case in a real power transformer. The obtained symmetrical circuit is shown in Figure 2.6.

Simulating the symmetrical circuit in Microtran and doing Fourier analysis in Matlab gives the results as shown in Figure 2.7. Only one resonance is found. The main disadvantage of this model lies in the still lumped parameters in Microtran transformer data card. Also, with the increase of frequency, the capacitance and skin effect will have big effects in the performance of the circuit. The parameters used here are not frequency dependent parameters.

The dropping of one parallel capacitance branch and one shunt capacitance done in the second decoupling conversion is another big factor that invalidates this high frequency model. For different values of high frequencies, these two branches sometimes act like an open circuit, sometimes act like a short circuit, or the situation in between.

Transmission Line Diagnostic

Therefore, above elimination of branches is only a very rough approximation and results in more inaccuracies.

2.4 Equivalent π Model by Nodal Analysis

Any transformer can be described as a two-port system as shown in Figure 2.8. From the line hyperbolic equations, i.e. formula (4) and (5), an equivalent π circuit can be derived to represent the entire line length, which takes the frequency dependence of the parameters into account. Instead of injecting any signal into the circuit, the equivalent admittance of the whole circuit by nodal analysis is evaluated as the transfer function for this model.

$$Z1 = (Z'l) \frac{\sinh(\gamma l)}{(rl)} = R1(\omega) + j\omega L1(\omega) \quad (4)$$

$$Y2 = (Y'l) \frac{\tanh(\gamma l/2)}{(rl/2)} = G2(\omega) + j\omega C2(\omega) \quad (5)$$

Where,

Z' : impedance per meter

Y' : admittance per meter

l : total length of the line or winding

$\gamma = \gamma l = l\sqrt{Z' \cdot Y'}$ propagation constant of the line

This equivalent π model can not be used directly in time-domain simulations because the circuit parameters are functions of frequency. It is only useful for one-frequency at a time steady state solutions, so it is simulated in Matlab. The script is as following. The simulation result is shown in Figure 2.9.

```
%matlab script for the equivalent pi model by using hyperbolic correction
%for the whole transformer, using pi circuit for both windings
%using inverse fft to get h(t) in time domain
f=[1e3:1e2:10e6];
w=2*pi.*f;
Sb=167000;
Vb1=14400;
Vb2=347;
Zb1=Vb1*Vb1/Sb;
Zb2=Vb2*Vb2/Sb;
```

Transmission Line Diagnostic

```

c12=352e-12;
z12=1./(j.*w.*c12)./Zb1;
c13=418e-12;
z13=1./(j.*w.*c13)./Zb1;
c30=50.9e-12;
z30=1./(j.*w.*c30)./Zb2;
%a=0.7*3e8;
%Yphase0=-len/a.*w/pi;
%tao=len/a;%8.37e-7;

%for high voltage winding
C1=0.014e-12;
L1=3e-4;
len1=175.83;
z1=(j.*w.*L1).*len1.*sinh(j.*w.*len1.*sqrt(L1*C1))./(j.*w.*len1.*sqrt(L1*C1))./Zb1;
y21=j.*w.*C1.*len1.*tanh(j.*w.*len1.*sqrt(L1*C1)/2)./(j.*w.*len1.*sqrt(L1*C1)/2);
z21=2./y21./Zb1;

%for inner section of low voltage winding
C2=398e-12;
L2=2.85e-4;
len2=13.33;
z2=(j.*w.*L2).*len2.*sinh(j.*w.*len2.*sqrt(L2*C2))./(j.*w.*len2.*sqrt(L2*C2))./Zb2;
y22=j.*w.*C2.*len2.*tanh(j.*w.*len2.*sqrt(L2*C2)/2)./(j.*w.*len2.*sqrt(L2*C2)/2);
z22=2./y22./Zb2;

%for outer section of low voltage winding
C3=452e-12;
L3=2.54e-4;
len3=14.94;
z3=(j.*w.*L3).*len3.*sinh(j.*w.*len3.*sqrt(L3*C3))./(j.*w.*len3.*sqrt(L3*C3))./Zb2;
y23=j.*w.*C3.*len3.*tanh(j.*w.*len3.*sqrt(L3*C3)/2)./(j.*w.*len3.*sqrt(L3*C3)/2);
z23=2./y23./Zb2;

%calculate equivalent circuit
%step 1
z4=z21.*z22./(z21+z22);
z5=z23.*z22./(z23+z22);
z6=z23.*z30./(z23+z30);
%step 2: y to delta
za=(z1.*z2+z1.*z4+z2.*z4)./z4;
zb=(z1.*z2+z1.*z4+z2.*z4)./z2;
zc=(z1.*z2+z1.*z4+z2.*z4)./z1;
%step 3
zf=z12.*za./(z12+za);
zd=z21.*zb./(z21+zb);

```

Transmission Line Diagnostic

```

ze=z5.*zc./(z5+zc);
%step 4: y to delta
zg=(zf.*z3+zf.*ze+z3.*ze)./ze;
zh=(zf.*z3+zf.*ze+z3.*ze)./z3;
zi=(zf.*z3+zf.*ze+z3.*ze)./zf;
%step 5
zk=zd.*zh./(zd+zh);
zm=zi.*z6./(zi+z6);
zn=zi+zm;
ye=abs((zk+zn)./(zk.*zn))./Zb1;
y=fft(ye);
plot(f/1e6,y);xlabel('Frequency in MHz');ylabel('Admittance');
title('Applying Correction Factor to Pi Model for the Transformer');grid;

```

The result gives many resonance frequencies, but the parameters used here are still lumped parameters. Non frequency-dependent parameters decide that the result obtained by this model is still unreliable.

From the above three models, we find that different disadvantages limit the development of an effective transformer model for winding movement detection. For a lumped circuit, the approach is inadequate since the approximation is too great. A distinguishing feature of the circuit with distributed constants is its ability to support travelling waves of current and voltage. This leads us to explore the transformer modeling based on the travelling wave theory of a transmission system in the next chapter.

CHAPTER 3 Transformer as a Transmission Line

The travelling wave theory for transmission systems has been extensively studied since 1930. In short, any disturbance, no matter whether it is electrical, magnetic, mechanical or audio, will cause a wave to propagate in the surrounding medium. On power transmission systems, for example, on a transmission line, any electromagnetic disturbance caused by switching operations, faults or lightning strikes will result in the initiation of travelling electromagnetic waves. These waves propagate along the transmission system until they reach a discontinuity, such as the end of the line, where they may be reflected and/or refracted and modified. The waves may also be attenuated and distorted by corona and other losses until they are completely dissipated and die out. The velocity of electromagnetic waves v_0 in free space is constant. By formula (1), regardless of the line geometry or conductor material, the electromagnetic wave always travels at the speed of light, i.e. 300km/ms. Approximately, it takes a wave 3.3 ms to travel 1000 km in free space.

$$v_0 = \frac{1}{\sqrt{\mu_0 \epsilon_0}} \quad (1)$$

Transmission Line Diagnostic

μ_0 : permeability of free space, $4\pi \cdot 10^{-7}$ H/m;
 ϵ_0 : permittivity of free space, $8.854 \cdot 10^{-12}$ F/m.

Another important term in travelling wave theory is the characteristic impedance Z_c , also called surge impedance, which is the amplitude ratio between the voltage wave and the current wave. Z_c represents the impedance which travelling waves encounter in the front along the line, so Z_c is constant for the entire length of a uniformly distributed line. Unlike the velocity of travelling waves, Z_c heavily depends on the geometry of the transmission systems. For example, for a single conductor above an ideal ground, Z_c is about 500 Ω ; while for two parallel conductors, Z_c is about 200 to 300 Ω . Any change in Z_c represents a discontinuity in the line, which may indicate an unusual condition of the line, for example, a short circuit fault.

Travelling wave theory has been applied for accurate location of faults on power transmission systems. Technology is available to determine fault location within a transmission span of 300 meters on 500 kV transmission lines. Any fault on the transmission line represents a discontinuity in the wave propagation along the line, which is caused by the change of the surge impedance. Each wave can be decomposed into different frequencies depends on the type of faults. These waves travel and reflect towards the two ends of the line at the velocity of light if one assumes the wave propagation in the air has no dielectric loss. In practice, the travelling speed along the transmission line in the air is a little bit less than the speed of light. By observing the travelling time from one discontinuity to another or end of the line, one can calculate the fault distance by the product of the velocity of light and the travelling time. In this way, a fault can be accurately located.

In practice, transformer winding is like a transmission line when the wave frequency is very high. According to the well known formula (2), for the power frequency 60 Hz, the wavelength along the transmission line is 5000 km; while for a higher frequency of 2 MHz, the wavelength along the transformer winding is only 150 m. In other word, high frequency waves make the transformer winding long enough to behave like a transmission line for wave propagation. In addition, measurements on many actual transformers have revealed that the internal capacitance between turns or coils are so small that the electromagnetic waves travel on conductors wound into coils of negligible internal capacitance, that is, ignoring the dielectric permittivity, with the same speed as on a straight line conductor. Like fault location technique in transmission line, wave propagation theory can be put into the use of transformer winding movement diagnosis, which is named the Transmission Line Diagnostics (TLD) method by Dr. Jose Marti.

$$\lambda = f \cdot \lambda \quad (2)$$

f : frequency
 λ : wavelength of that frequency

3.1 The Wave Propagation High-frequency Transformer Model

By taking advantage of the wave propagation property and frequency-dependent transmission line model, one can simulate the real transformer winding as a high frequency distributed transmission line, obtain the characteristic impedance and propagation constant of the winding, calculate the travelling time for certain frequency for the total equivalent length of the winding. By comparing the change of the characteristic impedance Z_c we can detect whether there is winding distortion or movement. The fault location results in an equivalent sublength, which can be compared with the total equivalent length and further used to determine where the winding movement or distortion has occurred.

This section is split into three subsections. A frequency-dependant model for a transmission line is presented in the first subsection. The model for a non-faulted winding is derived in the second subsection. The last subsection details the modification to the model for the case when a fault occurs in the winding.

3.1.1 Frequency-dependant Line Model

This subsection shows the derivation of a frequency-dependant line model for a transmission line. This model was originally presented by Dr. J. R. Marti in 1982.

Given a transmission line as shown in Figure 3.1, the following wave equations can be obtained:

$$V_x = V_{fk} e^{-\gamma x} + V_{bk} e^{+\gamma x} \quad (3)$$

$$I_x = \frac{1}{Z_c} V_{fk} e^{-\gamma x} - \frac{1}{Z_c} V_{bk} e^{+\gamma x} \quad (4)$$

where:

$$V_f = Z_c I_f \quad (5)$$

$$V_b = -Z_c I_b \quad (6)$$

$$Z_c = \sqrt{\frac{Z'}{Y'}} \text{ is the characteristic impedance of the line} \quad (7)$$

$$\gamma = \sqrt{Z' \cdot Y'} \text{ is per unit length propagation constant of the line} \quad (8)$$

Z' is the per unit length impedance of the line

Y' is the per unit length admittance of the line

By combining equations (3) and (4), a forward perturbation function can be found as given in equation (9) under the condition $V_k + Z_c I_k = 2V_{fk}$ at $x=0$.

$$V_x + Z_c I_x = (V_k + Z_c I_k) e^{-\gamma x} \quad (9)$$

Transmission Line Diagnostic

Therefore, at node m , equation (9) becomes:

$$V_m - Z_c I'_m = (V_k + Z_c I_k) e^{-\gamma l} \quad (10)$$

where:

$$I'_m = -I_m \quad (11)$$

l is the length of the transmission line

An equivalent circuit as shown in Figure 3.2 follows from equations (10) and (11).

E_{kh} and E_{mh} are history functions and are defined as:

$$E_{mh} = (V_k + Z_c I_k) e^{-\gamma l} \quad (12)$$

$$E_{kh} = (V_m - Z_c I_m) e^{-\gamma l} \quad (13)$$

From Figure 3.2 and the above equations, we can find that a complicated distributed frequency-dependent transmission line is simply modeled as two separate lumped circuits. Each circuit includes the characteristic impedance of the transmission line, the wave propagation constant, and a history function. For a given transmission line, its characteristic impedance and propagation constant are fixed, since they are determined by the geometry and composition of the transmission line. Typical Z_c of a transmission line is a smooth almost exponential curve, which decreases with frequency.

3.1.2 Non-faulted Winding Model

The windings of the transformer behave as transmission lines if the frequency of the exciting voltage is sufficiently high. An individual winding is modeled by a black box which has a specific structure. The frequency-dependent model that was presented in the previous subsection is used for the structure of the black box. This subsection details the derivation of the parameters of the black box given that the input voltage, input current, and output current are known or measured. The unknown parameters of the model are the characteristic impedance and propagation constant of the equivalent line model. This model is for a normal, non-faulted winding.

The winding under investigation is physically connected as shown in Figure 3.3.

The transmission line model for the winding as connected in Figure 3.3 is shown in Figure 3.4.

Applying Kirchhoff's voltage law around the voltage loop of the right-hand side circuit of Figure 3.4 gives:

Transmission Line Diagnostic

$$E_{mh} = (Z_c + R) I_m \quad (14)$$

Where:

$\bar{I}_m = I_m \angle \theta_m$ is the measured output current

Substituting the definition of E_{mh} from Equation (12) yields:

$$V_k e^{-\gamma} + Z_c I_k e^{-\gamma} = Z_c I_m + R I_m \quad (15)$$

Where:

$\bar{V}_k = E_k \angle 0^\circ$ is the measured input voltage

$\bar{I}_k = I_k \angle \theta$ is the measured input current

Equation (15) contains two complex unknowns, thus another equation must be obtained. The second equation comes from applying Kirchhoff's voltage law around the voltage loop of the left-hand side circuit as given by Equation (16):

$$V_k = E_{kh} + Z_c I_k \quad (16)$$

Using the definition of E_{kh} from equation (13) and noting the direction of I_m yields:

$$V_k - Z_c I_k = R I_m e^{-\gamma} - Z_c I_m e^{-\gamma} \quad (17)$$

Equations (15) and (17) can now be solved numerically to obtain the values for the characteristic impedance Z_c and propagation constant γ . Note that the propagation constant γ obtained by this method is the actual value not the per-unit length value, i.e. $\gamma = \gamma' * l$. While from formula (18), we can get τ , which is the travelling time of wave propagation corresponding to certain ω . Formula (19) enables us to find the equivalent length of the winding, i.e. l_e , which is in between the physical length of the winding and the height of the winding. v_0 is the velocity of wave propagation, which is $3e^8$ m/s in air.

$$\omega * \tau = \text{imaginary_part}(\gamma) \quad (18)$$

$$l_e = v_0 * \tau \quad (19)$$

From the above, we can see that by taking measurements of currents and voltages on the two ends of the winding, we obtain the Z_c and γ , which are the fingerprints of the winding without knowing the internal detailed physical parameters of the transformer. Z_c and γ are further used in the next section to detect the winding displacement.

3.1.3 Faulted Winding Model

Transmission Line Diagnostic

The model shown in the previous subsection is modified to account for a fault at impedance Z_x , an unknown location in the winding. The winding is split into two sections with effective lengths of l_1 and l_2 . The modified model is shown in Figure 3.5.

As with the non-faulted winding, the input voltage, input current, and output currents are known. The two sections on either side of the fault have, in general, different propagation constants; γ_1 for the leftmost section and $\gamma_2 = \gamma - \gamma_1$ for the rightmost section. Kirchhoff's voltage law is applied to all of the loops, as was done with the simpler non-faulted winding. Four equations result from the four loops in the model. Since there are only four unknowns, namely, V_f , I_f , Z_x , and γ_1 , the model has a unique solution. The four equations are given by:

$$V_k - Z_c I_k = (V_f - Z_c I_f) e^{-\gamma_1} \quad (20)$$

$$(V_k + Z_c I_k) e^{-\gamma_1} = V_f + Z_c I_f \quad (21)$$

$$(I_m R - I_m Z_c) e^{-(\gamma + \gamma_1)} - \frac{V_f Z_c}{Z_x} = V_f - Z_c I_f \quad (22)$$

$$(V_f + Z_c I_f - \frac{Z_c V_f}{Z_x}) e^{-(\gamma + \gamma_1)} = I_m R + Z_c I_m \quad (23)$$

Equations (20) – (23) can be solved numerically to obtain the value of γ_1 by the Matlab program. Above formulae are defined as function F1 to F4 respectively in the Matlab. The Matlab script is shown as following:

```
% Matlab script for solving the nonlinear equations
% Define the nonlinear equations
F1 = V_k - Z_c I_k - (V_f - Z_c I_f) e^{-\gamma_1}
F2 = (V_k + Z_c I_k) e^{-\gamma_1} - V_f + Z_c I_f
F3 = (I_m R - I_m Z_c) e^{-(\gamma + \gamma_1)} - \frac{V_f Z_c}{Z_x} - V_f - Z_c I_f
F4 = (V_f + Z_c I_f - \frac{Z_c V_f}{Z_x}) e^{-(\gamma + \gamma_1)} - I_m R + Z_c I_m
F = [F1; F2; F3; F4];
% Set initial values
x0 = [0; 0; 0; 0];
options = optimset('Display','iter');
% Solve
[x,fval] = fsolve(F,x0,options)
```

Transmission Line Diagnostic

Since the per-unit length propagation constant is assumed not to change as the result of a fault, the location of the fault is simply given by:

$$l_{e1} = l_e \cdot \frac{\gamma_1}{\gamma} \quad (24)$$

The fault impedance, Z_x , is also determined by the solution of Equations (20) – (23) by Matlab. The determination of the fault impedance Z_x can give insight into what type of fault occurred, for example, if Z_x is very small, it implies a short circuit happens inside the transformer.

Note: For the convenience of notation, in the following sections, V_{in} , I_{in} , V_{out} and I_{out} will replace the V_k , I_k , V_m , I_m of above formulae respectively.

3.2 Laboratory Experiments and Simulation Results

Experimental works have been performed in the university High Voltage Lab and the utility research lab (Powertech Labs. Inc).

3.2.1 Initial Experiments Performed in the University Labs

The excitation of input signal can be created by two means in the laboratory: a function generator or a network analyzer. A good network analyzer can produce discrete frequencies one at a time with a high resolution, record all the input and output signals in the time and frequency domain, calculate the transfer function both in magnitude and phase angle. However, the equipment is very expensive. An alternative way is to use a simple function generation, which either injects a sinusoidal signal, at a given frequency, to the tested transformer or produces a low voltage impulse signal for the test. In our experiment, a sinusoidal signal was adopted as the input voltage source. The WAVETEK function generator used has a maximum frequency of 2MHz with the 50 kHz frequency resolution. The oscilloscope is Tektronix TDS 220 with 2 channels. The experimental circuit is set up as figure 3.6.

In the above figure, the input resistor R_{in} is 20 Ω with 0.5% precision. The output resistor is made of one 20 Ω and one 30 Ω resistors both with 0.5% precision. A function generator injects low voltage sinusoidal wave into the circuit at every 100 kHz from 500 kHz to 2 MHz.

The first set of transformers for test is four 16.7kVA 240V/280V variacs in series. The negative terminals have been shorted together. The connecting cables between them are made as short as possible, since the cable itself can act like a transmission line. Because of the small gauge of the windings of these Variacs and antenna effect, only a very small amount of current is drawn. Stray capacitance is everywhere, which causes big loss. For an open circuit test, the output voltage is only a few tens of mV when the input voltage is a few tens of volts. Therefore the measurements are not acceptable.

Transmission Line Diagnostic

The second transformer tested is a 3-phase 60 cycle 10kVA transformer as shown in Figure 3.7. The voltage rating is 220/220V and total weight is 275 pounds. In order to have a solid ground, the core and the chassis are shorted together. Initially, the experiments are performed in an undergraduate lab. However, antenna effect and bad grounding conditions have a huge influence on the measurement, which leads to a low signal-to-noise ratio. In order to improve the accuracy of the experiments, the transformer has been moved into a special high voltage lab, where good shielding and good grounding are obtained. Both the wall and the floor of the high voltage lab are made of aluminum, which provide evenly distributed stray capacitance and hence make it more like the enclosed coils inside a tank environment. To avoid electromagnetic interference (EMI), both the function generator and the oscilloscope are shielded by an aluminum case.

From Figure 3.7, we can see the transformer is a dry type transformer without a tank. In order to simulate the physical transformer which is usually inside a metal case, we wound an aluminum foil to the top of the winding. We also use the insulation sticker and paper ball to separate the aluminum cylinder from the winding with different separations. The change of the separation between the winding and the aluminum tank will vary the inductance of the winding and the capacitance in between, and therefore vary the values of Z_c for different frequencies.

Ideally, according to formula (25) and (26) below, we can see that the changes in the winding distances (i.e. the separation b and d) vary both the capacitance and the inductance. The increase of the separation reduces the capacitance between the winding and the ground and raises the self-inductance of the winding. Formula (27) further defines that Z_c is directly proportional to $\frac{b}{1+b/d}$. When b is much less than d , which is usually the case for real transformers, the denominator of the fraction equals 1, hence the Z_c is directly proportional to b . We can conclude here that the internal insulation distance plays a key role in the value of Z_c . When b is in the same order as d , both of them determine the value of Z_c .

$$C = \frac{\epsilon \omega h}{4\pi v_0} \frac{b+d}{bd} \cdot 10^9 \quad \text{F} \quad (25)$$

$$L = 4\pi\mu \frac{\omega}{h} N^2 \frac{bd}{b+d} \cdot 10^{-9} \quad \text{H} \quad (26)$$

$$Z_c = 120\pi \sqrt{\frac{\mu}{\epsilon}} \frac{N}{h} \frac{b}{1+b/d} \quad \Omega \quad (27)$$

Where,

μ : magnetic permeability of the material

ϵ : dielectric constant of the insulation material

N : total number of the turns of the winding

h : axial length of the winding

b : internal insulating distance, i.e. distance between the inner winding and the core

d : external insulating distance, i.e. distance between the outer winding and the tank

v_0 : velocity of light in a vacuum, 300m/us.

Transmission Line Diagnostic

The relationship that Z_c is directly proportional to the inner separation can be proved in another way. Taking a simple case, for two parallel plates, the capacitance is inversely proportional to the separation between the plates by the well-known relationship/formula (28).

$$C = k_1 A / D \quad (28)$$

Where;

k_1 : constant

A: area of the plate

D: the distance between two plates

By extending the formula (7), we get $Z_c = \sqrt{\frac{Z'}{Y'}} = \sqrt{\frac{R + j\omega L}{G + j\omega C}}$, with the

increasing of frequency, R and G are negligible, therefore we get the formula (29). In formula (30), v_0 is a constant, i.e. the speed of light. Combining these two formulae, we can get the direct relationship between Z_c and C (31).

$$Z_c = \sqrt{\frac{L}{C}} \quad (29)$$

$$v_0 = \sqrt{\frac{1}{LC}} \quad (30)$$

$$Z_c = \frac{1/v_0}{C} = \frac{k_2}{C} \quad (31)$$

Comparing formulae (28) and (30), we get

$$Z_c = \frac{k_2}{k_1 A} D = k \circ D \quad (32)$$

From the above we can find that formula (32) is consistent with formula (27), which leads us to focus more on the variation of the separation between the winding and the core of a transformer. It also gives us some general idea that Z_c increases with the increase of the separation; it can be either the separation between the winding and the core, or the separation between the winding and the tank.

However, in the above ideal situation, Z_c is linear to the separation and independent of frequency, which is usually not the case for practical transformers. More often, transformers are made of concentric core and tank, which provide nonlinear capacitances and Z_c as well. For example, the capacitance is the logarithm of the separation of two concentric cylinders; also, the dielectric constant becomes frequency dependent. Therefore, separation between the winding and the core, separation between the winding and the tank, and frequency are the main factors to be varied in our technique.

By measuring the input voltage, input current and output voltage, we simulate the winding performance of the unity transformer in Matlab based on the formulae described in section 3.1. The Matlab script is as following:

Transmission Line Diagnostic

```
%Matlab script for experiments performed in the univeristy lab
%Frequency scan

%Experimental results of input voltage, input current and output current
%are 3 knowns. Hence, we set them as constant A, B, and C.
%Source voltage is the reference voltage which has zero phase angle

close all;

Rin=20;%input resistor is adjustable
A=data(:,4).*exp(2*pi*1000*data(:,1)*1e-9.*data(:,5)*j)/2;%input voltage Vk(to
the winding)
B=(data(:,2)/2-A)/Rin;%input current Ik
R=50;%output resistor is adjustable
C=data(:,6).*exp(2*pi*1000*data(:,1)*1e-9.*data(:,7)*j)/R/2;%output current Im

k1=A+B*R;
k2=C+B.*C*R./A;
m1=C-B.*B./C;
m2=B+C.*C*R./A;
n1=C.*R+A.*B./C;
n2=C.*C*R*R./A-A;

%set the parameters aa, bb, cc for solving Zc
aa=m1.*k2;
bb=n1.*k2-m2.*k1;
cc=-n2.*k1;
Zc=(-bb+sqrt(bb.*bb-4*aa.*cc))./(2*aa);
Zc_mag=abs(Zc);
Zc_angle=unwrap(angle(Zc));

%Zc plots
figure(1)
subplot(2,1,1);
plot(data(:,1),Zc_mag);ylabel('Magnitude of Zc');grid;title('Zc');
axis([500 2000 100 1300]);%parameters are adjustable & The command may not
be needed.
subplot(2,1,2);
plot(data(:,1),Zc_angle/pi);xlabel('Frequency in KHz');ylabel('Phase angle of Zc
in pi');grid;
```

The characteristic impedance Z_c of the transformer winding is obtained in the unshielded lab as shown in Figure 3.8. The results have been smoothed out because the geometrical irregularity of the transformer results in the oscillation of Z_c . The winding of the transformer is very short. In the normal lab, there are stray capacitances all over the place, to the supporting poles, to the wall, to the nearby objects, to the floor, and to the

Transmission Line Diagnostic

chassis. All create the irregularity and uncertainty, which degrades the transmission line behavior of the winding. Antenna effect is another factor which worsens the experimental condition. More important, the ground is not evenly distributed, which is not the situation for an over head transmission line.

In the experiments, the internal insulating distance b is fixed, and the only thing we can change is the outer insulating distance d . With the increase of d , Z_c decreases correspondingly. In Figure 3.8, we can find that when changing the transformer tank from closed foil to open foil, i.e. increasing d , Z_c goes up dramatically. Z_c of open foil is almost one and a half times of Z_c of close foil. We can find the same phenomenon between 0.5 cm and 5 cm separations. The Z_c curve of 5 cm separation is always above the Z_c curve of 0.5 cm separation. They are like in parallel, which demonstrates that the increment of Z_c from one separation to another separation is fixed, determined by the fraction $\frac{b}{1+b/d}$. However, the oscillation of the curves reflects the inferior experimental conditions, like bad grounding and antenna effect.

After moving the transformer into the HV lab, the grounding and shielding conditions improve dramatically, but the presence of other HV gas insulation testing equipments in the HV lab creates the extra irregularity problem. Simulation results among different locations are shown as Figure 3.9. It shows that the location or the experimental condition plays a critical role in the accuracy of the simulation results.

From the Figure 3.8 and 3.9, we can find that no matter how big the external insulating distance is and no matter where the experiment is performed, the general shape of Z_c of the transformer winding is just like the characteristic impedance of transmission line.

However, there are still some other factors which limit the accuracy of the simulation. Factors like the minimal frequency resolution, the recording length of the samples and the data-reading by human (when using the cursor to get the phase angle), the bad grounding condition, the uncontrolled stray capacitance, the small signal to noise ratio, the temperature (if the winding is too thin and therefore susceptible to temperature change), the test set-up and especially the old equipment, they all reduce the accuracy of the simulation results. For example, the links of the wire or the scope cables will create an extra phase delay because they act like a transmission line for high frequency wave as well. In order to improve the accuracy of the simulation results, experiments need to be implemented in a utility research lab which has advanced function generator and better digital oscilloscope.

3.2.2. Experiments Performed in the Powertech Labs

Under private communication protected under a confidentiality agreement, similar experiments are performed on a 167kVA distribution reactor in a utility research lab. A fast pulse generator, a high precision measuring equipment and automatic data recording were used. As the above, three parameters are recorded in the time domain: input voltage, input current and output current. The internal impedance of the pulse generator is 50 Ω . While the output current is measured on a 1 Ω shunt. Different from the previous

Transmission Line Diagnostic

experiments in the UBC lab, the input is not a sinusoidal signal. Instead, an impulse signal is injected. The sampling frequency is 500 MHz, which implies that the maximum frequency from the signal we can get is 25 MHz. Hence, the time-step is 2 ns. The number of the sampling points is 30,000 and the time window is 60 μ s. The minimal recording data value is $1e^{-8}$. The original measurement obtained from the research lab is shown in Figure 3.10. In order to have a detailed look of the waveform when the impulse signal is injected, figure 3.10 only shows the waves from 11.8 μ s to 13 μ s.

The data obtained from the research lab is not put into use directly. Some modifications have been made. Firstly, the time window is chopped for all three waveforms. From the data file obtained, we can find that there are lots of noise during the whole time period. After examining the input voltage data file, we find that at 11.988 μ s, the input impulse voltage is being injected; while at 12.108 μ s, the impulse signal has its first zero crossing. In order to remove the noise, we set the signal before 11.988 μ s and after 12.108 μ s to 0. Therefore, a better impulse input signal is generated without noise before and after. Correspondingly, the input current and output current are chopped at 11.988 μ s and 12.108 μ s as well, and only the signals in the time interval 11.988 μ s and 12.108 μ s are kept nonzero. Furthermore, in order to get almost continuous frequency response, the time window has been extended to double as before. By chopping and extending the time window, an impulse response is represented in a better way. Figure 3.11 shows the modified measurements in the time domain.

By applying the formulae developed in section 3.1, we can obtain the characteristic impedance Z_c of the winding in both magnitude and phase as shown in Figure 3.12, based on the following Matlab script. Furthermore, the travelling time and equivalent length of the winding for different frequencies are obtained, as shown in Figure 3.13.

```
%Matlab script for experiments performed in a utility reserach lab
%Inject Impulse Signal
%chop the time window from first zero crossing
%add another 30,000 points---i.e. zero padding

close all;
dt=2e-9;
n=60000;%number of points
tmax=dt*n;
t=[dt:dt:tmax];
fmax=1/dt;%sampling frequency is 500MHz
df=fmax/n;%frequency resolution
freq=[df:df:fmax];
f=transpose(freq);
w=2*pi*f;

v_in=data(:,3);
i_in=data(:,4).*50;
```

Transmission Line Diagnostic

```

i_out=data(:,5);

v_in_f=fft(v_in);%convert input voltage into frequency domain
i_in_f=fft(i_in);%convert input current into frequency domain
i_out_f=fft(i_out);%convert output current into frequency domain

%Experimental results of input current, input voltage and output current
%are 3 knowns. Hence, we set them as constant A, B, and C.
A=v_in_f;
B=i_in_f;
C=i_out_f;
R=1;% resistor connected to the bottom end of the reactor in ohms

k1=A+B*R;
k2=C+B.*C*R./A;
m1=C-B.*B./C;
m2=B+C.*C*R./A;
n1=C.*R+A.*B./C;
n2=C.*C*R*R./A-A;

%set the parameters aa,bb,cc for solving Zc
aa=m1.*k2;
bb=n1.*k2-m2.*k1;
cc=-n2.*k1;
Zc=(-bb+sqrt(bb.*bb-4*aa.*cc))./(2*aa);
Zc_mag=abs(Zc);
Zc_angle=unwrap(angle(Zc));

%plots
%time domain plots
figure (1)
subplot(3,1,1),plot(t/1e-6,v_in);grid;
title('input voltage');ylabel('voltage in volt');
axis([11.8 13 -2 15]);%The parameters are changeable according to when the impulse
signal is injected.
%This command may not be needed if we want the full range plot.
subplot(3,1,2),plot(t/1e-6,i_in);grid;
title('input current');ylabel('current in ampere');
axis([11.8 13 -0.5 0.5]);%changeable or not needed.
subplot(3,1,3),plot(t/1e-6,i_out);grid;
title('output current');xlabel('time in μs');ylabel('current in ampere');
axis([11.8 13 -0.4 0.3]);%changeable or not needed.

%FRA plots
figure (2)
subplot(2,1,1),plot(t/1e-6,i_in./i_out);grid;%v_out=i_out, Rout=1ohm

```

Transmission Line Diagnostic

```

title('Transadmittance of the Reactor');xlabel('time in  $\mu$ s');ylabel('Transadmittance in
siemens');
axis([11.8 13 -100 150]);%changeable or not needed
subplot(2,1,2),plot(f/1e6,(i_in_f)/(i_out_f));grid;
title('Frequency Response of the Reactor');xlabel('frequency in
MHz');ylabel('Transadmittance in siemens');
axis([0 25 -50 100]);%Only take the values up to Nyquist frequency & parameters are
adjustable

%TLD plots (Zc)
figure(3)
subplot(2,1,1);
plot(freq/1e6,Zc_mag);ylabel('Zc');title('Magnitude of Zc');grid;
axis([0 25 0 300]);%parameters are adjustable
subplot(2,1,2);
plot(freq/1e6,Zc_angle/pi);xlabel('Frequency in MHz');ylabel('Phase angle of
Zc');title('Phase angle of Zc1 in pi');grid;
axis([0 25 -1300 100]);%parameters are adjustable

```

From figure 3.12, we can find the Z_c of the transformer winding has the exactly same wave shape as the Z_c of a typical transmission line up to 17.5MHz. With the increase of the frequency, the magnitude of Z_c decays exponentially and the phase angle of Z_c decreases linearly. Therefore, we can verify that it is valid to model the transformer winding as a transmission line as long as the frequency is high enough. The signal with high frequency travels fast and has a small wavelength so that the transformer winding is long enough to allow the wave to travel along as if the wave travels along the transmission line.

When the frequency is relatively low, for example in our case lower than 0.5MHz, the corresponding wavelength of the frequency is very long. Especially, if the wavelength is longer than the physical length of the winding, the injected signal will not really travel along the winding like along a transmission line. In other words, the winding is not long enough to act like a transmission line for any low frequency signals. This explains the phase angles for the lower frequency range.

When the frequency is extremely high, the Z_c response is becomes more sensitive to the test set-up, the noise and the accuracy of the measuring equipment. We can find in figure 3.12 that the magnitudes of Z_c above 17.5 MHz begin to increase. It should be corrected by further improvement on the overall test design and more advanced measuring equipment.

From figure 3.13, we can see that the results are consistent with the conclusion in section 3.1.2. Like in a transmission line, high frequency signal oscillates faster. Moreover, the equivalent length of the winding decreases with the increase of the

Transmission Line Diagnostic

frequency. It proves again that the transmission line diagnostic model in transformer is valid and efficient.

3.2.3 Configuration of a Single Phase Transformer

In order to further the study of the winding movement diagnosis, a single phase power transformer is assembled in the laboratory as shown in Figure 3.14 and 3.15. Two identical disk-type copper coils are used as the two windings. Conductors of both the windings have square cross sections about 0.2 cm^2 . They are wound as concentric disks. The radius of the innermost layer is 8.5 inches, while the radius of the outermost layer is 12.5 inches. The number of the disks for each winding is 23, and the number of layers is 28. The height of each winding is 4.75 inches. The insulation between turns and layers is varnish. The insulations between the two windings and between the lower winding and ground are wooden spacers. The two windings are connected in series.

According to the formula (33) below, we roughly calculate the total length of the windings (L), which is 7081 feet, that is, 2158 meters. Comparing L with the wavelength of 600 meters at 0.5 MHz obtained by formula (2), we know that in a homogeneous lossless medium, the wave travels about 3 wavelengths at such frequency. In the other word, it provides 3 full waveforms. Similarly, the wavelength is 150 meters for a 2MHz signal, which will give us about 14 full waveforms of the signal. Again, the higher the frequency is, the shorter the wavelength will be, and therefore the more full waveforms will be obtained. Therefore, the windings with such length are reasonable and practical for our travelling wave based transmission line diagnostic modeling.

$$L = 2 * \pi * \text{average winding radius} * \text{number of the turns} * \text{number of the layers} \quad (33)$$

The core is made up of the very thin aluminum cylinder, which is wound from an aluminum sheet. Compared with aluminum, steel is a very good type of magnetic material due to its high permeability, around 2000 times of air and aluminum. However, steel is usually very heavy and hard to bend. Although aluminum doesn't have as good a magnetic permeability as steel, it is suitable for high frequency study due to the skin effect explained later.

The aluminum cylinder or sheet is 31 inches tall. The whole transformer is put on the top of a mobile wooden stand with wheels underneath. The height of the stand is around 6 inches and the wooden spacer between two windings is around 5 inches. In order to shield the magnetic flux and to reduce end effect and proximity effect, the height of the core has to be larger than the total height of the windings, i.e. overheads has to be added up to the total height. Here we chose the height of the core to be about two times the total height of the windings. After rounding it, the maximum radius of the hollow core is approximately 8.5 inches, which equals the radius of the most inner layer of each winding. In such a way, we can simply adjust the separation between the windings and the core, i.e. b in formula (27), by compressing or expanding the very thin aluminum cylinder. A cross-section view of the transformer is shown in Figure 3.16.

Transmission Line Diagnostic

The thickness of the core is calculated based on the skin depth in a conducting material. When a magnetic field B travels inside a lossy conducting medium, it attenuates in magnitude exponentially according to the attenuation constant α as shown in Equation (34). Skin depth is defined as the field attenuated by a factor e^{-1} or 0.368 in a distance equal to $1/\alpha$. This distance is known as the skin depth and is denoted by the symbol d . Skin depth sometimes is also named space constant. Equations 33 and 34 derive and verify the relationship between α and d . From these equations, we can find that for a given magnetic material, the depth of the magnetic field penetration is inverse proportional to the square root of frequency applied. The higher the value of the frequency, the larger the value of the attenuation constant α , the smaller the value of the skin depth d , and therefore the shallower the magnetic wave can penetrate. This phenomenon is illustrated in Figure 3.14.

$$B = B_0 e^{-\alpha} \quad (34)$$

B_0 is the surface magnetic flux density

$$\alpha = \sqrt{\pi f \mu \sigma} \quad (35)$$

$$\delta = \frac{1}{\sqrt{\pi f \mu \sigma}} \quad (36)$$

Where,

σ is the conductivity of the material

From figure 3.17, we can observe that at skin depth, the flux density declines to about one third of surface flux density; at a depth of two skin depths, the flux density decreased to about one seventh of surface flux density; at a depth of three skin depths, the flux density is only five percentage of the surface flux density. From the last observation, we can design our aluminum core with proper thickness in order to minimize the leakage magnetic flux. The minimum frequency we are interested in is 0.5MHz, the permeability and conductivity of aluminum are $4\pi \times 10^{-7}$ henries/meter and 1.03×10^7 siemens/meter respectively. Put the above parameters into equation (36), we get the skin depth of aluminum is 0.115mm. Therefore we choose our aluminum sheet with 0.5mm thickness, which is much larger than 3 skin depths.

The tank is chosen and configured in the same way as the core. It is made of aluminum sheet, which provides very good electromagnetic shielding. The height of the tank is same as the core. The radius is adjustable by compressing or expanding as well. The minimum radius that the tank can round is 12.5 inches, i.e., the radius of the most outer winding; while the maximum radius that the tank can provide is 18.5 inches.

The choosing of the parameters above for both the core and the tank facilitate the changing of b and d in formula (27), which are the keys factors of Z_c .

3.2.4 Experiments Performed with a New Power Transformer in the University Labs

We use the same waveform generator to produce one sinusoidal signal once at a time to the one terminal of the winding, with starting frequency of 500 KHz and up to

Transmission Line Diagnostic

2MHz generated by the same waveform generator. The experiment circuit is same as figure 3.6 except that here both R_{in} and R_{out} are 220 ohms. As discussed in the TLD method, we measure the input voltage, input current and output voltage both in magnitude and phase angle. After importing the measurements into Matlab script in section 3.2.1, we can get the experimental results of Z_c . To reduce the measurement errors and EMI nearby, we smooth the experimental results by fitting it into exponential curve. Here we use the first order exponential fitting model I and second order exponential fitting model II respectively. In the following part, we will discuss about the winding overall movement both in axial and radial direction of the transformer.

Firstly, discuss about the radial winding movement. We vary the inner separation b while keeping the outer separation d constant. In practice, the winding is usually very close to the core, so we vary b from 0 to 0.25 inches and to 0.5 inches. d is usually very big compared with b , so here we set b as 2.25 inches. The Z_c result curves obtained for different inner separations are shown in figure 3.18 and figure 3.19. Both figures show that for given b and d , the surge impedance Z_c exponentially decreases with the increase of frequency, which is consistent with the Z_c of a transmission line. Furthermore, when b is decreasing; in other word, the inner winding is expanding to the core as analyzed in chapter 1, Z_c vertically shifts down. For example, in figure 3.18, when we reduce inner separation from 0.5 inches to 0.25 inches and then to 0 inch, Z_c is correspondingly shifted from the upper curve to the middle curve and then to bottom curve. It verifies the conclusion in formula (32), i.e. Z_c is directly proportional to inner separation b when b is much less than d . Figure 3.19 gives the same result and conclusion about the numerical relationship between Z_c and b .

Taking Z_c at 500KHz in figure 3.18, we can find that when b changes from 0 to 0.25 inch, i.e. 3% ($0.25/8.5$) separation change based on the inner radius of the winding, Z_c changes 12% ($(470-420)/420$). If the change percentage of Z_c is linear to the change percentage of b , then when b changes from 0 to 0.5 inch, i.e. 6% ($0.5/8.5$), Z_c should correspondingly change to 24%. However, Z_c only changes 18% ($(495-420)/420$). This shows that the smaller the separation, the more sensitive the Z_c is. In reality, b is usually close to zero, which will lead the TLD method to a very high accuracy. Figure 3.19 also proves the nonlinearity between the change percentage of b and the change percentage of Z_c . It shows the high sensitivity of Z_c when b is very close to the core as well.

From the curves in figure 3.18 and figure 3.19, we find that the distance between the two curves is not always the same. The discussion about the shortest distances between any two curves is made here and plots are as shown in figure 3.20. The curves are almost straight lines, where the data is well behaved. Figure 3.21 shows the percentage comparison of the shortest distance among any two curves, where the data is well behaved as well.

When b is large, we do the same measurements and plot Z_c versus frequency as shown in figure 3.22. Again, it shows Z_c exponentially decreases with the increase of the frequency for the same separation b . Also, Z_c shifts vertically with the change of the separation. It is consistent with the results in figure 3.18 and figure 3.19, that is, Z_c

Transmission Line Diagnostic

decreases with the decrease of the inner separation b . In other words, when a short circuit happens, the inner winding bulges out and therefore reduce the inner separation d . As a result of the reduced b , Z_c decreases as well. By comparing the percentage changes of b and Z_c , we conclude again that smaller the b , the more sensitive the Z_c is. For example, when b changes from 18% to 26.5% (i.e. b changes from 1.5 inches to 2.25 inches), Z_c changes from 15.5% to 26% based on the Z_c at 500kHz.

Shortest distances between the above curves are shown in figure 3.23. Like the curves in figure 3.20, they are almost straight lines as well. This should be analyzed in further work of the TLD method. The shortest distance percentage comparison is shown in figure 3.24.

Now we vary the outer separation d while keeping the inner separation b constant. Here, d changes from 1.5 inches to 2.25 inches and then to 3 inches. b stays at 0.5 inches. Simulation results are shown in figure 3.25. Z_c obtained shows the same shape and shift tendency as Z_c when varying b .

The shortest distance comparison is shown in figure 3.26; while the shortest distance percentage comparison is shown in figure 3.27.

From the above experiments and simulation, we find that Z_c of the TLD method is just like the Z_c of the transmission line. By checking the general shape of the Z_c , we can determine whether there is a discontinuity. For the overall winding movement in radial direction, we can find out by the shift of two Z_c curves.

Secondly, we will discuss the overall winding movement in axial direction. We simply lift up the transformer core and tank by 1.5 inches, and then we equivalently lower the winding by 1.5 inches. Figure 3.28 and figure 3.29 show the Z_c comparison results, before and after the lifting.

From the two comparison curves of Z_c , before lifting and after lifting, we find that when the winding is moving down, Z_c shifts up and vice versa. Therefore, the shifting direction of Z_c can be used to determine the winding movement in axial direction.

The shortest distance and the distance percentage comparison are shown in figure 3.30 and figure 3.31. Again, the shortest distance percentage is a straight line in the plots.

From above discussion, we can conclude that by checking the vertical shifting of Z_c , we can detect the overall winding movement in both axial and radial directions. In addition, TLD method is very sensitive when the separation is small.

How will Z_c change if we still apply the same algorithm as the above into the fault situations? The several fault situations are discussed as follows. Firstly, we assume that a short circuit happens in the connecting point of the two windings. Secondly, we assume that a fault shunt branch with 220 ohms resistance occurs at the same location as the first case. Thirdly, we assume that a fault shunt branch with 330 ohms resistance occurs at the same location as the first case. Lastly, we assume that a fault shunt branch

Transmission Line Diagnostic

with 4700 ohms resistance, which is similar to the arcing resistance caused by partial discharge, occurs at the same location as the first case.

After applying the algorithm developed in the section 3.1.2, the Z_c results are compared as shown in figure 3.32. We can find that in the short circuit case, Z_c decreased dramatically. Compared with the Z_c of the original curve under normal condition, Z_c of the short circuit case is about half of it. In the 220 and 330 ohms fault cases, Z_c curves cross the original curve. In the 4700 fault case, Z_c curve is above the original curve. We can conclude that with the increase of the fault resistance, Z_c begins to increase, and crosses the original non-fault curve at some certain fault impedances, and continues to go up until it is above the non-fault curve. Also, we can detect a short circuit fault by observing the dramatic decrease of Z_c .

3.3 Need for Baseline Historical Data

A significant disadvantage of the FRA technique is the need of the baseline data or reference values, because basically it is a method of comparison rather than of absolute values. Unfortunately, the baseline data or fingerprints from the similar units are usually not available. Also, for the power transformers with the same voltage rating and power ratings, the internal physical structures may be totally different and hence the FRA signatures. Even for the same transformer manufacturer, the assembly process and technique may change and evolve therefore changing the signatures. These factors limit the development of the FRA technique in winding movement detection.

It is believed that most mechanical damages only occur to one of the winding assemblies, therefore the separate examination or measurement of each winding can be compared for the detection of irregularities. The basic assumption is that there is structural three-phase symmetry in the core-and-coil-assembly. Specifically, while the coils are quite identical and the core is symmetric, tap changer and conductor configurations around the coils compose a non-symmetric assembly. In a simple example, if phase A and phase C are symmetrically located at the left and right sides of phase B, then one should expect that the transfer functions for phase A and phase C obtained by exciting and measuring them separately should be quite similar. If any of the three phases has some geometrical change, the symmetry will be broken. By further examining the trend and extent of the asymmetry, one should be able to determine which phase causes the asymmetry.

Some experimental works have been published. Two transfer functions are used: grounded neutral current and transferred voltage. Experimental results show that transfer function of neutral current gives no significant indication of the winding deformation for both radial shifts and axial shifts. In other words, it still presents good symmetric properties for the three phases. On the other hand, transfer function of transferred voltage of the low voltage winding indicates noticeable changes for the winding movements, i.e. the absence of the symmetry reflects the geometrical distortion of one of the phases.

Not only the choice of the transfer function, but quite a few other factors, will determine the validity and sensitivity of this no-need-of-reference method. The set-up of

Transmission Line Diagnostic

the test may affect the sensitivity of the experimental results and the assessment of the different transfer functions. How good is the symmetry is another major factor. Different transformers have different extent of symmetry/asymmetry in the core-and-coil-assembly. It largely influences the sensitivity of the method for different transformers. Furthermore, if the results need to be interpreted in more details, a large amount of the know-how database is still needed, which includes an amount of experimental experiences and rules of correlations of transfer function characteristics and changes in core-and-coil assembly.

At the XIIIth International Symposium on High Voltage Engineering of August 2003, a second paper claiming no need of baseline data was presented by researchers from USA and Germany. The new technique is called Objective Winding Asymmetry (OWA), which takes advantage of the similarities among the three phases.

OWA is a software-based version of FRA(I). Spectral Density Estimate (SDE) building blocks are used to formulate the final transfer function based on the optimum transfer function models, which was originally applied in sound, motion and vibration studies. To improve the accuracy of the estimated transfer function, averaging and weighting techniques have been used. Also, coherence function and random error function are used to reduce the noise and random error. The improved transfer functions then will be compared across phases and provide a single condition number which presents the weighted difference among phases. According to the paper, OWA technique can allow the normal phase-to-phase difference caused by the physical asymmetric layout, and detect the abnormal phase-to-phase difference caused by the winding displacement. Since this technique is patented in USA, the detailed explanation of the software and firmware is not provided in the paper. However, this technique is more like a software based mathematical tool. It is computationally intensive and requires specific and powerful software to assist. In addition, the disadvantages of the conventional FRA exist here as well, such as the test set up and the choice of transfer function.

The variety of the physical layouts of different transformers with different ratings complicates the validity and generalization of the above two methods. The sensitivity of the two methods not only depends on the choice of the transfer function or the estimated spectral density, as noted in the second paper, but also largely depends on the extent of the symmetry of the transformer structure under study. Furthermore, there are no proposed criteria for assessing the severity of the winding deformation. The assessment criteria will vary case by case.

Notwithstanding, the limitations and the disadvantages of the above new methods, they do shed light on the present investigation. The new built-up transformer for experiments has perfect symmetry, and therefore can be explored for the no-need-of reference diagnostic method in the future work.

Another significant advantage for the transmission line diagnostic technique over the FRA technique is the independence from the changes in the measuring circuit. Since Z_c is the characteristic impedance of the winding, it doesn't depend upon the external

Transmission Line Diagnostic

circuit. No matter whether the external measuring impedance changes or not, Z_c is always the fingerprint or signature of the winding. Z_c keeps constant at a given frequency and is independent of both the source and the measuring impedance.

3.4 Other Long Winding Equipment

In power apparatus, wave propagation theory applies to the homogenous lines, the composite lines, cables, the transformer windings and any other machine windings, for example, large generator and motor windings. In all the above cases, the characteristic impedance Z_c and velocity v_0 are defined according to the corresponding dielectric constant, magnetic permeability and physical parameters.

While winding movement contributes to a large percentage of power transformer failures, winding movement and fault discontinuities in other machinery may also lead to equipment failure, economical loss and a hazardous working environment for personnel. While the TLD technique can be used in the detection of transformer winding movement/distortion, it can also be used in the movement and fault detection of any other type of machine windings. The electric wave in such windings still propagates in a similar manner as it travels in the transformer windings. With TLD, one would be able to obtain Z_c by measuring the input and output voltages and currents of each winding. Comparing the deviations of the Z_c curves, one would be able to detect the winding movements of large generators and motors.

Summary

[0016] The invention has many aspects including:

- apparatus which is described herein and includes new and inventive features, combinations of features, or sub-combinations of features; and
- methods which are described herein and include new and inventive steps and/or acts, combinations of steps and/or acts or sub-combinations of steps and/or acts.

[0017] As will be apparent to those skilled in the art in the light of the foregoing disclosure, many alterations and modifications are possible in the practice of this invention without departing from the spirit or scope thereof.

Transmission Line Diagnostic

Abstract of the Disclosure

A new Transmission Line Diagnostic (TLD) approach for winding movement detection is proposed based on the wave propagation property and the frequency dependent transmission line model. In this method, the surge impedance Z_c of the winding can be uniquely obtained by measuring the input and output voltages and the currents. Z_c is the signature of the winding and it is independent of the external circuits. Any changes of Z_c will reflect movements of the winding. Z_c obtained by TLD is a simple exponential-like curve, whose vertical shift gives obvious indication to the overall axial or radial winding movements. This is different from the complex transfer function of numerous resonant frequencies in FRA. TLD is very efficient in low frequency range. TLD can be effectively applied to on-line winding condition monitoring.

Drawings

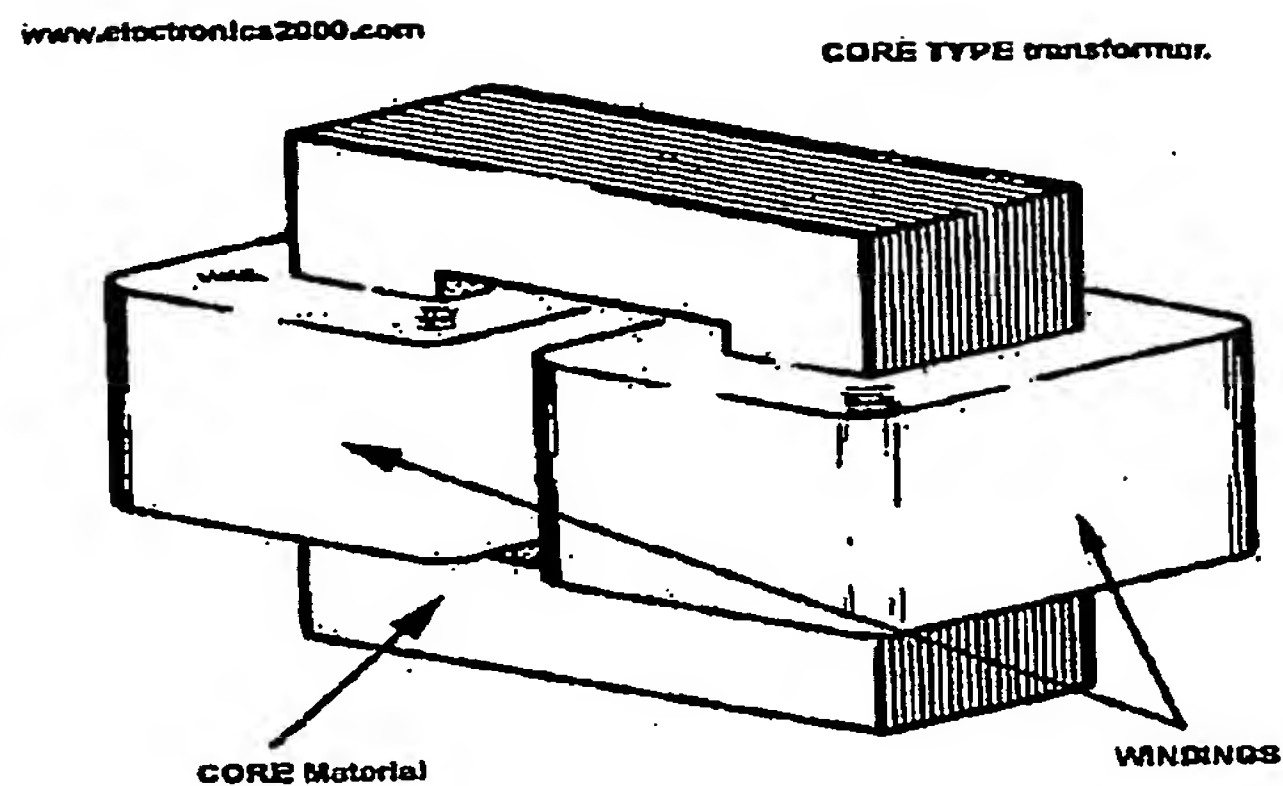


Figure 1.2 Core Type Transformer

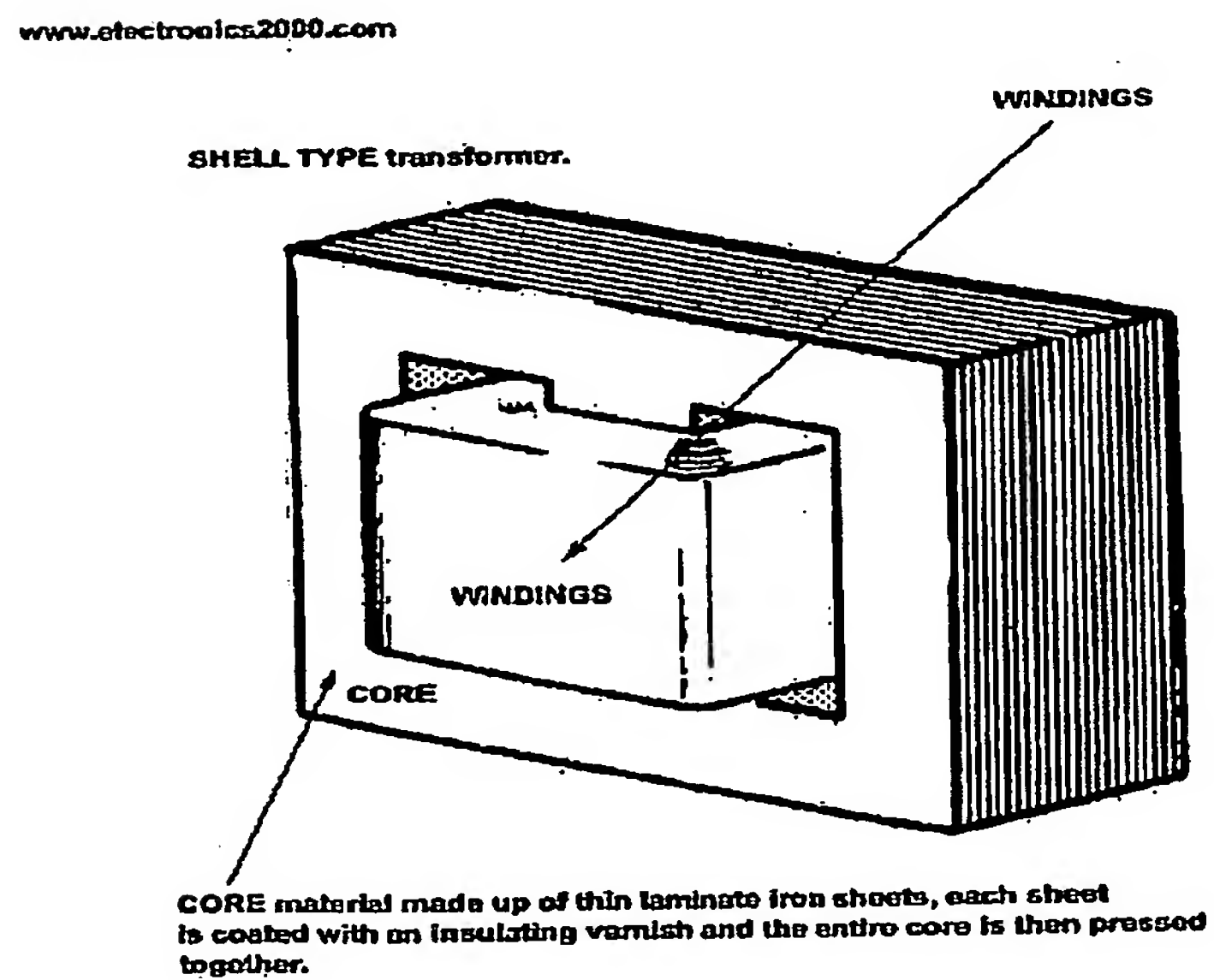


Figure 1.3 Shell Type Transformer

Transmission Line Diagnostic

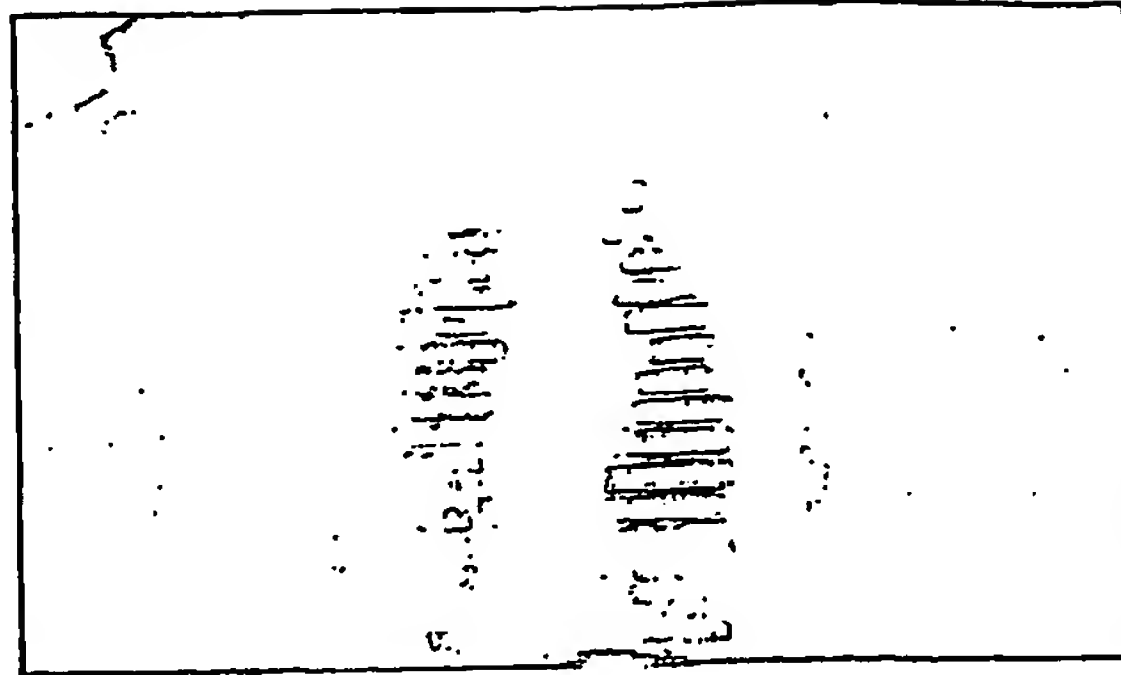


Figure 1.4 Distortion of a Transformer Winding

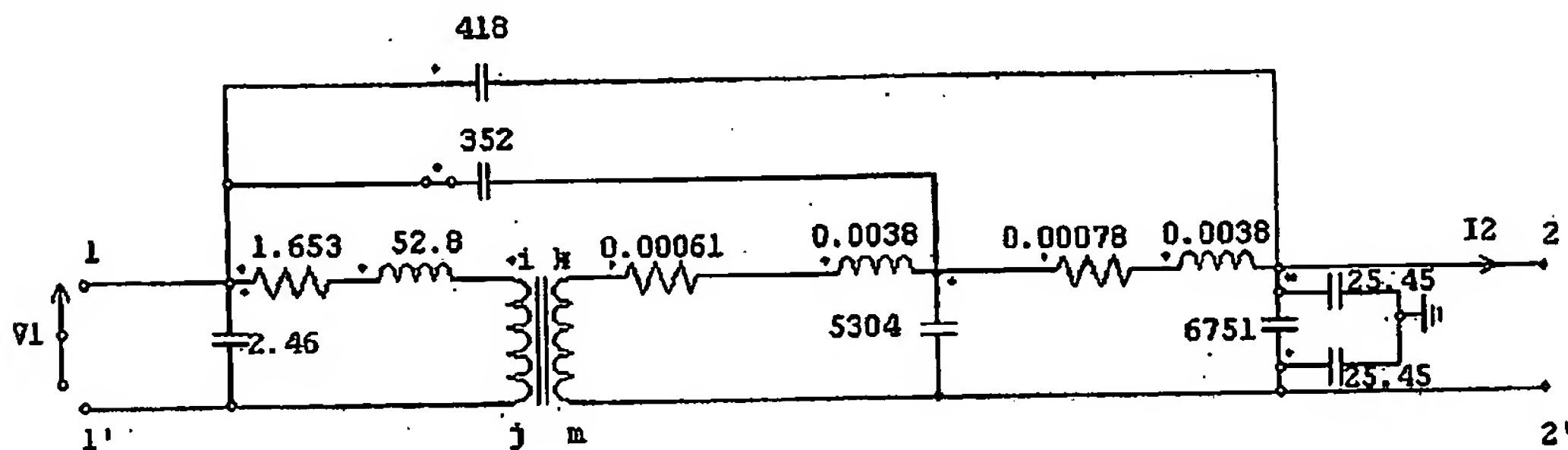


Figure 2.2 The Transformer Circuit by Physical Parameters

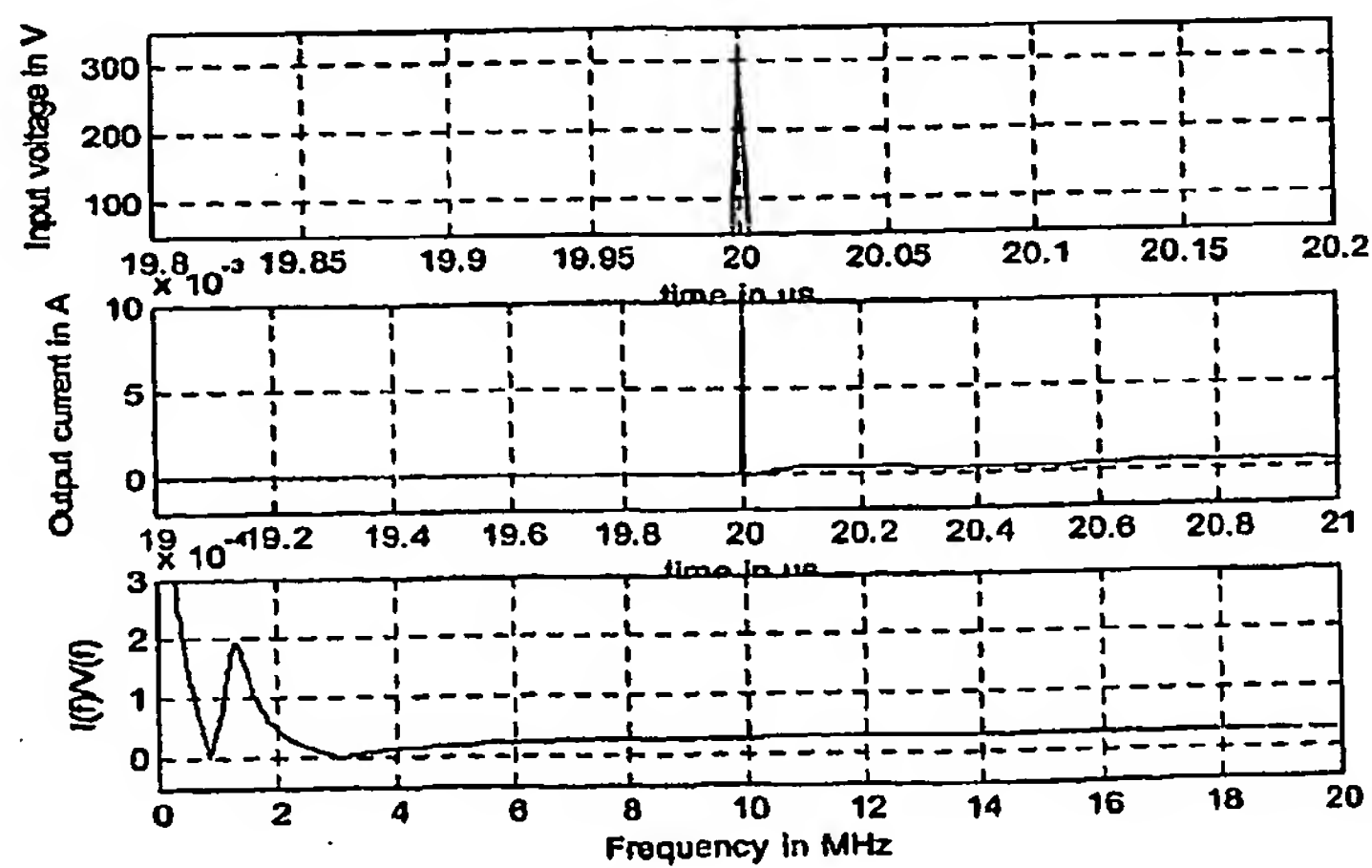


Figure 2.3 Frequency Response for the Physical Transformer Model with 8 Sections

Transmission Line Diagnostic

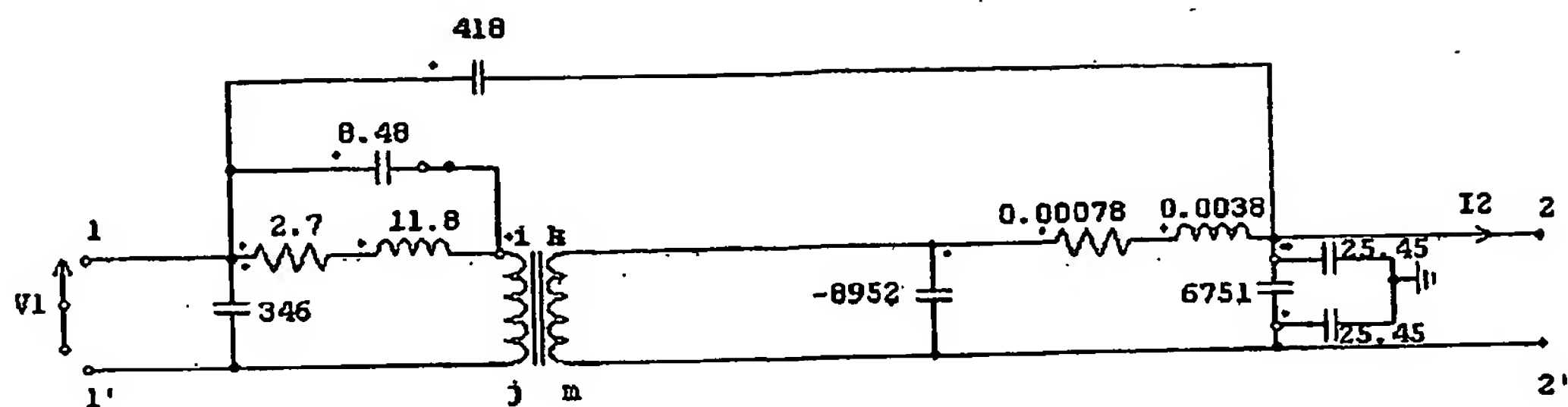


Figure 2.4 Decoupled Circuit I by High Frequency Transformer Model

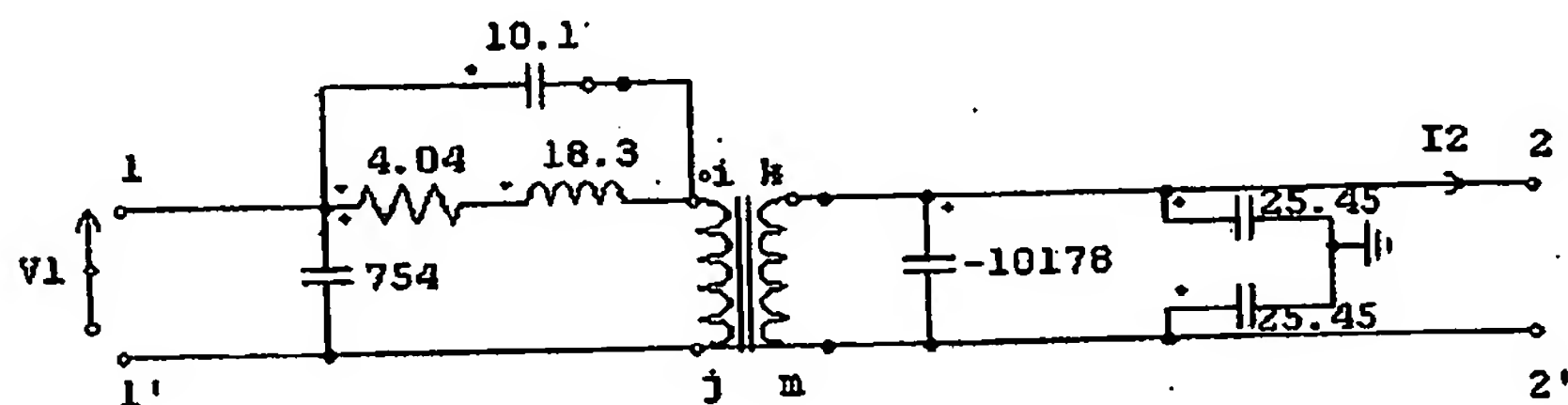


Figure 2.5 Decoupled Circuit II by High Frequency Transformer Model

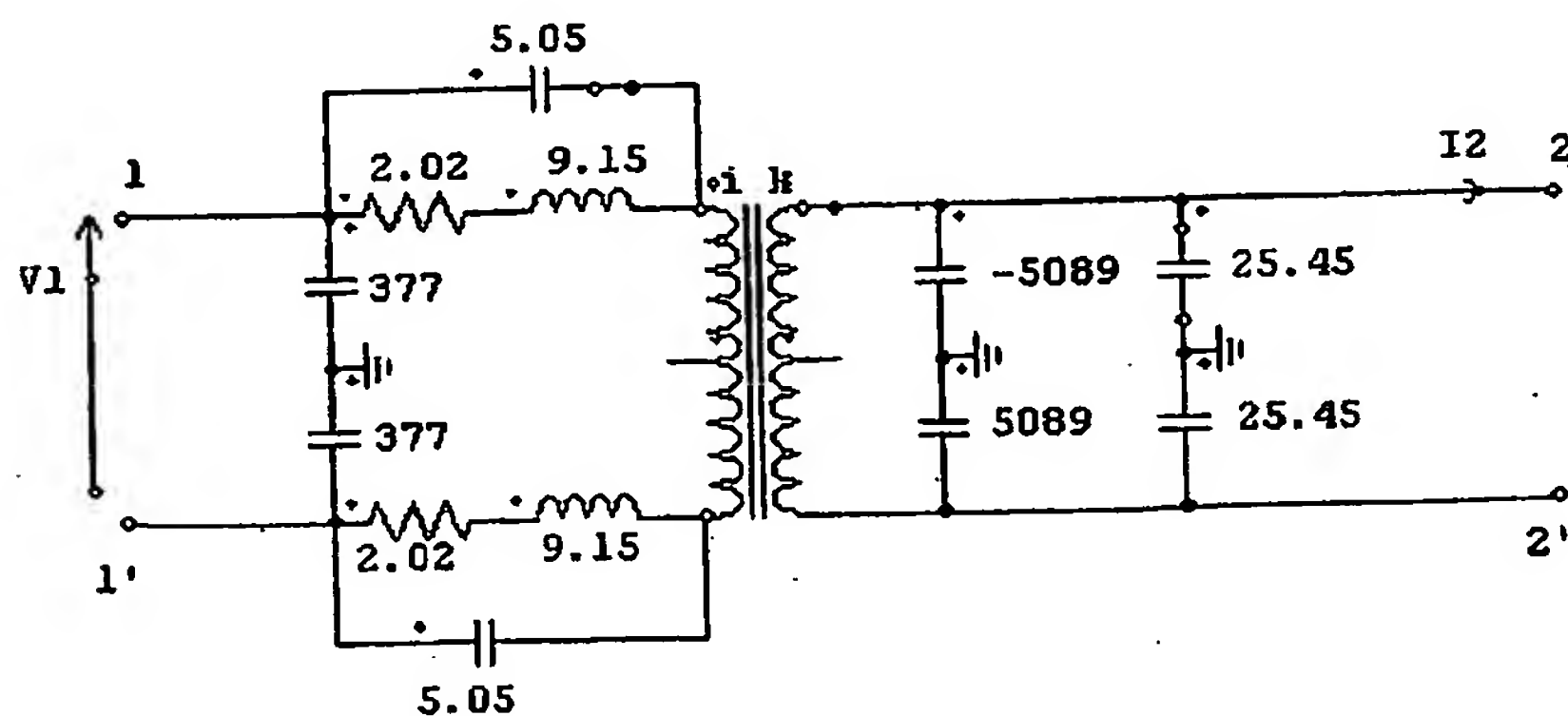


Figure 2.6 Symmetrical Circuit by High Frequency Transformer Model

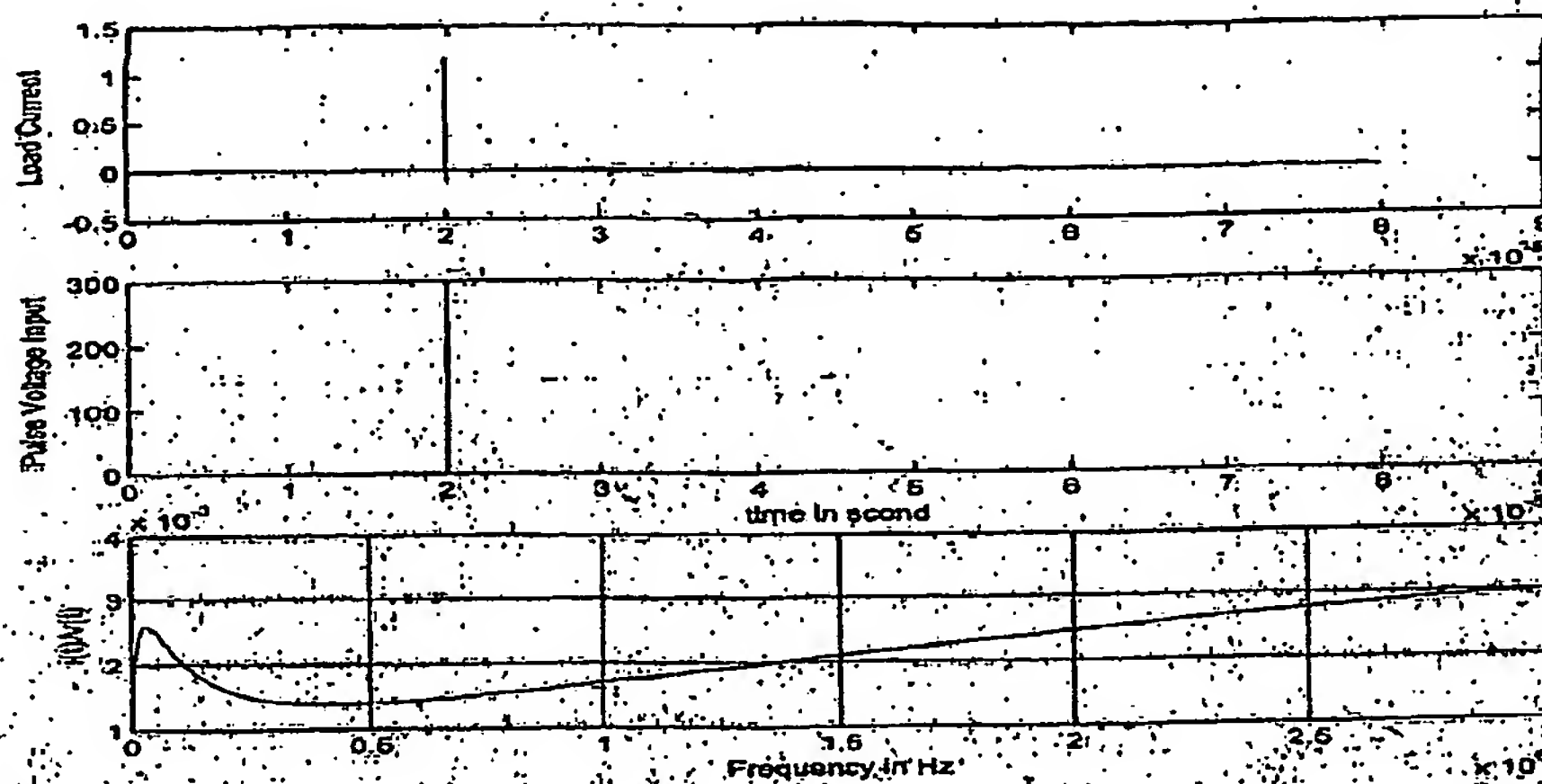


Figure 2.7 Simulation Result for the High Frequency Transformer Model

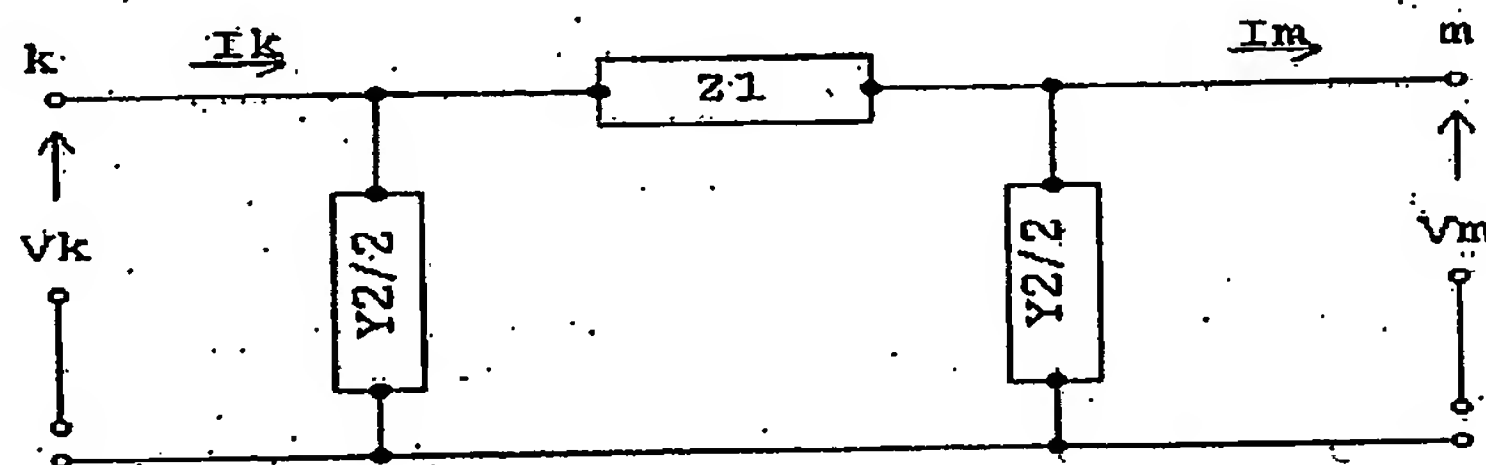


Figure 2.8 Equivalent pi Model by Nodal Analysis

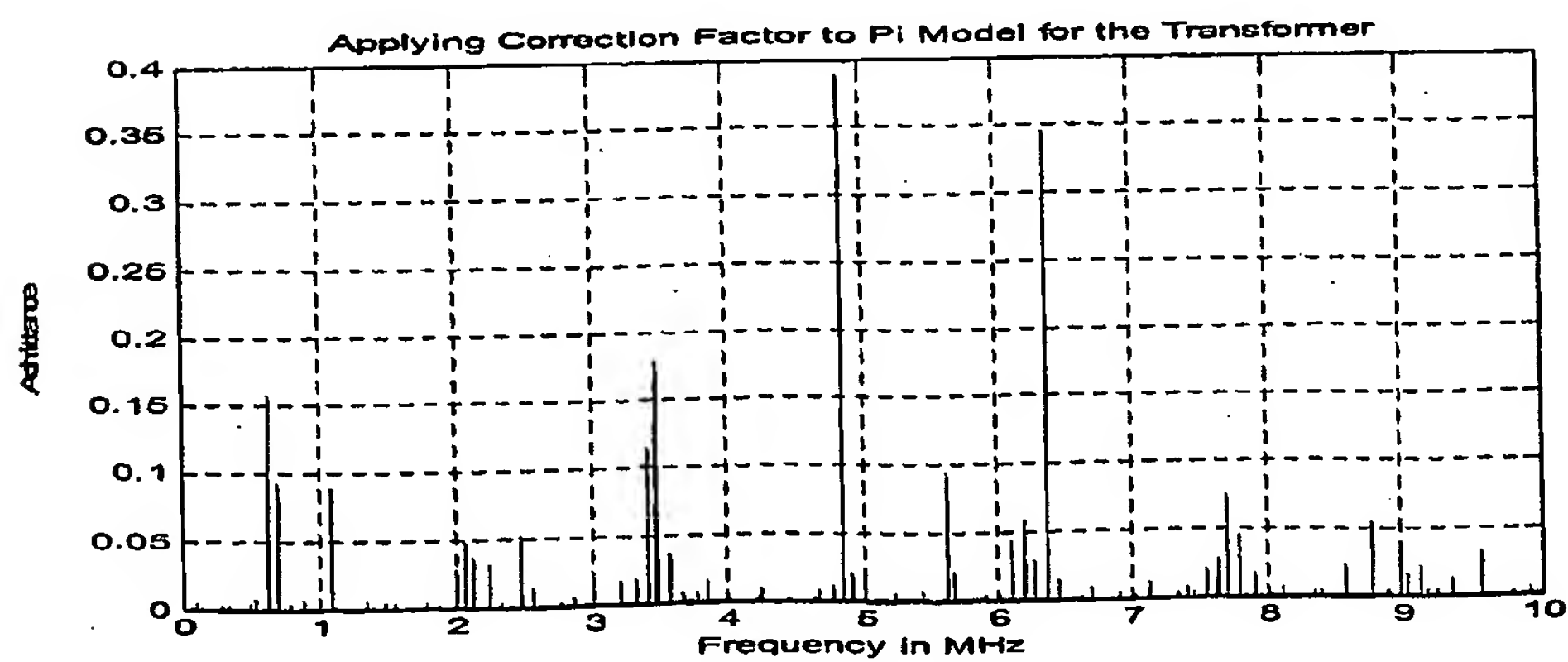


Figure 2.9 Simulation Results for Equivalent pi Model Using Nodal Analysis

Transmission Line Diagnostic

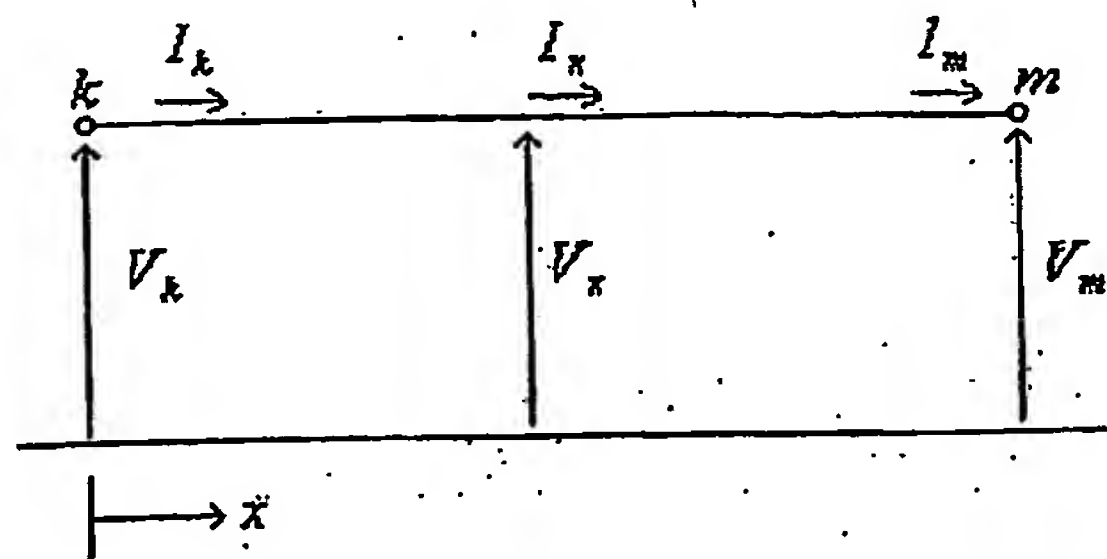


Figure 3.1 A Transmission Line

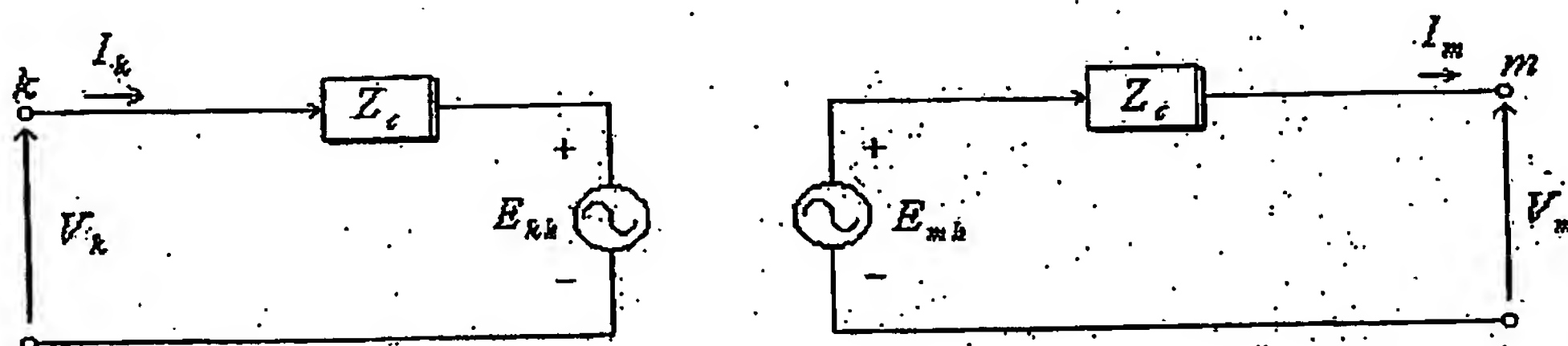


Figure 3.2 Equivalent Frequency-dependent Line Model

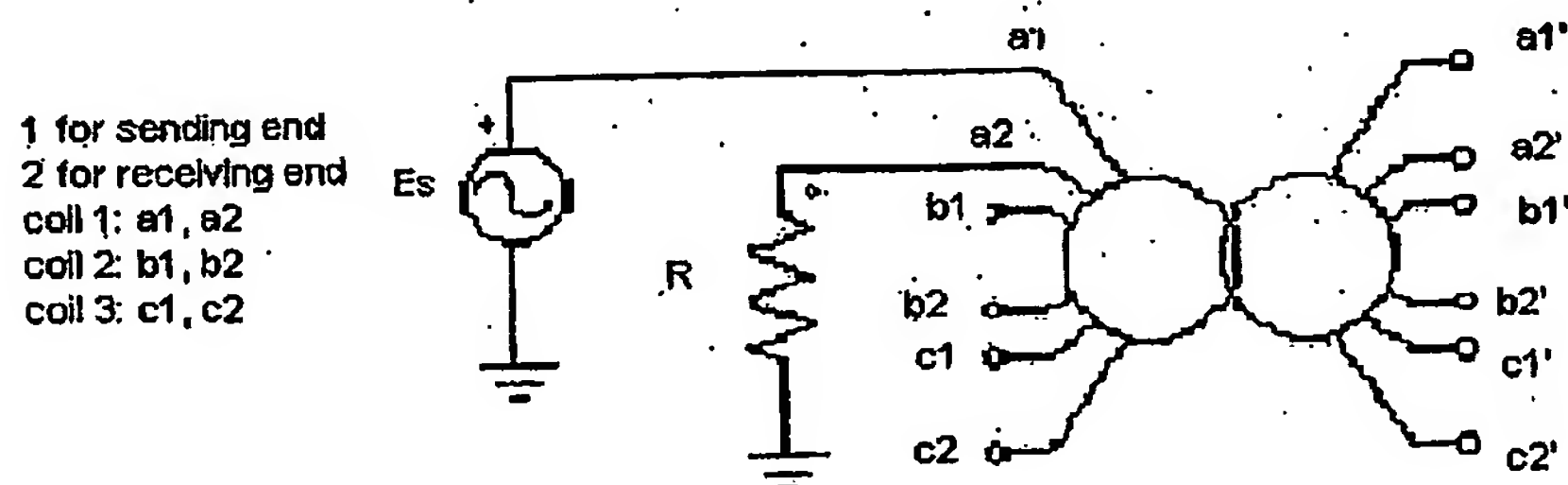


Figure 3.3: Connection of the Winding under Investigation

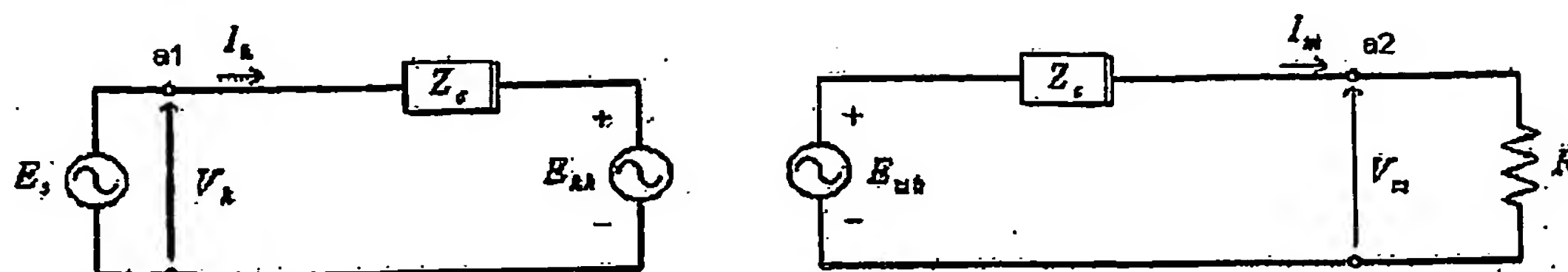


Figure 3.4 Winding Model

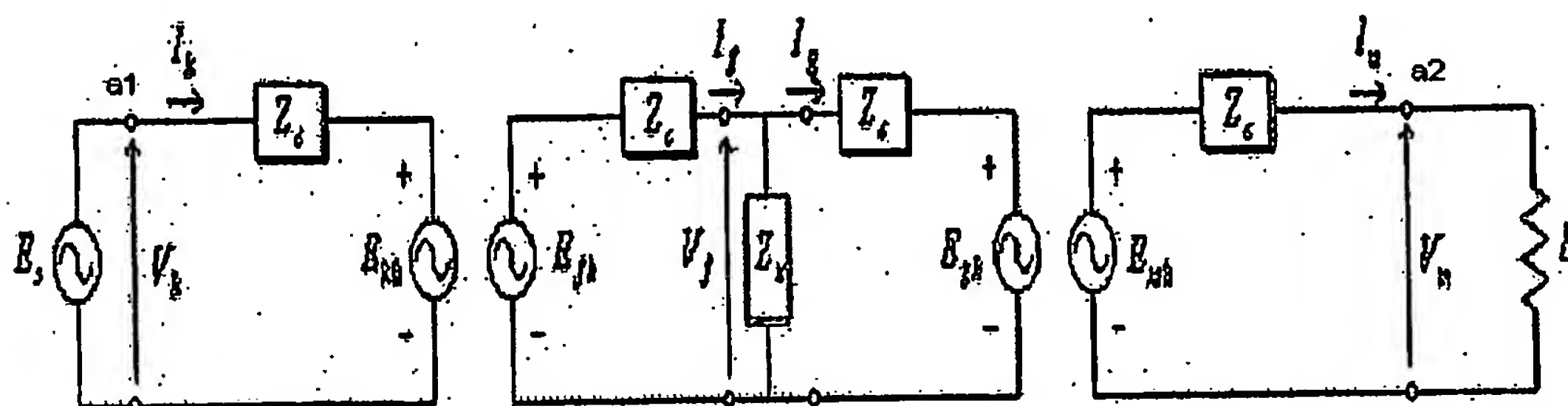


Figure 3.5 Faulted Winding Model

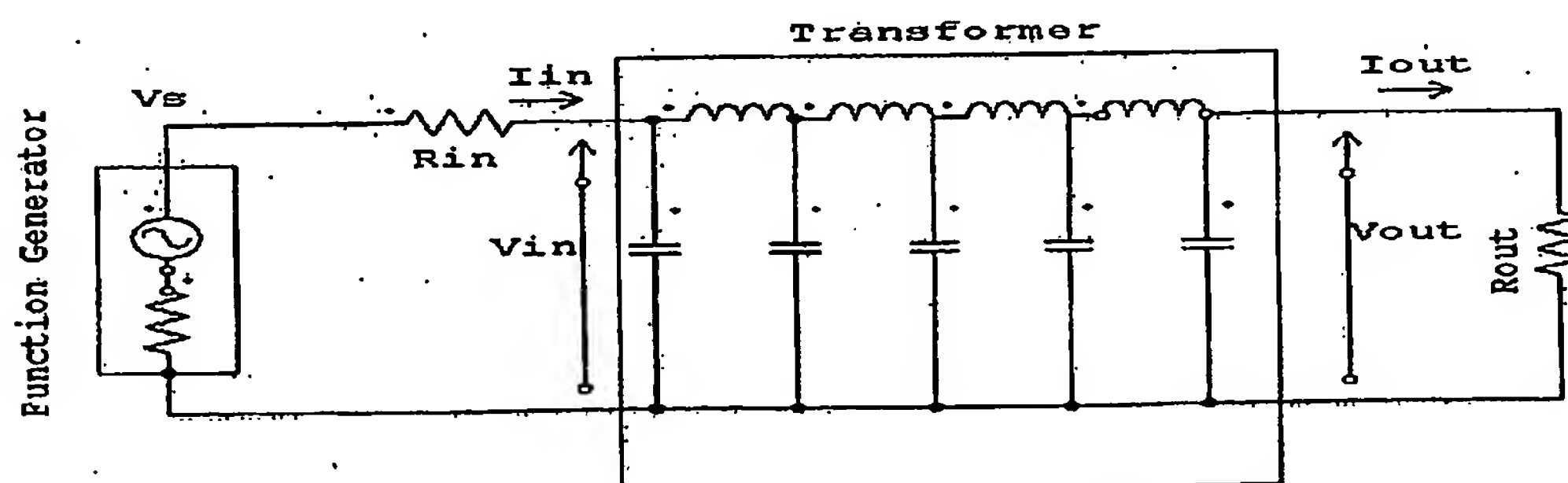


Figure 3.6 Experiment Set-up

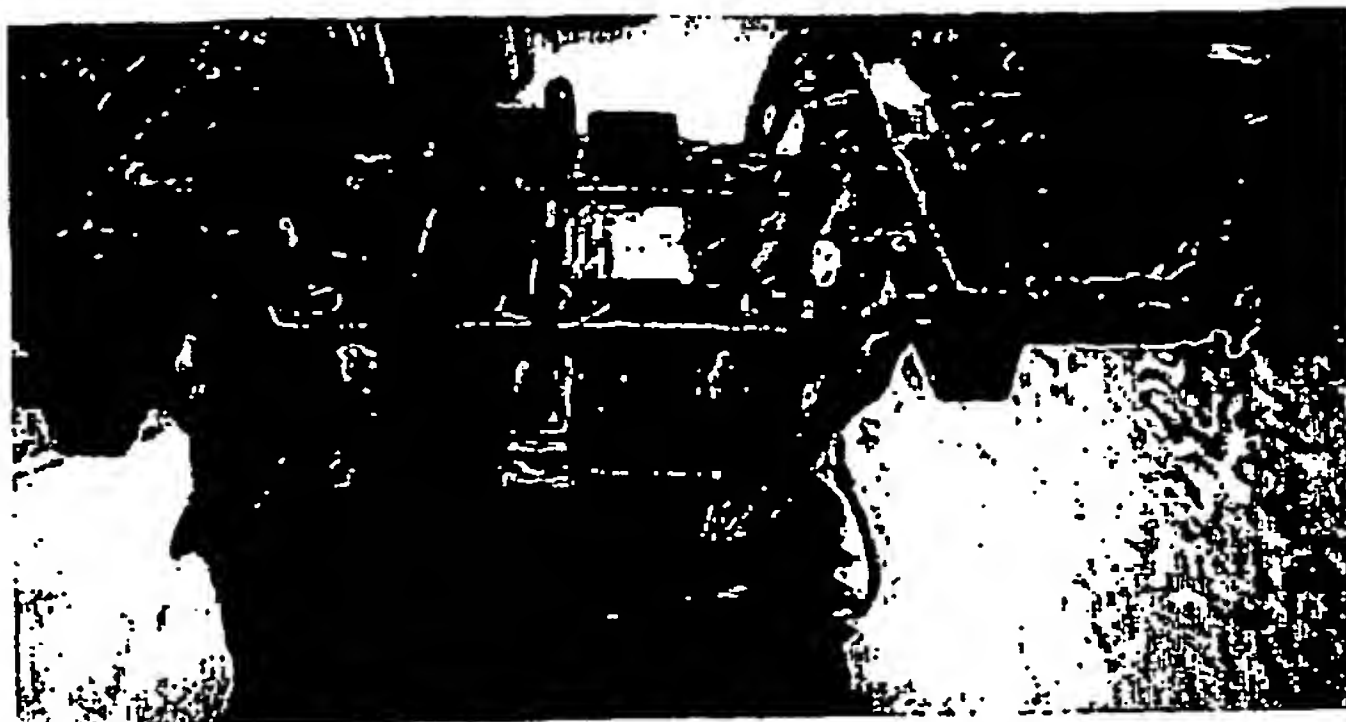


Figure 3.7 The 10kVA Transformer in the University Lab

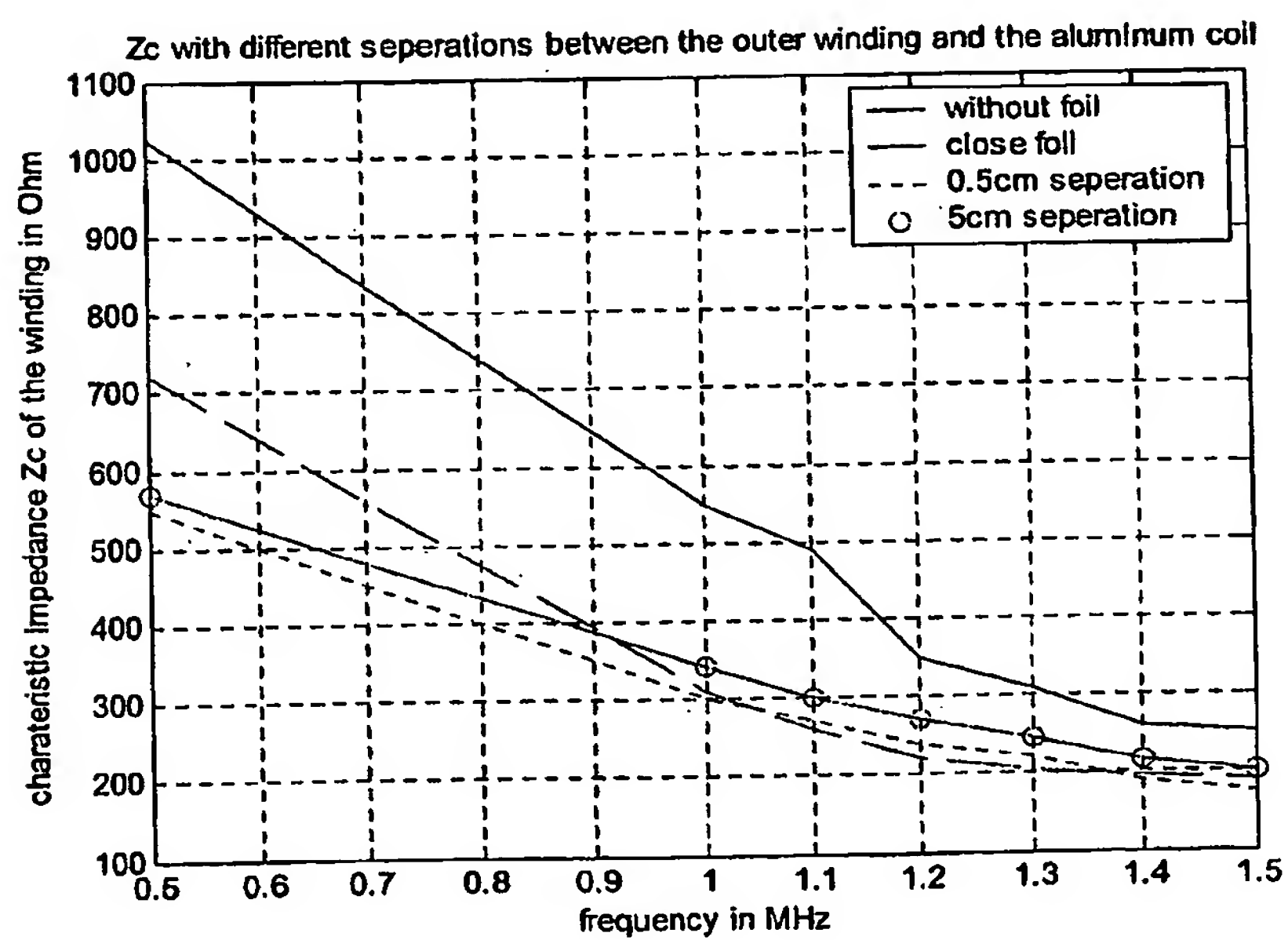


Figure 3.8 Zc with Different External Insulating Distances

Transmission Line Diagnostic

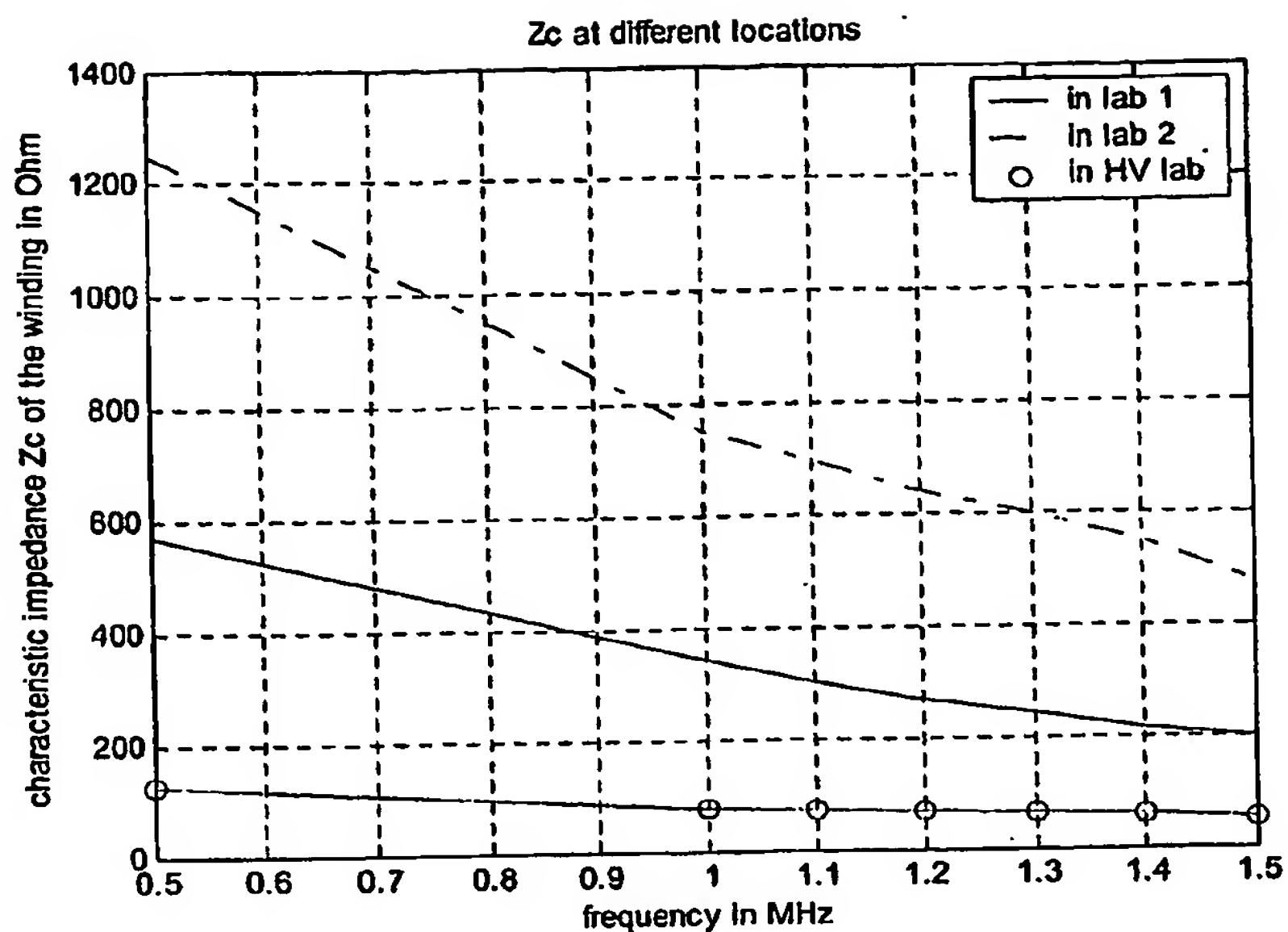


Figure 3.9 Z_c Obtained from Different Experiment Locations

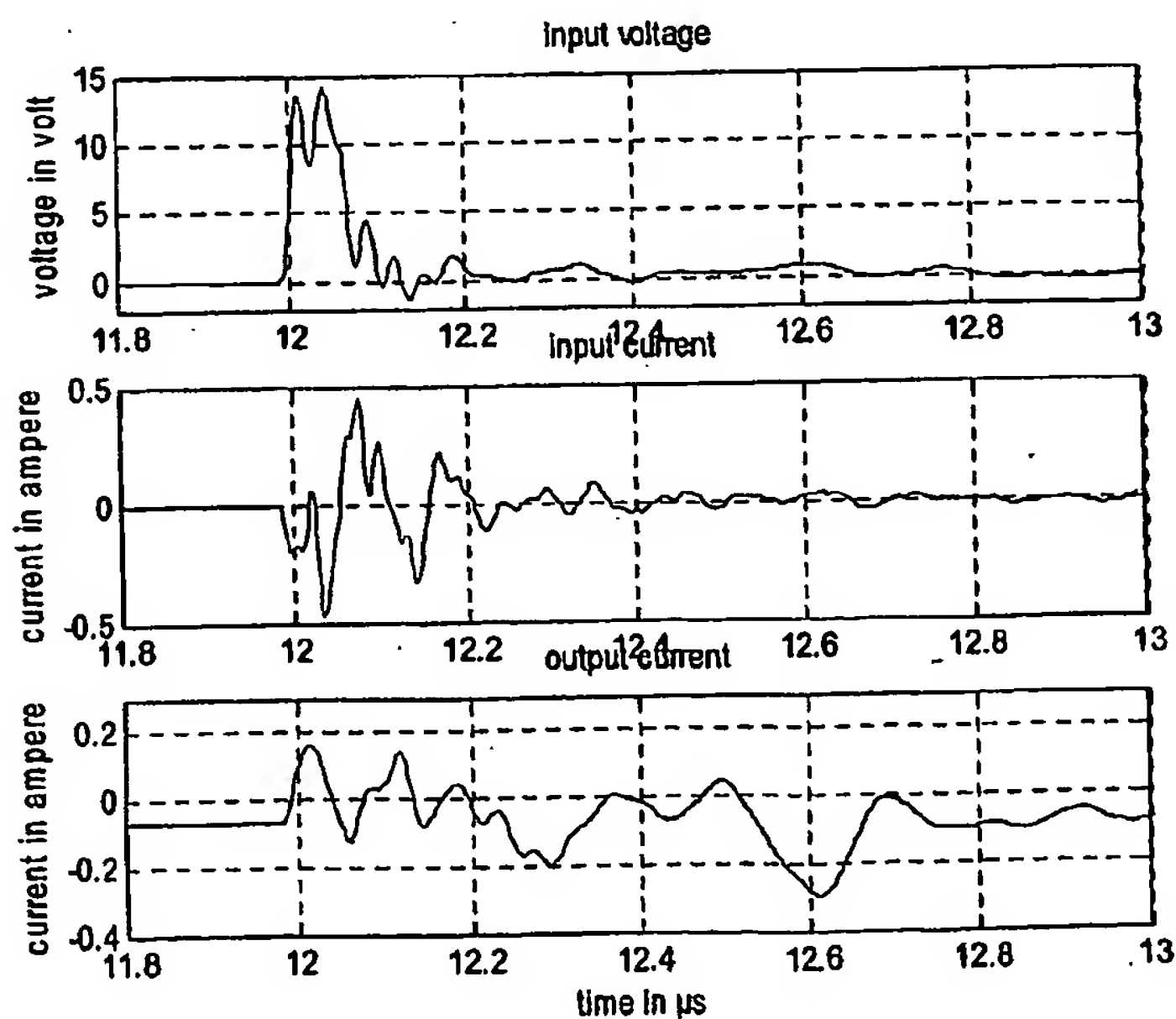


Figure 3.10 Original Time Domain Measurements in a Utility Research Lab

Transmission Line Diagnostic

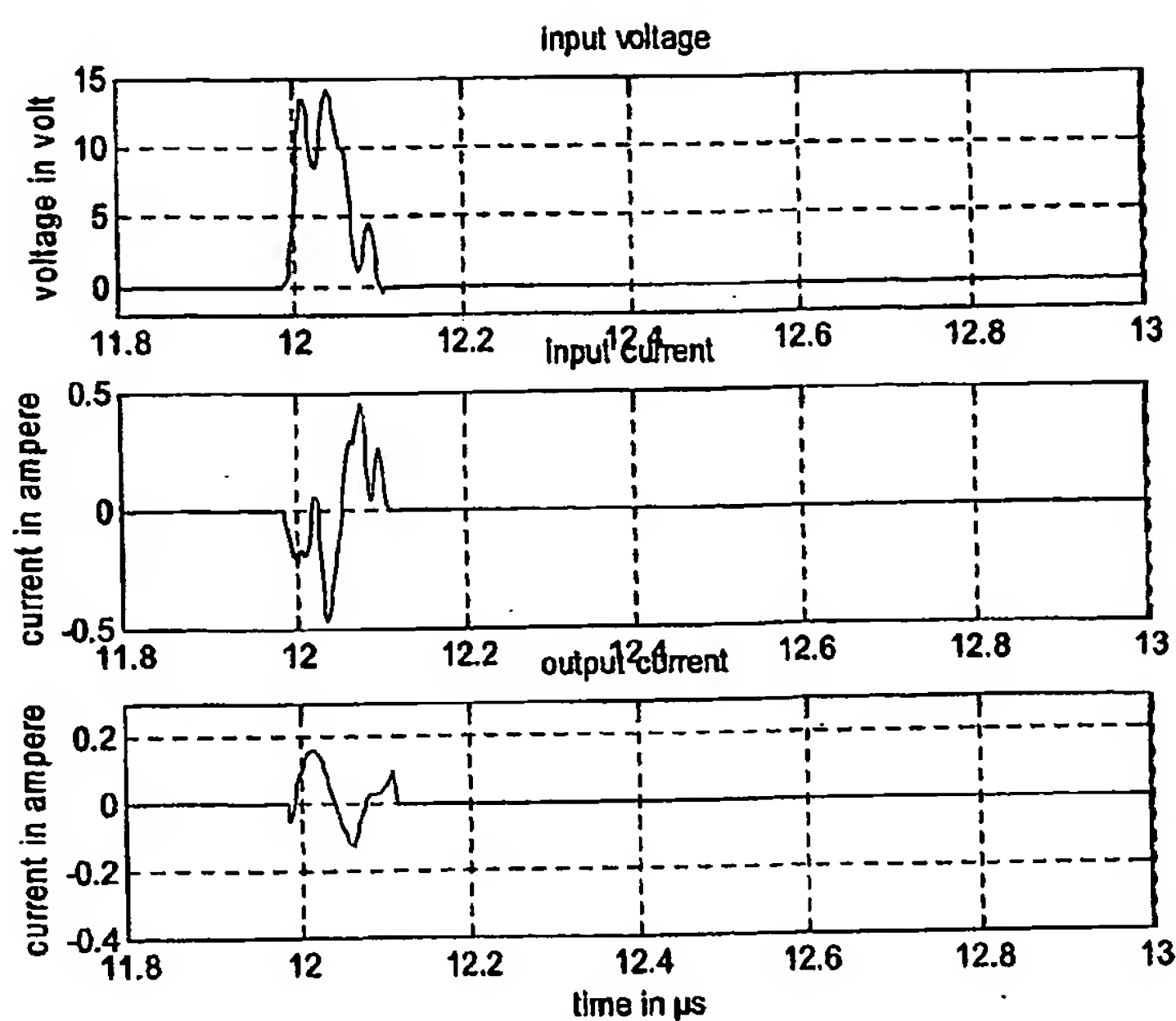


Figure 3.11 Modified Time Domain Measurements in a Utility Research Lab

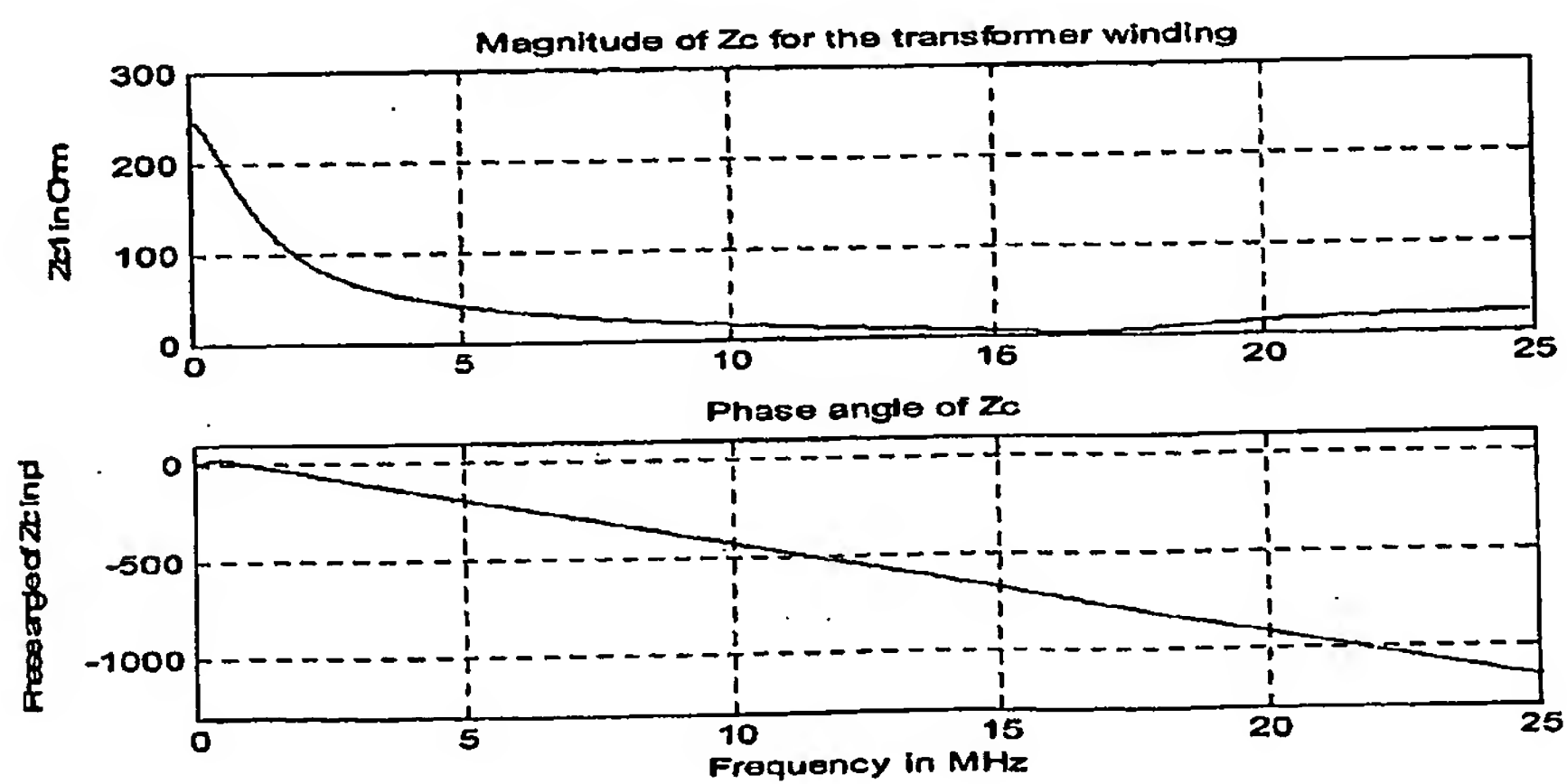
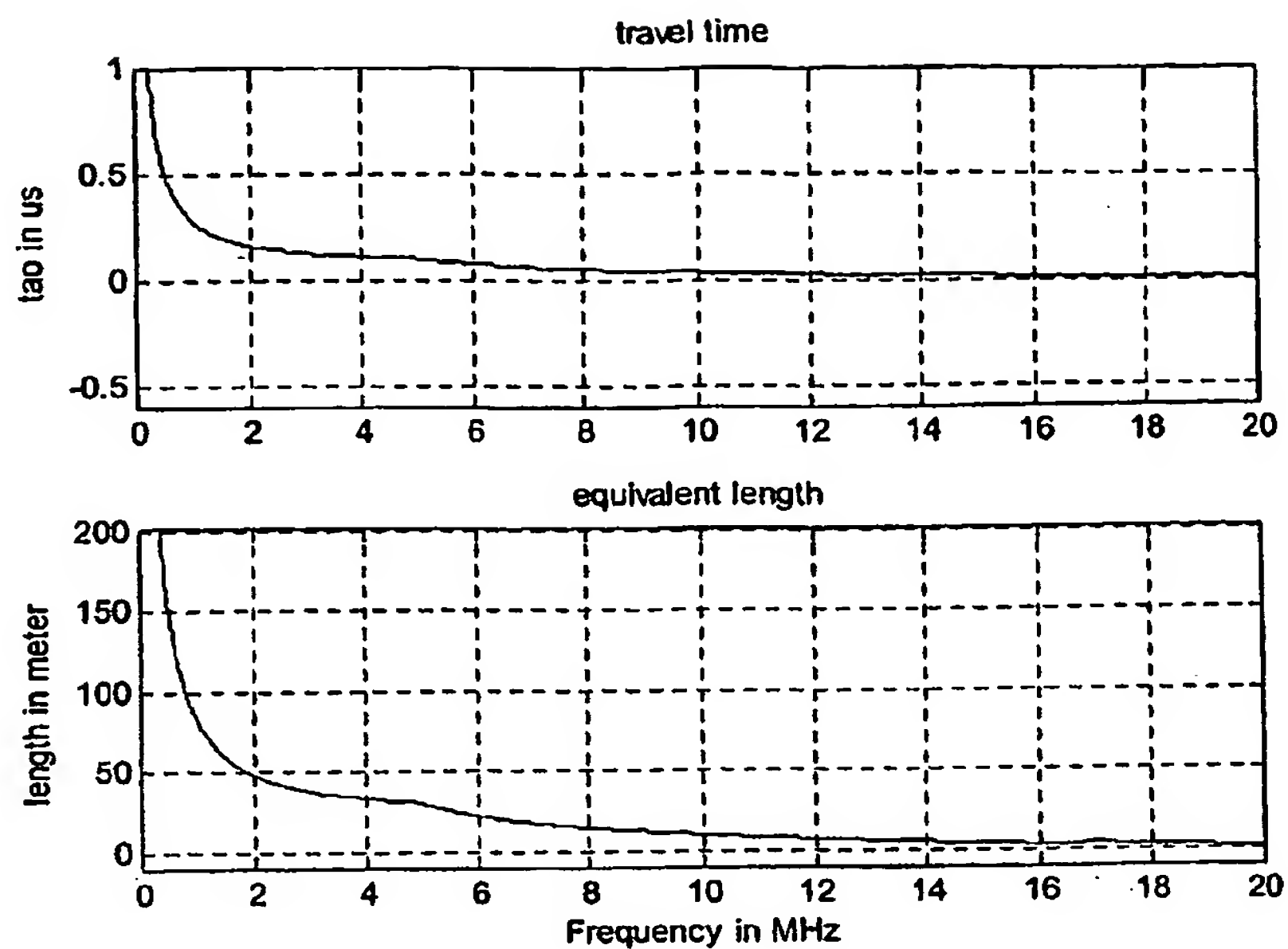


Figure 3.12 Simulation Results of Z_c in a Utility Research Lab



**Figure 3.13 Simulation Results of Travelling Time and Equivalent Length
in a Utility Research Lab**

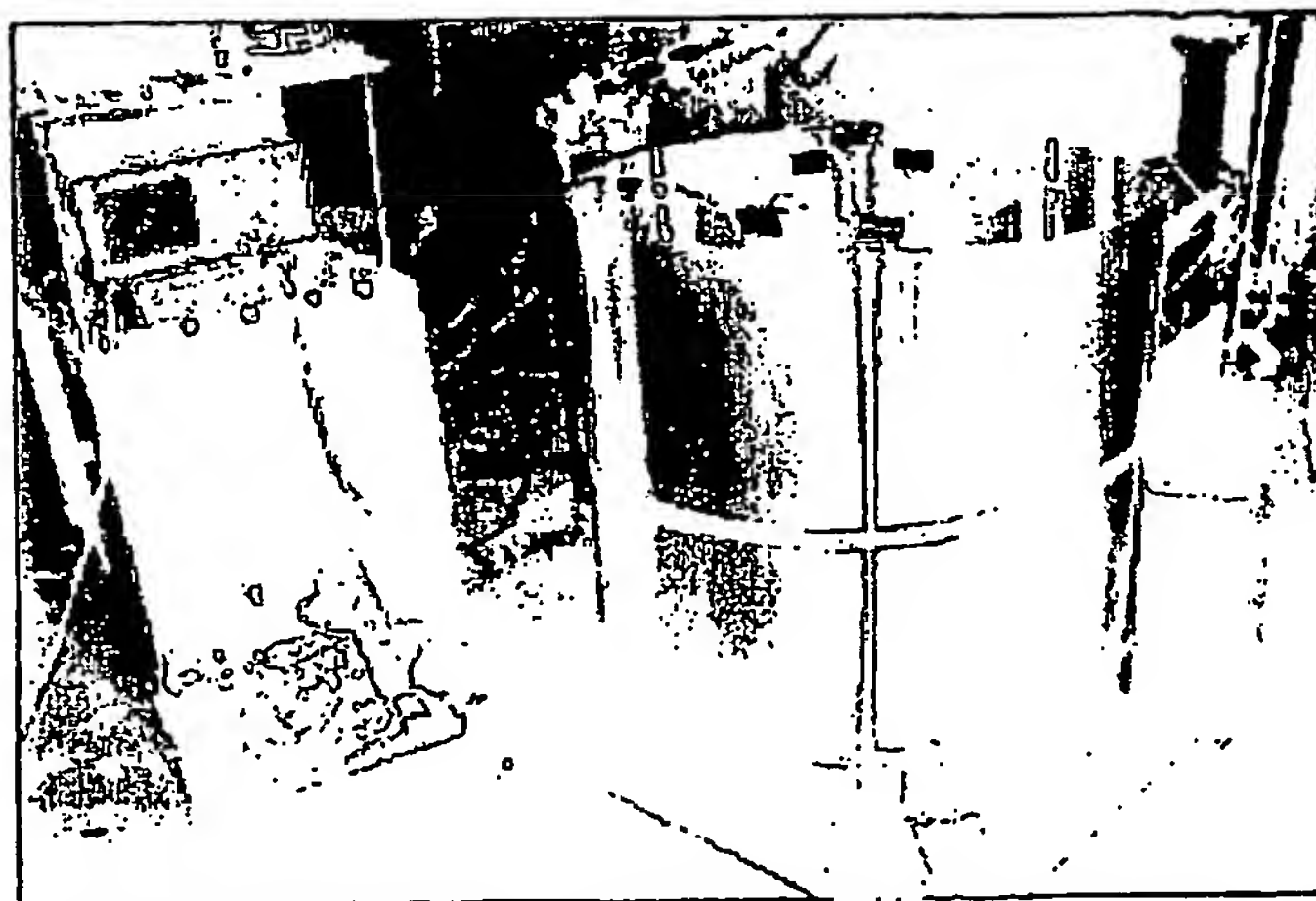


Figure 3.14 Overall View of the Transformer

Transmission Line Diagnostic



Figure 3.15 Cross-section View of the Transformer

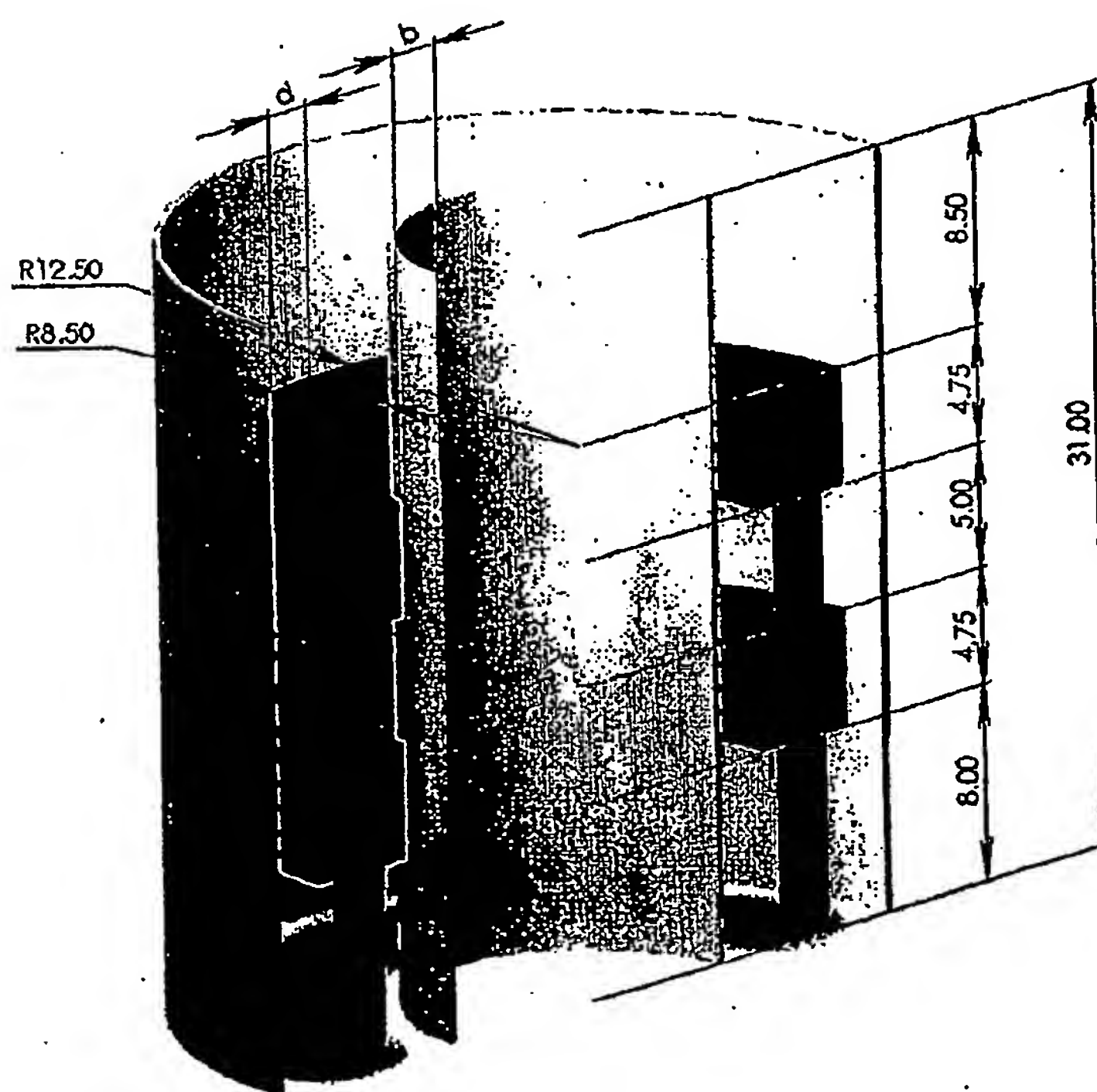


Figure 3.16 Cross-section View of the Transformer

Transmission Line Diagnostic

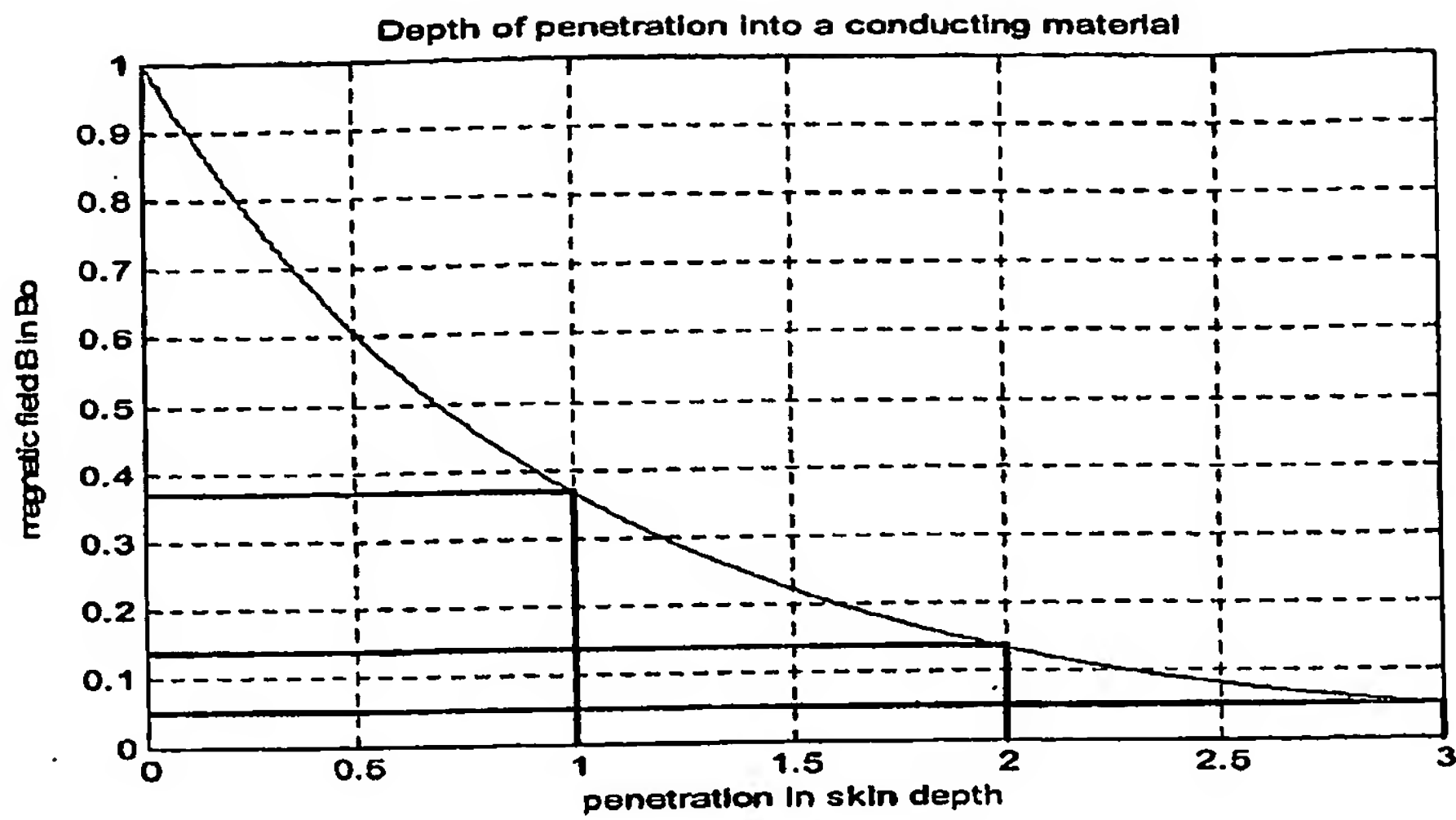


Figure 3.17 Illustration of the Skin Depth of a Conducting Material

Surge Impedance when b is very small
 $b_5 = \text{top}$; $b_7 = 0.25''$; $b_8 = 0.5''$; $d = 2.25''$
 Fitting Model II : $Z_c = a \cdot \exp(b \cdot f) + c \cdot \exp(d \cdot f)$

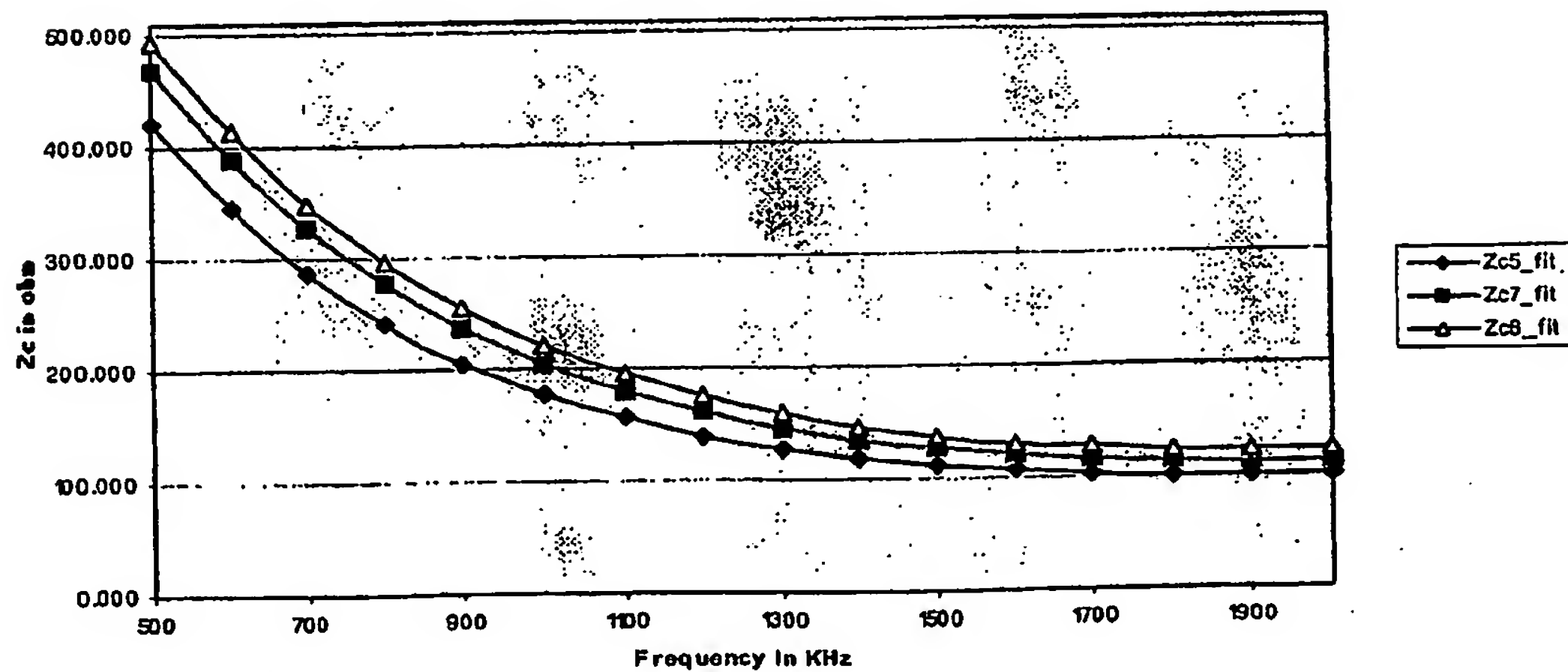


Figure 3.18 Z_c for Different Inner Separation by TLD Method with Model II

Transmission Line Diagnostic

Surge Impedance Z_c when b is very small
 $b_5 = \text{top}$; $b_7 = 0.25''$; $b_8 = 0.5''$; $d_5 = d_7 = d_8 = 2.25''$
 Fitting Model I: $Z_c = a \cdot \exp(b \cdot f)$

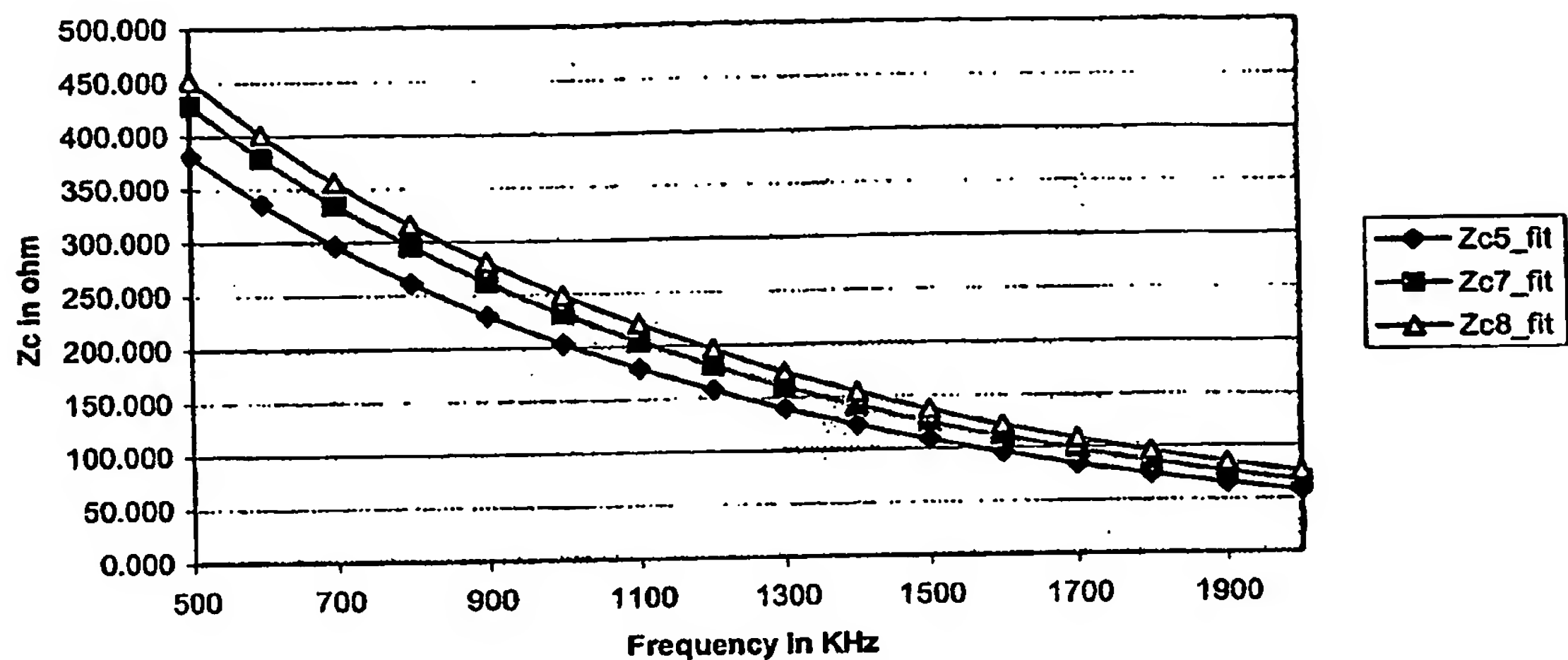


Figure 3.19 Z_c for Different Inner Separation by TLD Method with Model I

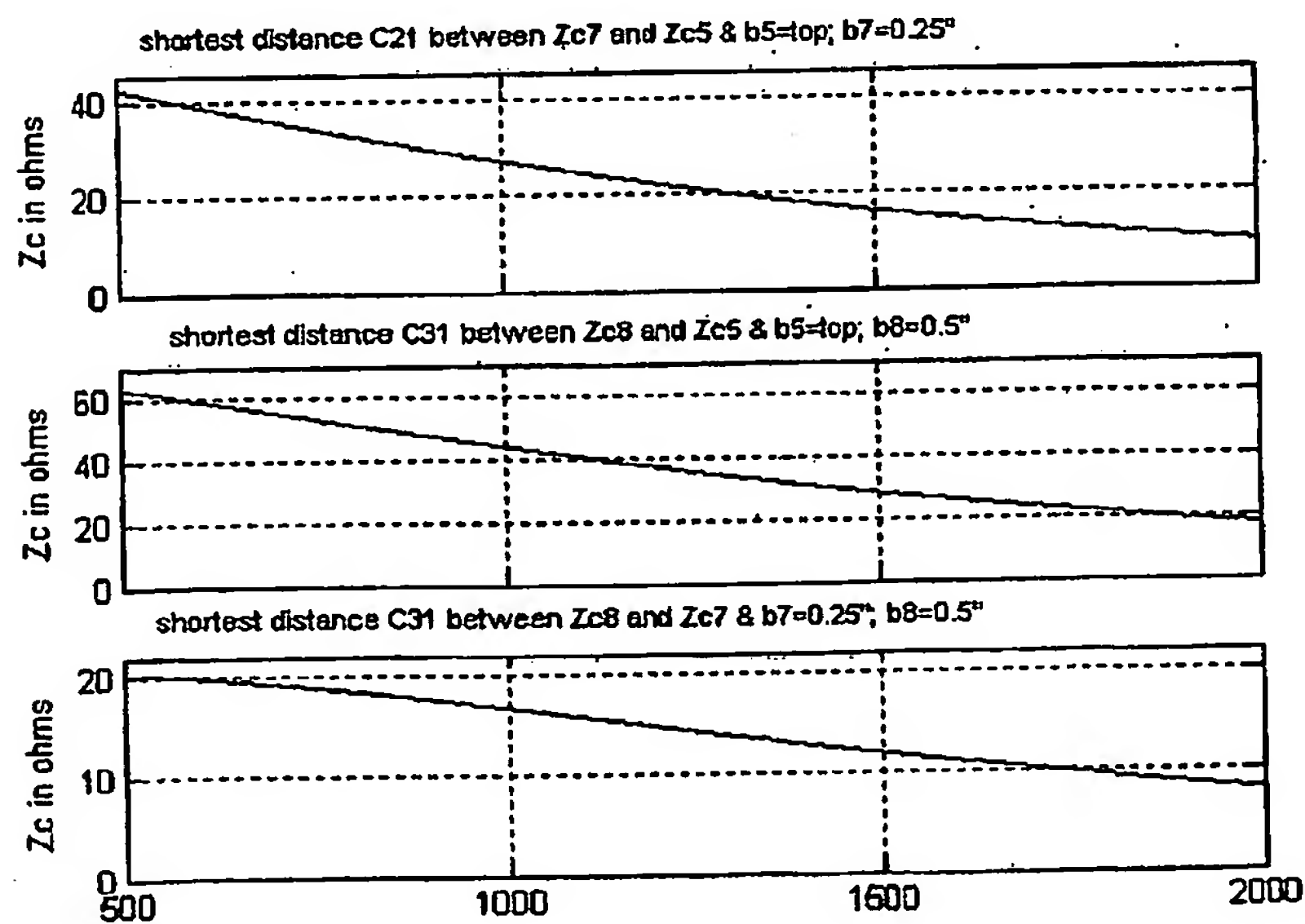


Figure 3.20 Shortest Distance among Z_{c5} , Z_{c7} and Z_{c8}

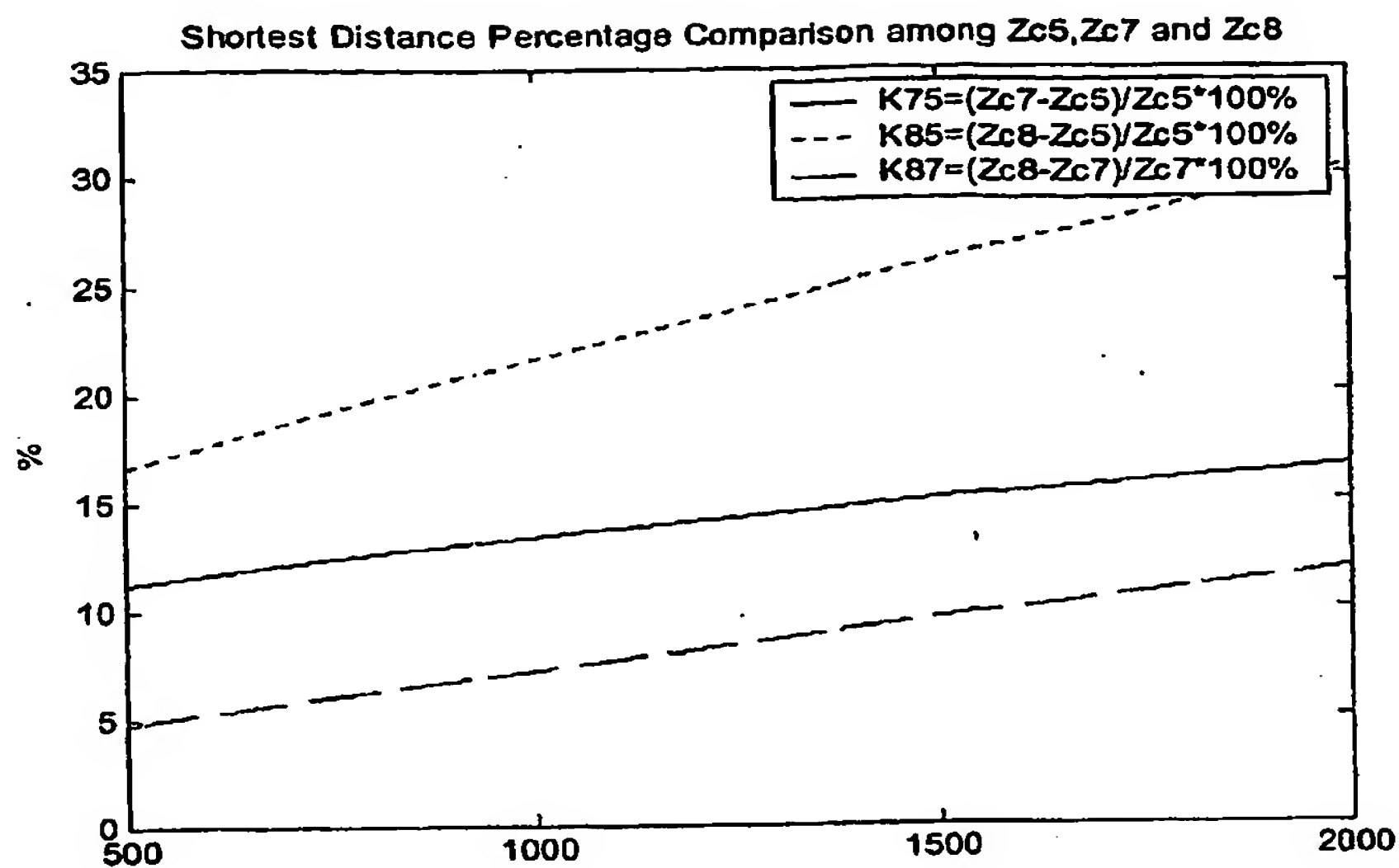


Figure 3.21 Shortest Distance Percentage Comparison When b is Small

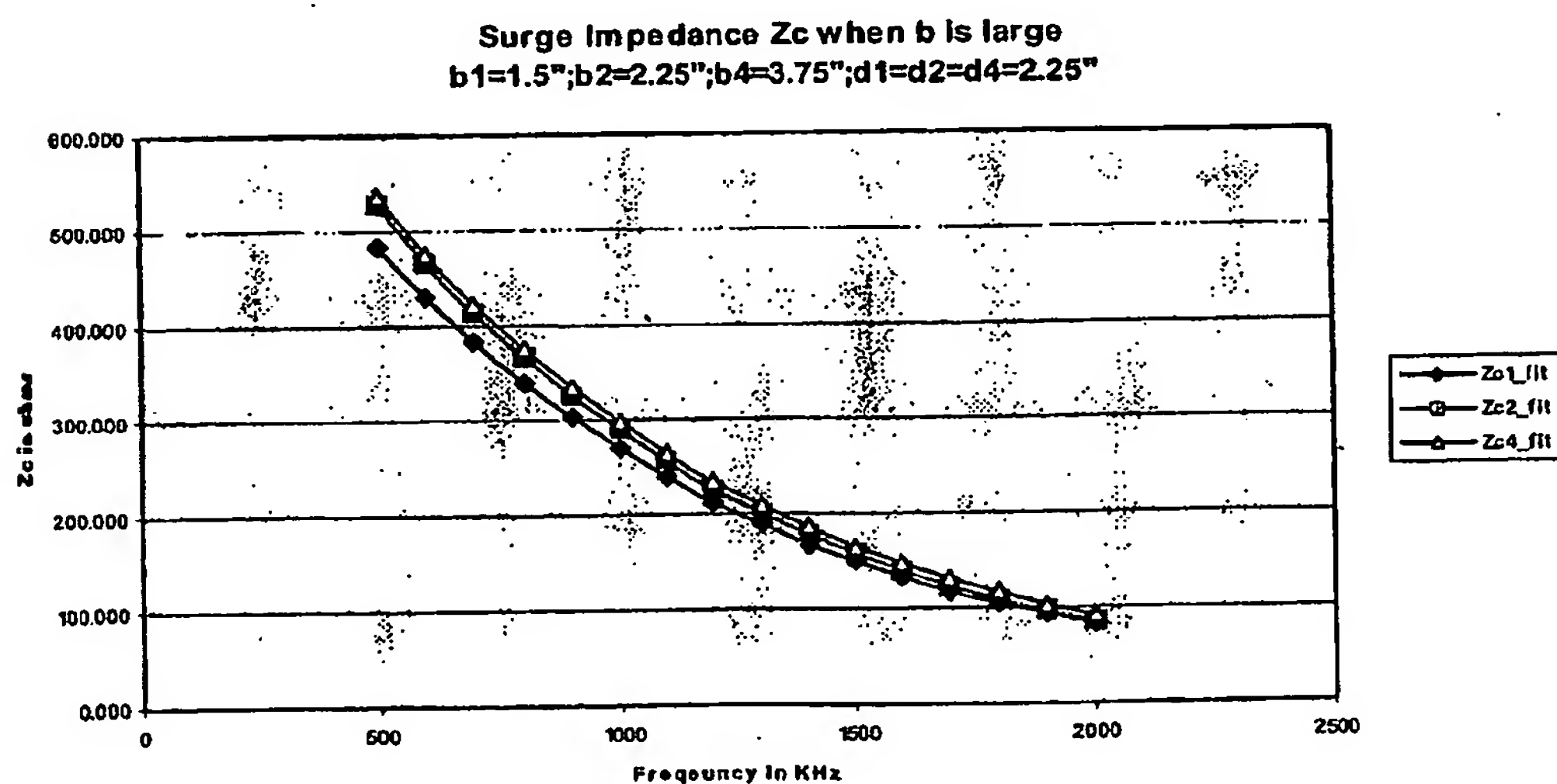


Figure 3.22 Zc for Bigger Inner Separation by TLD Method

Transmission Line Diagnostic

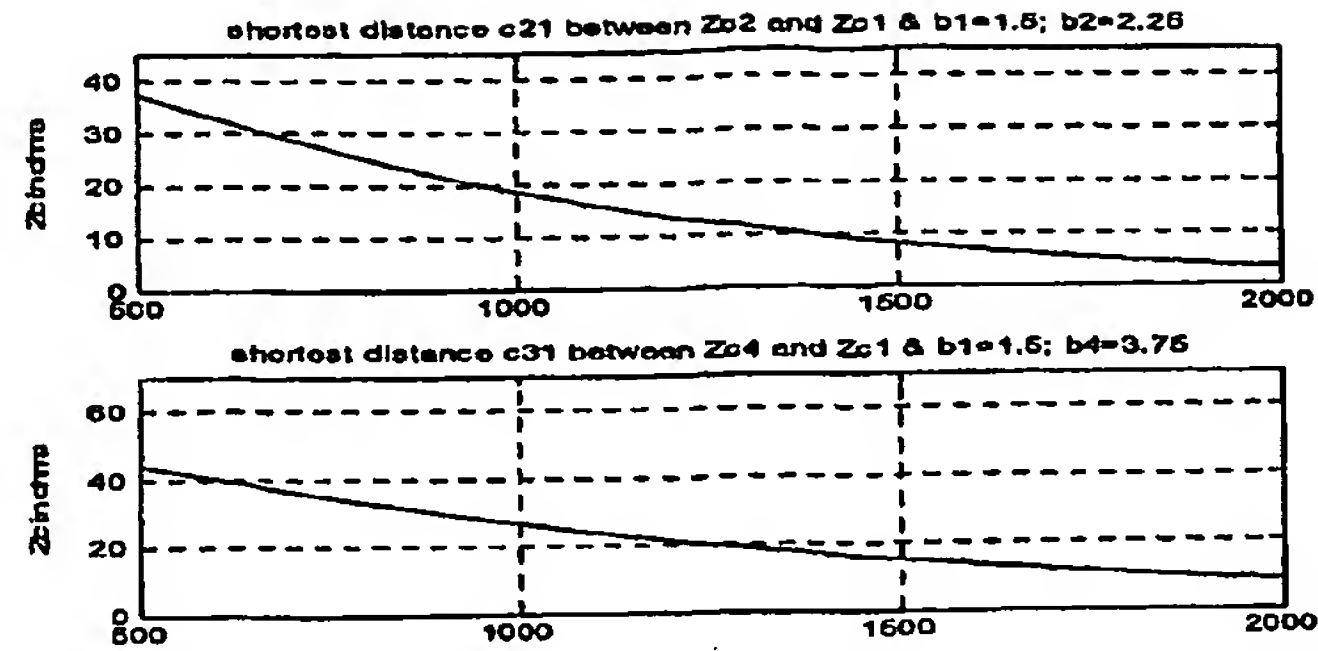


Figure 3.23 Shortest Distance among Zc1, Zc2 and Zc4

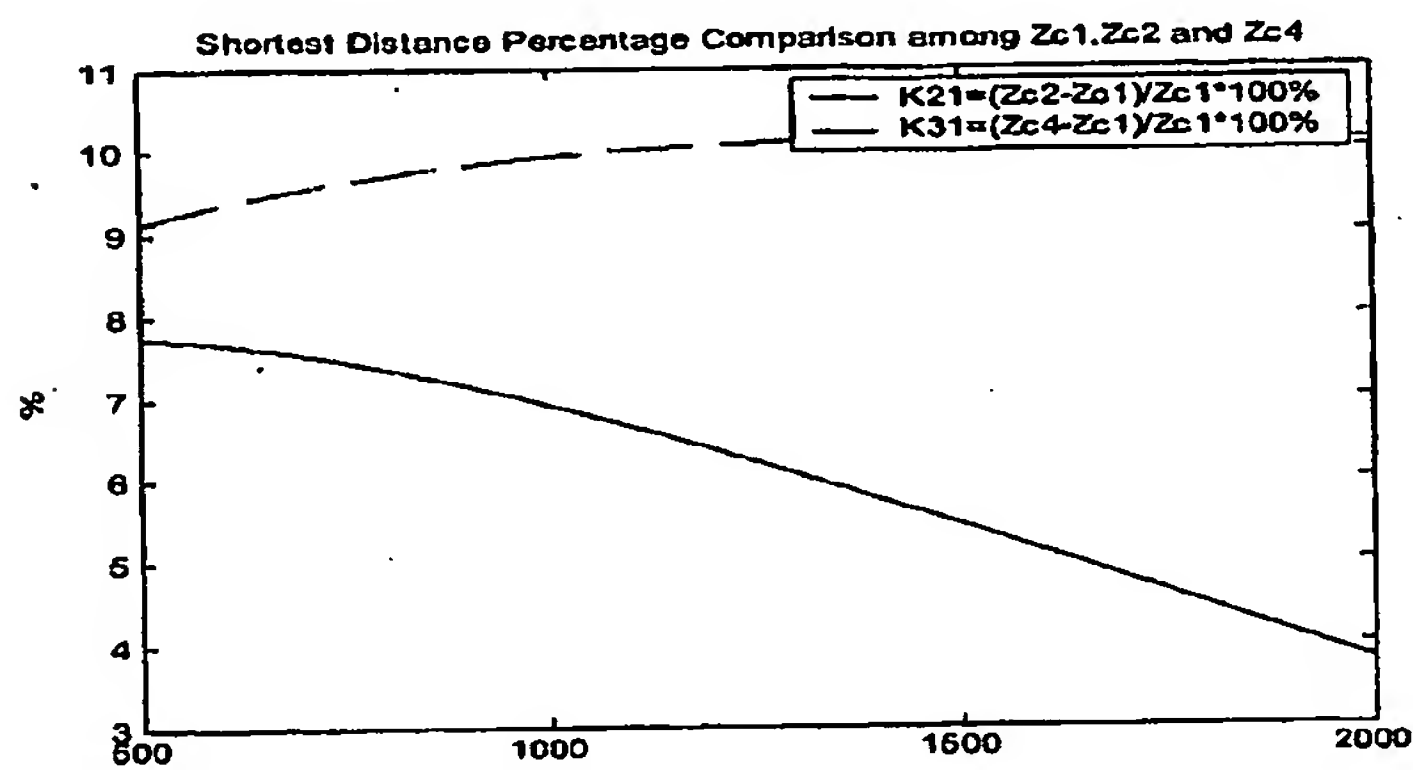


Figure 3.24 Shortest Distance Percentage Comparison When b is Large

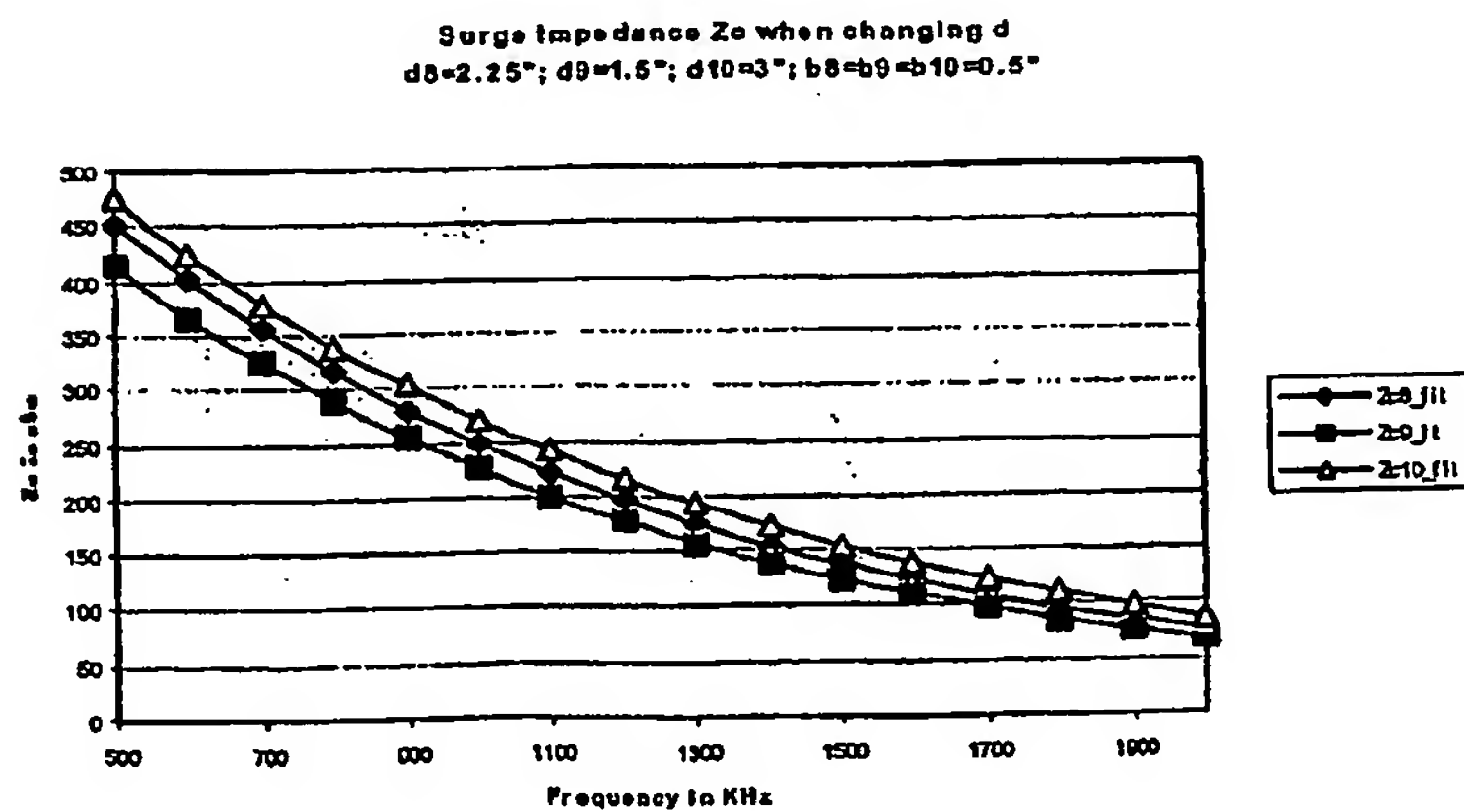


Figure 3.25 Zc for Different Outer Separation by TLD Method

Transmission Line Diagnostic

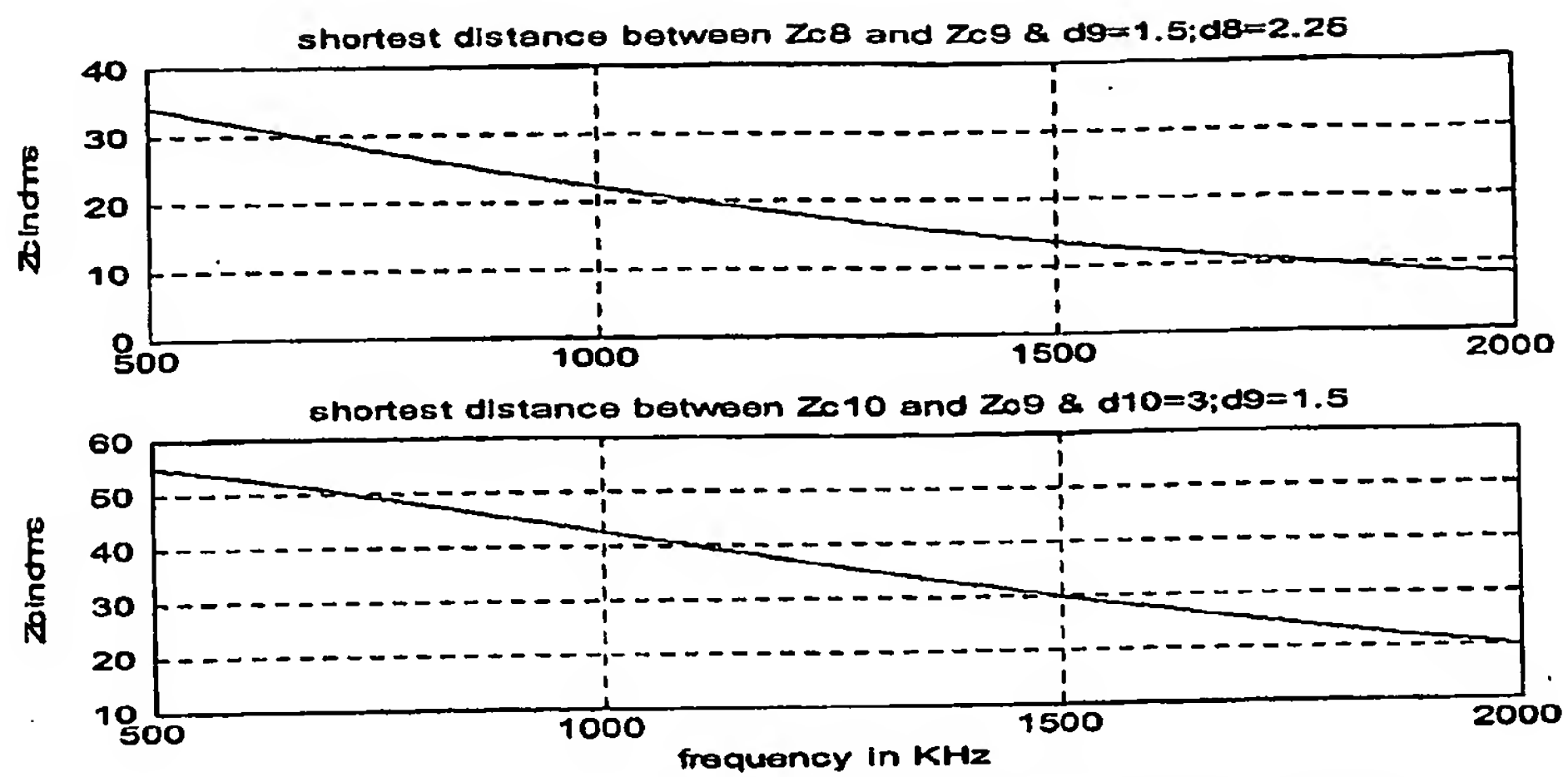


Figure 3.26 Shortest Distance among Zc8, Zc9 and Zc10

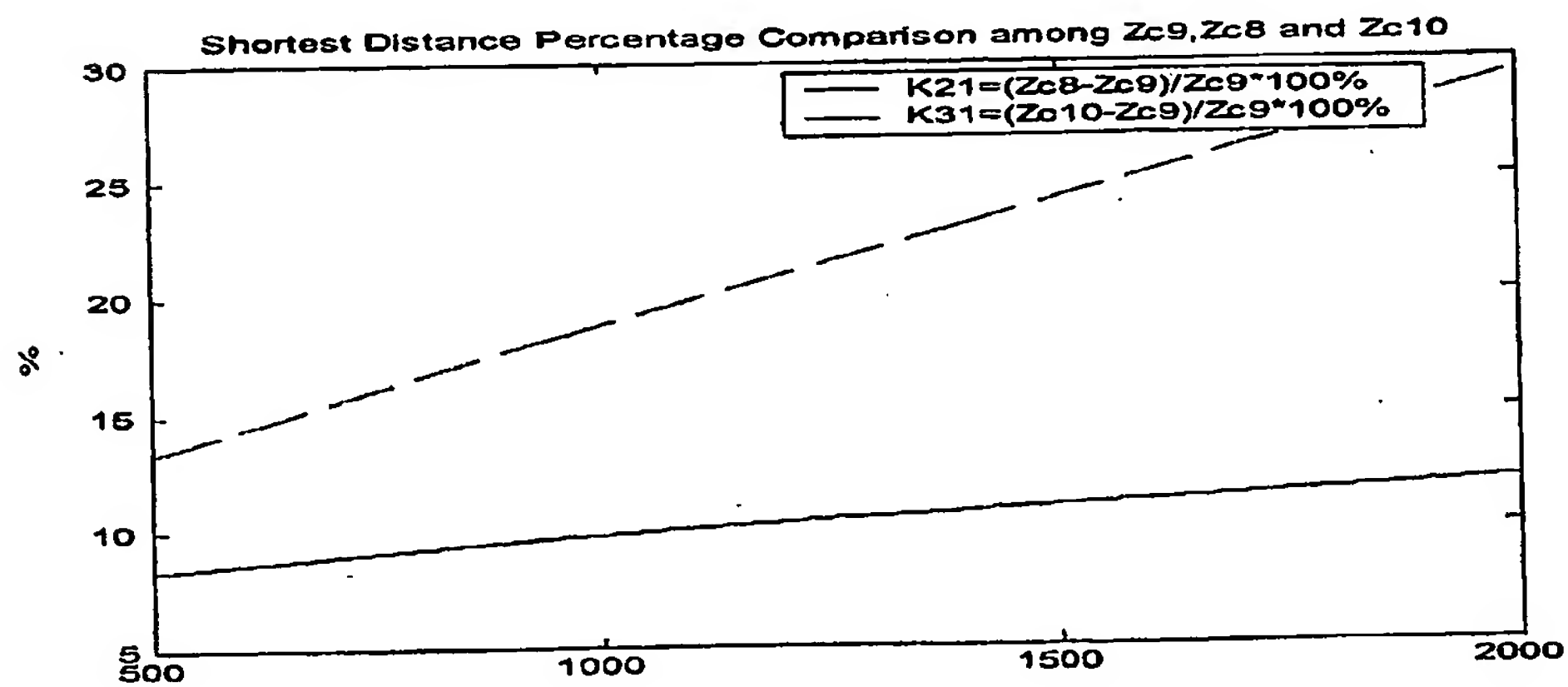


Figure 3.27 Shortest Distance Percentage Comparison among Zc9, Zc8 and Zc10

Transmission Line Diagnostic

Zc5 (before lifting) vs Zc14 (after lifting)
b=top=0; d=2.25"

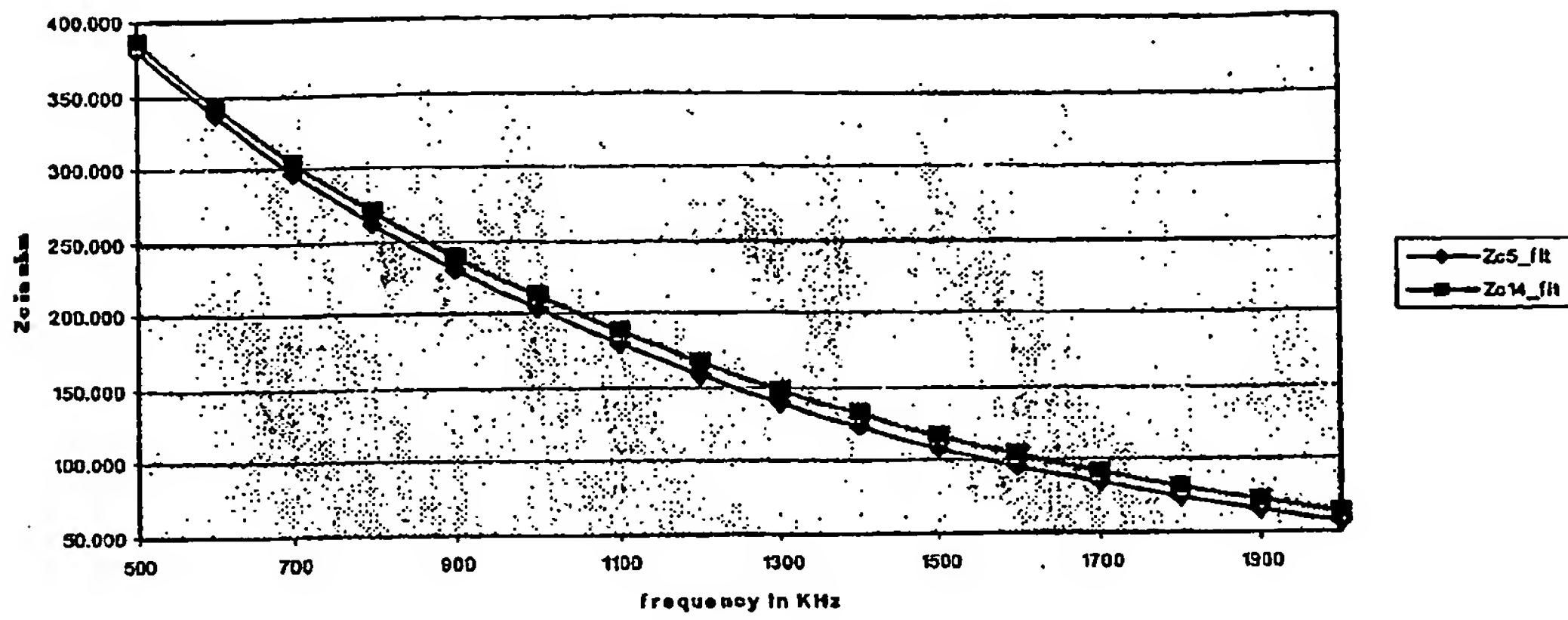


Figure 3.28 Zc Comparison 1

Zc8 (before lifting) vs Zc16 (after lifting)
b=0.5"; d=2.25"

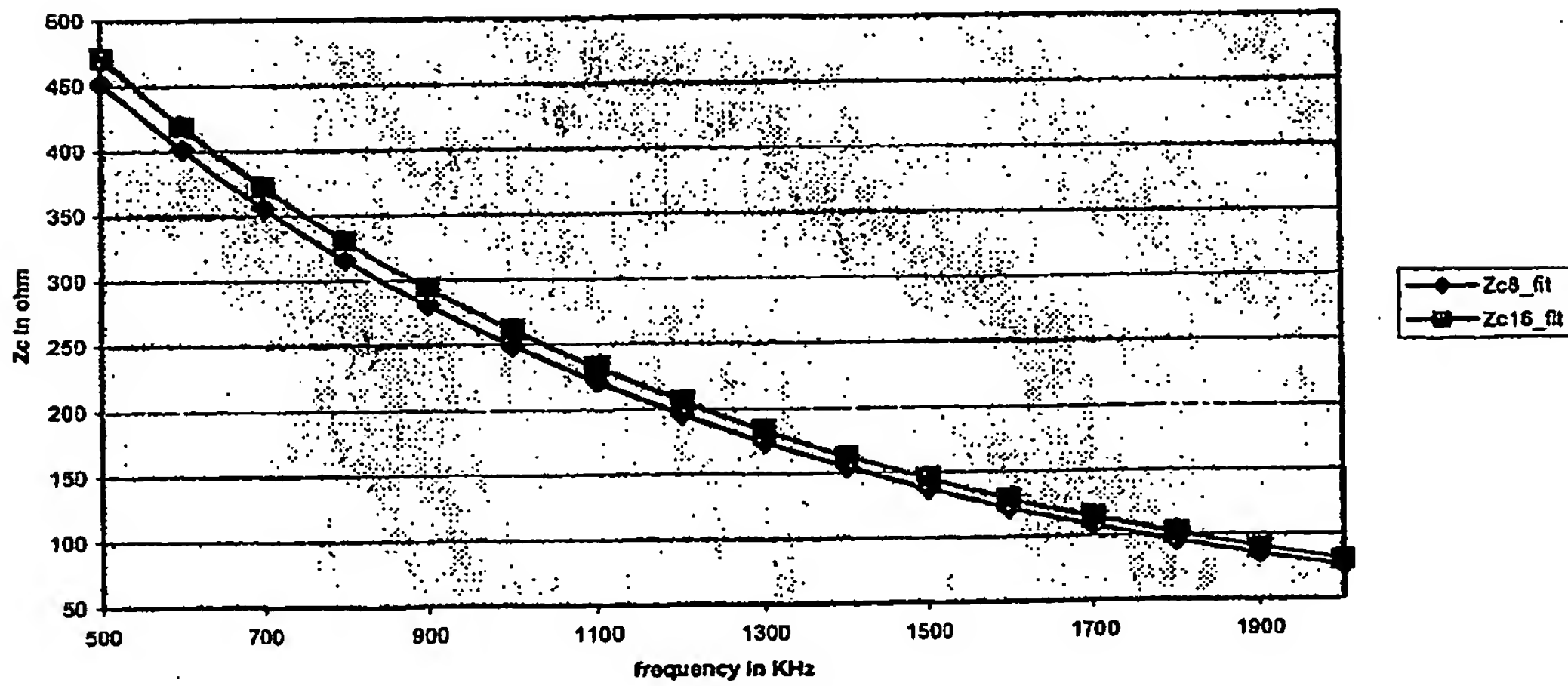


Figure 3.29 Zc Comparison 2

Transmission Line Diagnostic

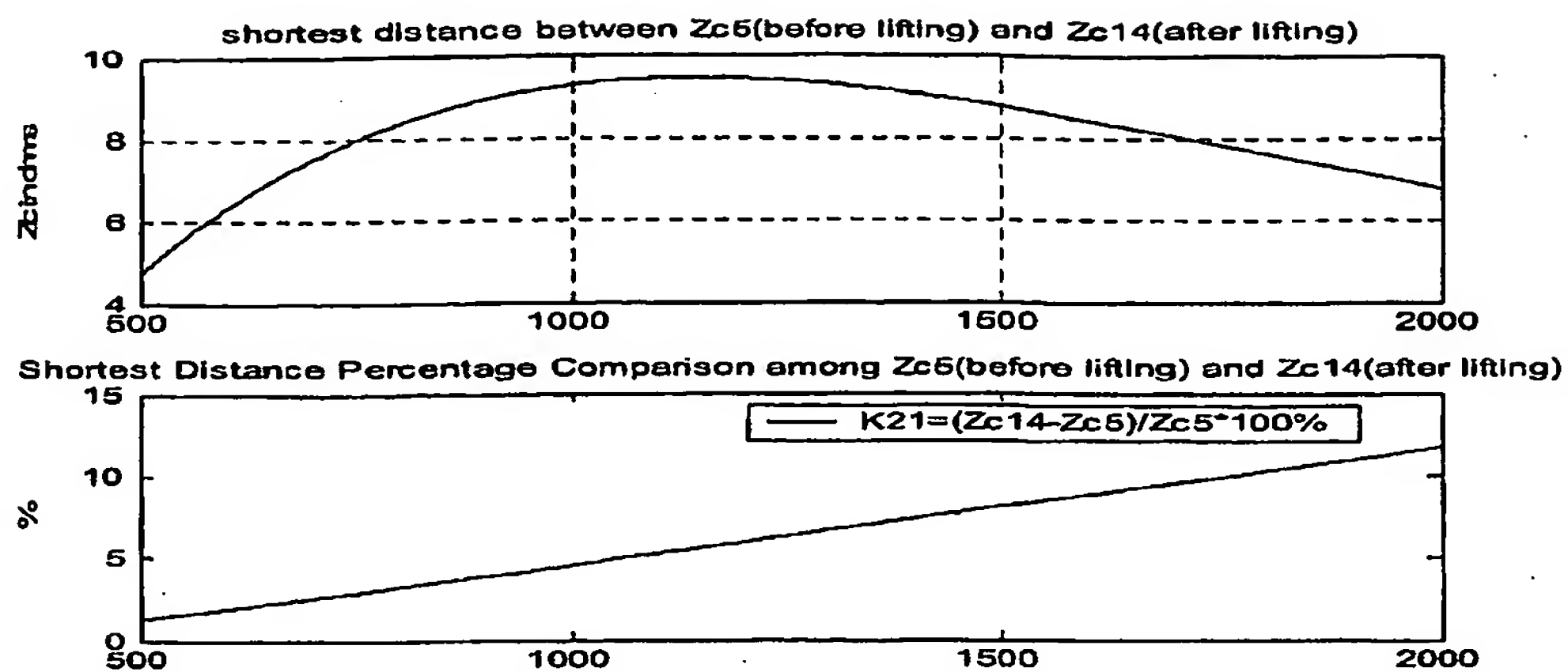


Figure 3.30 Shortest Distance & Distance Percentage Comparison 1

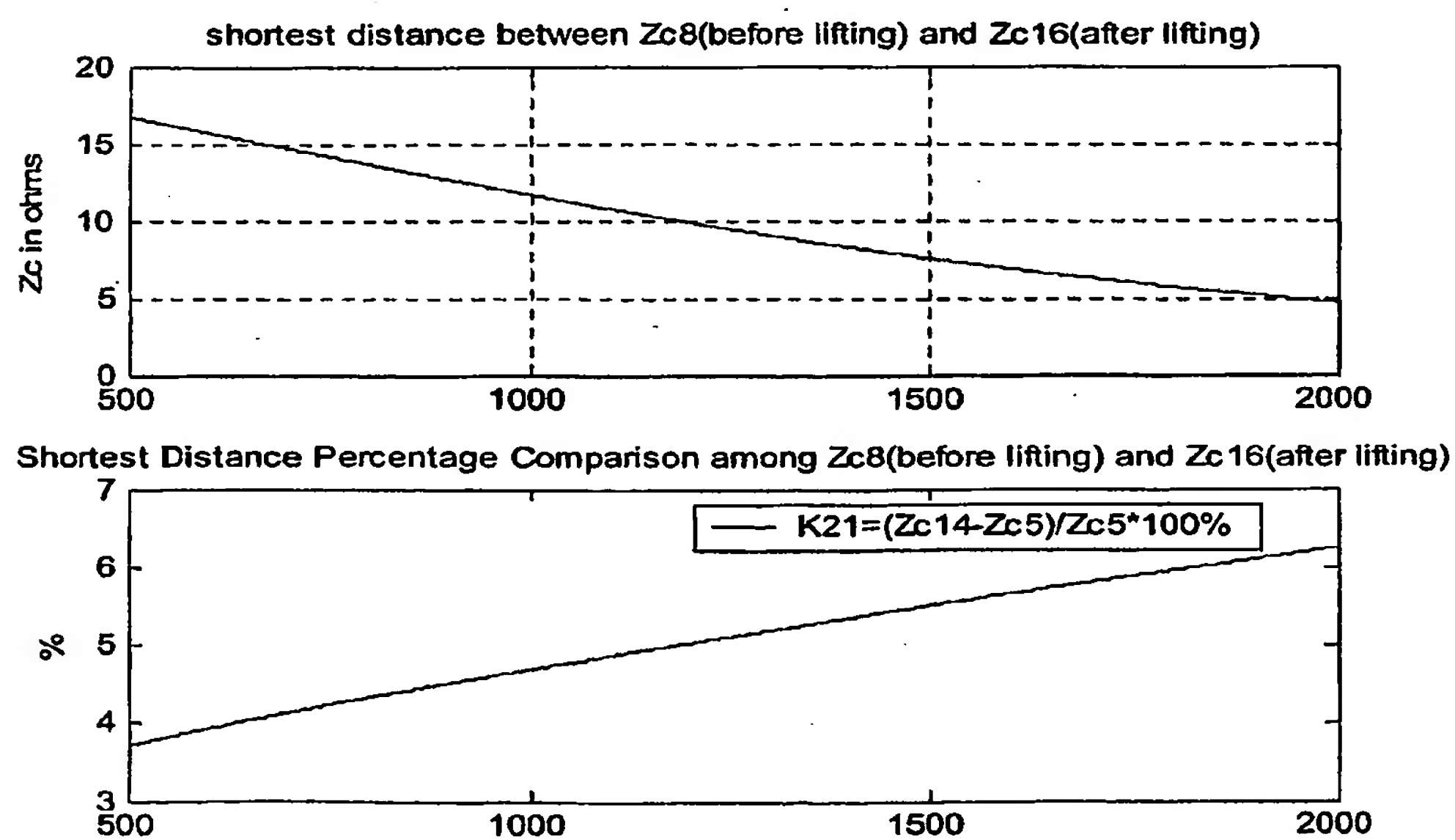
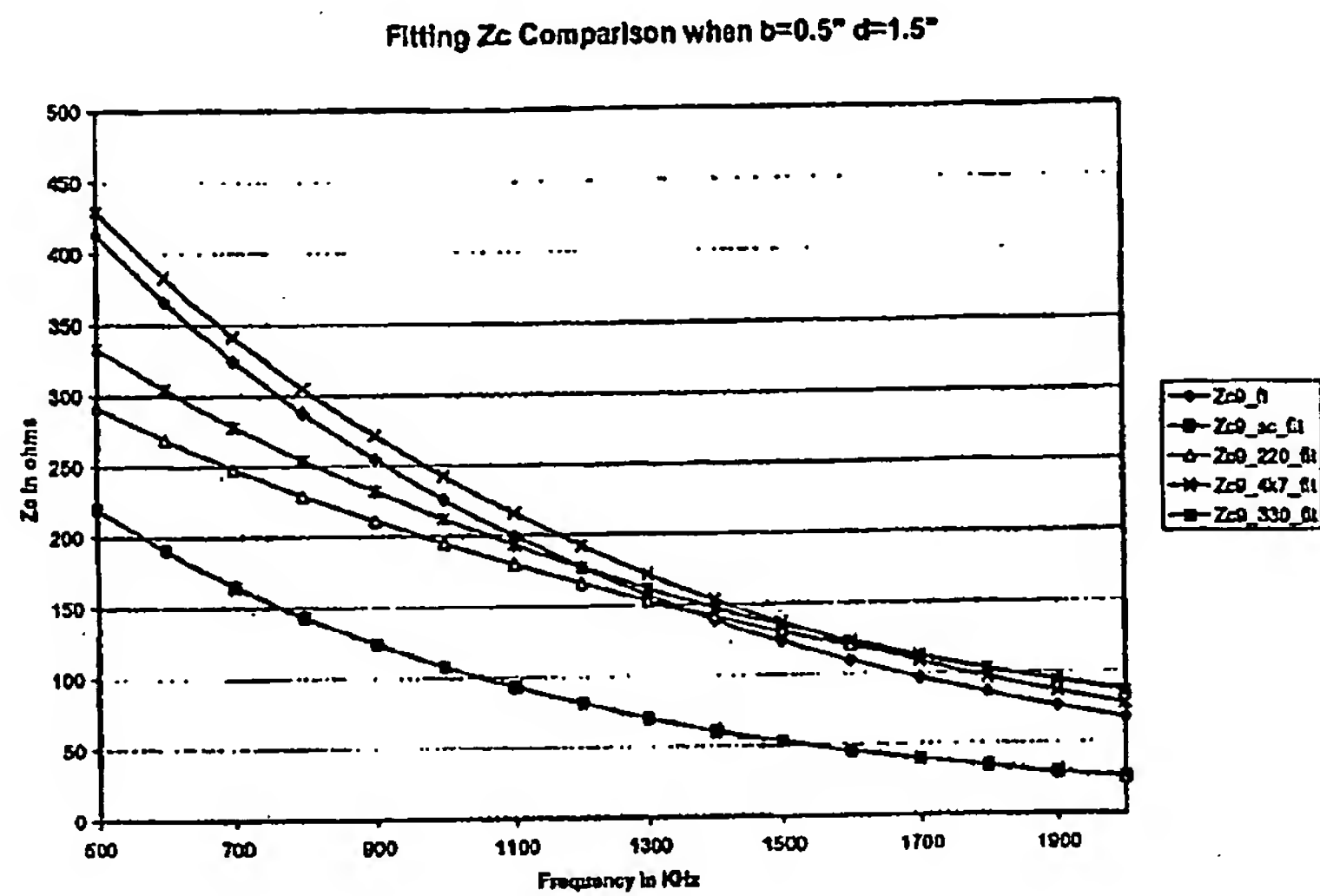


Figure 3.31 Shortest Distance & Distance Percentage Comparison 2

Figure 3.32 Z_c Comparison for Fault Situations